Electronic Supplementary Information for

Iodo-Bodipys as Visible-light-absorbing Dual-functional Photoredox Catalysts for Preparation of Highly Functionalized Organic Compounds by Formation of C–C bonds via Reductive and Oxidative Quenching Catalytic Mechanisms

*Ling Huang and Jianzhang Zhao**

State Key Laboratory of Fine Chemicals, School of Chemical Engineering, Dalian University of Technology, E-208 West Campus, 2 Ling-Gong Road, Dalian 116024, China

E-mail : zhaojzh@dlut.edu.cn

http://finechem.dlut.edu.cn/photochem

Index

The molecular structure characterization data of the photoredox catalytic reactions. The structural characterization data of the substrates and products in Table 6 and Table 7, **1g-1*l*, 1h-1k, 2gh-2gk**, **2*l*h-2*l*k**, were reported previously.[1] For the following compounds, the yields in the photocatalysis are exemplified with **B-1** as the photocatalysts. The results with **B-2** as the photocatalyst were presented in the Tables.

1. L. Huang and J. Zhao, *Chem. Commun,*. **2013**, 49, 3751–3753.

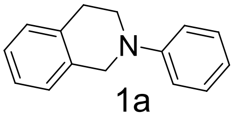

1a

1a. Yield: 714 mg (68 %). ^{1}H NMR (400 MHz, CDCl$_3$): δ 7.35–7.31 (m, 2H), 7.22–7.21 (m, 4H), 7.04–7.02 (d, J = 8.0 Hz, 2H), 6.89–6.86 (m, 1H), 4.45 (s, 2 H), 3.62–3.59 (m, 2H), 3.04–3.01 (m, 2H). TOF HRMS ESI$^+$: Calcd [$C_{15}H_{15}N+H$]$^+$ m/z 210.1283 found m/z 210.1288.

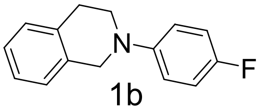

1b

1b. Yield: 650 mg (57 %). ^{1}H NMR (400 MHz, CDCl$_3$): δ 7.35–7.31 (m, 2H), 7.22–7.21 (m, 4H), 7.04 (d, J = 8.0 Hz, 2H), 6.89–6.86(m, 1H), 4.45 (s, 2 H), 3.62–3.59 (m, 2 H), 3.04–3.01 (m, 2H). TOF HRMS ESI$^+$: Calcd [$C_{15}H_{14}FN+H$]$^+$ m/z 228.1189, found m/z 228.1183.

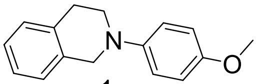

1c

1c. Yield: 858 mg (71 %). ^{1}H NMR (400 MHz, CDCl$_3$): δ7.17–7.11 (m, 4H), 6.98 (d, J = 8.0Hz, 2H), 6.86 (d, J =8.0 Hz, 2H), (d, J =8.0 Hz, 2H),4.28 (s, 2H), 3.76 (s, 3 H), 3.45–3.42 (m, 2 H), 2.99–2.96 (m, 2H). TOF HRMS ESI$^+$: Calcd [$C_{16}H_{17}NO+H$]$^+$ m/z 240.1388, found m/z 240.1391.

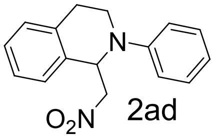

2ad

2ad. Yield: 82.8 mg (77 %). ^{1}H NMR (400 MHz, CDCl$_3$): δ 7.34–7.28 (m, 4H), 6.92–6.90 (m, 2H), 7.24–7.22 (m, 1H). 7.18–7.17 (m, 1H), 7.04 (d, *J*= 8.0 Hz, 2H), 5.61–5.58 (m, 1H), 4.94–4.91 (m, 1H), 3.71–3.66 (m, 2H), 3.13–3.15 (m, 1H), 2.85 –2.81(m, 1H). TOF HRMS ESI$^+$: Calcd [$C_{16}H_{16}N_2O_2$+H]$^+$ *m*/*z* 269.1290, found *m*/*z* 269.1285.

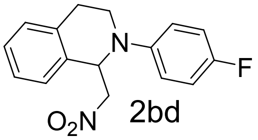

2bd

2bd. Yield: 87.1 mg (76 %). ^{1}H NMR (400 MHz, CDCl$_3$): δ 7.28–7.22 (m, 2H), 7.21–7.14 (m, 2H), 6.97–6.89 (m, 4 H). 5.43–5.41 (m, 1H), 4.85–4.83 (m, 1H), 4.60–4.55 (m, 2H), 3.62–3.58 (m, 2H), 3.03–3.01 (m, 1H), 2.75–2.74 (m, 1H), TOF HRMS ESI$^+$: Calcd [$C_{16}H_{15}N_2O_2F$+H]$^+$ *m*/*z* 287.1196 found *m*/*z* 287.1199.

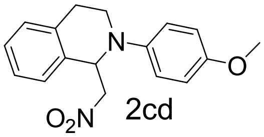

2cd

2cd. Yield: 92.1 mg (77 %). ^{1}H NMR (400 MHz, CDCl$_3$): δ 7.25–7.21 (m, 2H), 7.17–7.13 (m, 2H), 6.93 (d, *J* = 8.0 Hz, 2H), 6.83 (d, *J* = 8.0 Hz, 2H), 5.39–5.371 (m, 1H), 4.84–4.81 (m, 1H), 4.59–4.54 (m, 1H), 3.75 (s, 3H), 3.58–3.55 (m, 2H), 3.02–3.00 (m, 1H), 2.73–2.68 (m, 1H), TOF HRMS ESI$^+$: Calcd [$C_{17}H_{18}N_2O_3$+H]$^+$ *m*/*z* 299.1396, found *m*/*z* 299.1394.

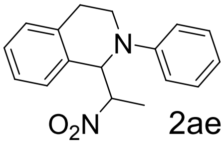

2ae

2ae. Yield: 103.0 mg (91 %). ^{1}H NMR (400 MHz, CDCl$_3$): δ 7.29–7.09 (m, 6H), 7.01–6.98 (m, 2H), 6.84–6.79 (m, 1H), 5.26 – 5.22(m, 1H), 5.07–4.89 (m, 1H), 3.83–3.56 (m, 2H), 3.10–2.89 (m, 2H), 1.71–1.53 (m, 3H). TOF HRMS ESI$^+$: Calcd [$C_{17}H_{18}N_2O_2$+H]$^+$ *m*/*z* 283.1447, found *m*/*z* 283.1441.

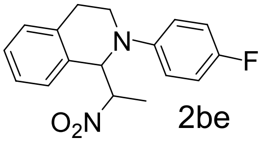

2be

2be. Yield: 71.0 mg (59 %). ^{1}H NMR (400 MHz, CDCl$_3$): δ 7.29–7.04 (m, 4H), 6.97–6.90 (m, 4 H), 5.13–5.02 (m, 2H), 3.82–3.52 (m, 2H), 2.99–2.84 (m, 2H), 1.69–1.56 (m, 3H). TOF HRMS ESI$^+$: Calcd [$C_{17}H_{17}N_2O_2F$+H]$^+$ *m*/*z* 301.1352, found *m*/*z* 301.1352.

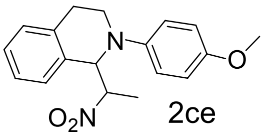
2ce

2ce. Yield: 71.4 mg (57 %). ^{1}H NMR (400 MHz, CDCl$_3$): δ 7.24–7.09 (m, 4H), 6.92–6.90 (m, 2H), 6.83–6.76 (m, 2H). 5.06–4.86 (m, 2H), 3.79–3.72 (m, 4H), 3.52–3.48 (m, 1H), 2.97–2.95 (m, 1H), 2.83–2.78 (m, 1H), 1.68–1.52 (m, 3H). TOF HRMS ESI$^+$: Calcd $[C_{18}H_{20}N_2O_3+H]^+$ *m/z* 313.1552, found *m/z* 313.1546.

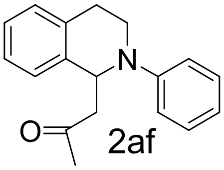
2af

2af. Yield: 26.6 mg (50 %). ^{1}H NMR (400 MHz, CDCl$_3$): δ 7.25–7.23 (m, 2H), 7.16 (m, 4H), 6.95(d, *J* = 8.0 Hz, 2 H), 6.79–6.76 (m, 1H), 5.41–5.38 (m, 1H), 3.68–3.52 (m, 2H), 3.07–3.03 (m, 2H), 2.85–2.79 (m, 2H), 2.07 (s, 3H). TOF HRMS ESI$^+$: Calcd $[C_{18}H_{19}NO+H]^+$ *m/z* 266.1545, found *m/z* 266.1545.

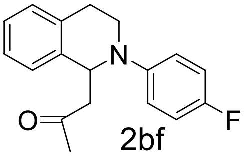
2bf

2bf. Yield: 44.9 mg (79 %). ^{1}H NMR (400 MHz, CDCl$_3$): δ 7.18–7.11 (m, 4H), 6.95–6.91 (m, 4H), 5.30–5.27 (m, 1H), 3.57–3.49 (m, 2H), 3.04–3.00 (m, 2H), 2.82–2.76 (m, 2H), 2.07 (s, 3H). TOF HRMS ESI$^+$: Calcd $[C_{18}H_{18}NOF+H]^+$ *m/z* 284.1451, found *m/z* 284.1445.

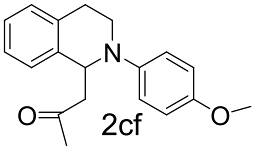
2cf

2cf. Yield: 37.9 mg (64 %). ^{1}H NMR (400 MHz, CDCl3): δ 7.15–7.11 (m, 4H), 6.93–6.91 (m, 2H), 6.82–6.80 (m, 2H), 5.26–5.23 (m, 1H), 3.74 (s, 3H), 3.56–3.45 (m, 2 H), 3.04–2.98 (m, 2H), 2.79–2.75 (m, 2H), 2.06 (s, 3H). TOF HRMS ESI$^+$: Calcd $[C_{19}H_{21}NO_2+H]^+$ *m/z* 296.1651, found *m/z* 296.1650.

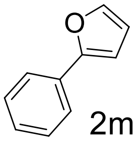
2mr

2mr. Yield: 59.1 mg (82 %). ^{1}H NMR (400 MHz, CDCl$_3$): δ 7.77 (d, *J* = 7.6 Hz, 1H), 7.65–7.60 (m, 2H), 7.39–7.33 (m, 3H), 6.62 (d, *J* = 4.0 Hz, 1H), 6.46 (d, *J*=8.0Hz 1H). TOF HRMS EI$^+$: Calcd [$C_{10}H_8O$]$^+$ *m/z* 144.0575. found *m/z* 144.0582.

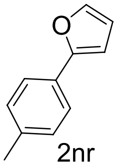

2nr

2nr. Yield: 48.2 mg (61 %). ^{1}H NMR (400 MHz, CDCl$_3$): δ 7.57 (d, *J* = 8.0 Hz, 2H), 7.43 (s, 1H), 7.19 (d, *J*=7.2Hz 2H), 6.58 (d, *J*=7.6 Hz 1H), 6.44 (s, 1H), 2.35 (s, 3H). TOF HRMS EI$^+$: Calcd [$C_{11}H_{10}O$]$^+$ *m/z* 158.0732 found *m/z* 158.0735.

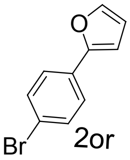

2or

2or. Yield: 96.1 mg (87 %). ^{1}H NMR (400 MHz, CDCl$_3$): δ 7.60 (d, *J*=2.8 Hz, 1H), 7.55–7.47 (m, 4H), 6.62 (d, *J*=4.0Hz 1H),6.46 (d, *J*=8.0Hz 1H).TOF HRMS EI$^+$: Calcd [$C_{10}H_7BrO$]$^+$ *m/z* 221.9680, found *m/z* 221.9689.

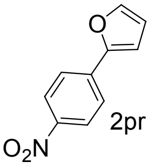

2pr

2pr. Yield: 70.9 mg (75 %). ^{1}H NMR (400 MHz, CDCl$_3$): δ 8.26 (d, *J* = 8.0 Hz, 2H), 7.81 (d, *J*= 7.6 Hz, 2H), 6.89 (d, *J* = 4.0 Hz, 1H), 6.56 (s, 1H). TOF HRMS EI$^+$: Calcd [$C_{10}H_7NO_3$]$^+$ *m/z* 189.0426, found *m/z* 189.0432.

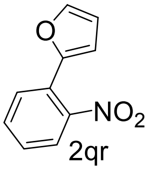

2qr

2qr. Yield: 67.1 mg (71 %). ^{1}H NMR (400 MHz, CDCl$_3$): δ 7.74–7.68 (m, 2H), 7.61–7.57 (m, 1H), 7.53 (s, 1H), 7.44–7.41 (m, 1H), 6.96 (d, *J*=4.0 Hz 1H), 6.52 (d, *J* = 4.0 Hz, 1H). TOF HRMS EI$^+$: Calcd [$C_{10}H_7NO_3$]$^+$ *m/z* 189.0426, found *m/z* 189.0435.

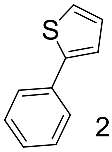

2ms

2ms. Yield: 65.6 mg (82 %). ^{1}H NMR (400 MHz, CDCl$_3$): δ 7.63–7.59 (m, 2H), 7.46–7.44 (m, 1H), 7.40–7.36 (m, 2H), 7.32–7.28 (m, 2H), 7.09–7.07 (m, 1H),. TOF HRMS EI$^+$: Calcd [$C_{10}H_8S$]$^+$ *m/z* 160.0347 found *m/z* 160.0354.

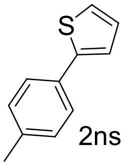

2ns

2ns. Yield: 60.9 mg (70 %). ^{1}H NMR (400 MHz, CDCl$_3$): δ 7.51–7.48 (m, 2H), 7.44–7.29 (m, 2H), 7.24–7.22 (m, 1H), 7.19 (d, *J* = 8.0Hz 1H), 7.13–7.05 (m, 1H), 2.36 (s, 3H). TOF HRMS EI$^+$: Calcd [$C_{11}H_{10}S$]$^+$ *m/z* 174.0503, found *m/z* 174.0503.

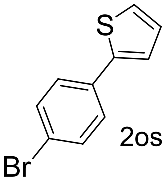

2os

2os. Yield: 92.4 mg (78 %). ^{1}H NMR (400 MHz, CDCl$_3$): δ 7.37 (d, *J* = 4.0Hz, 2H), 7.25 (d, *J* = 4.0 Hz, 2H), 6.94 (s, 1H), 6.82–6.80 (m, 2H). TOF HRMS EI$^+$: Calcd [$C_{10}H_7BrS$]$^+$ *m/z* 237.9452, found *m/z* 237.9458.

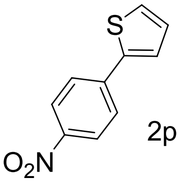

2ps

2ps. Yield: 72.8 mg (71 %). ^{1}H NMR (400 MHz, CDCl$_3$): δ 8.28 (d, *J*=8.0Hz, 2H), 7.76 (d, *J*=8.0Hz, 2H), 7.49–7.44 (m, 2H), 7.17–7.15 (m, 1H). TOF HRMS EI$^+$: Calcd $[C_{10}H_7NO_2S]^+$ *m/z* 205.0198, found *m/z* 205.0203.

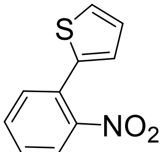

2qs

2qs. Yield: 71.8 mg (70 %). ^{1}H NMR (400 MHz, CDCl$_3$): δ 7.76 (d, *J* = 8.0 Hz, 2H), 7.58–7.56 (m, 1H), 7.47–7.42 (m, 2H), 7.09 ppm (d, *J*=4.0, 2H). TOF HRMS EI$^+$: Calcd $[C_{10}H_7NO_2S]^+$ *m/z* 205.0198, found *m/z* 205.0204.

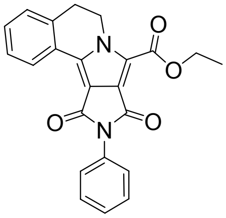

^{1}H NMR (400 MHz, CDCl$_3$) δ = 8.61 (d, *J* = 12.0 Hz, 1H), 7.50 –7.47 (m, 2H), 7.42–7.37 (m, 5H), 7.31 (d, *J* = 8.0 Hz, 1H), 4.80 (t, *J* = 6.9 Hz, 2H), 4.46–4.41 (m, 2H), 3.21 (t, *J* = 6.4 Hz, 2H), 1.49 ppm (t, *J* = 7.2 Hz, 3H).

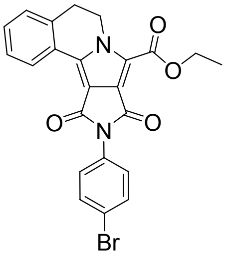

^{1} H NMR (400 MHz, CDCl$_3$) δ = 8.58 (d, *J* = 8.0 Hz, 1H), 7.62 (d, J = 8.0 Hz, 2H), 7.43 –7.37 (m, 2H), 7.32–7.29 (m, 3H), 4.80 (t, *J* = 6.9 Hz, 2H), 4.47–4.41 (m, 2H), 3.21 (t, *J* = 6.4 Hz, 2H), 1.49 ppm (t, *J* = 7.2 Hz, 3H).

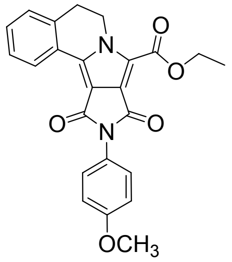

^{1} H NMR (400 MHz, $CDCl_3$) δ = 8.60 (d, *J* = 8.0 Hz, 1H), 7.43 –7.38 (m, 2H), 7.32–7.30 (m, 3H), 7.01 (d, *J* = 7.6 Hz, 2H), 4.79 (t, *J* = 6.9 Hz, 2H), 4.46–4.41 (m, 2H), 3.84 (s, 3H), 3.20 (t, *J* = 6.4 Hz, 2H), 1.48 ppm (t, *J* = 7.2 Hz, 3H).

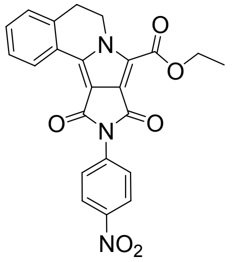

^{1}H NMR (400 MHz, $CDCl_3$) δ = 8.56 (d, *J* = 8.0 Hz, 1H), 8.36 (d, J = 7.2 Hz, 2H), 7.73 (d, J = 8.0 Hz， 2H), 7.46–7.41 (m, 2H), 7.32 (d, *J* = 4.0 Hz, 1H), 4.82 (t, *J* = 6.9 Hz, 2H), 4.49–4.43 (m, 2H), 3.22 (t, *J* = 6.4 Hz, 2H), 1.50 ppm (t, *J* = 7.2 Hz, 3H).

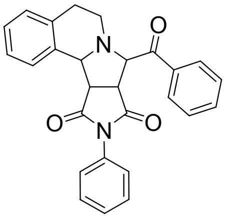

^{1}H NMR (400 MHz, $CDCl_3$): δ = 8.16 (d, 2 H, *J* = 8.0 Hz), 7.64–7.61 (m, 1H), 7.54–7.50 (m, 2 H), 7.42–7.38 (m, 3 H), 7.35–7.29 (m, 1 H), 7.24–7.20 (m , 1 H), 7.18–7.14 (m, 3H), 7.09 (d, 1 H, *J* = 8.0 Hz), 5.32 (s, 1 H), 4.87–4.85 (m, 1 H) , 4.05–4.03 (m, 1 H), 3.96–3.93 (m, 1 H), 3.33–3.31 (m, 1 H), 3.05–2.86 ppm (m, 3 H)

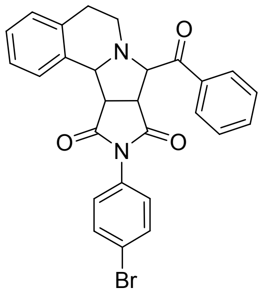

^{1}H NMR (400 MHz, $CDCl_3$): δ = 8.14 (d, 2 H, *J* = 8.0 Hz), 7.65–7.61 (m, 1H), 7.54–7.50 (m, 4 H), 7.39–7.37 (m, 1 H), 7.24–7.20 (m, 1 H), 7.17–7.15 (m , 1 H), 7.09–7.05 (m, 3H), 5.30 (s, 1 H), 4.84–4.82 (m, 1 H) , 4.04–4.02 (m, 1 H), 3.94–3.91 (m, 1 H), 3.29–3.28 (m, 1 H), 3.02–2.90 ppm (m, 3 H).

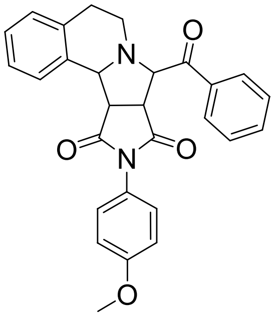

^{1}H NMR (400 MHz, $CDCl_3$): δ = 8.15 (d, 2 H, *J* = 8.0 Hz), 7.64–7.60 (m, 1H), 7.53–7.50 (m, 2 H), 7.39–7.38 (m, 1 H), 7.23–7.14 (m, 2 H), 7.08–7.05 (m, 3H), 6.90–6.88 (m, 2 H), 5.34 (s, 1 H), 4.91–4.90 (m, 1 H) , 4.03–3.93 (m, 1 H), 3.89–3.85 (m, 1 H), 3.77 (s, 3H), 3.34–3.30 (m, 1 H), 3.01–2.90 ppm (m, 3 H).

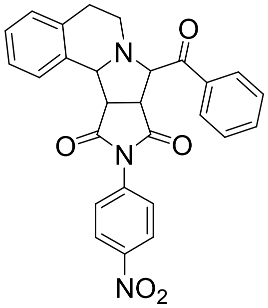

^{1}H NMR (400 MHz, $CDCl_3$): δ = 8.20 (d, 2 H, *J* = 8.0 Hz), 8.07 (d, 2 H, *J* = 4.0 Hz) 7.59–7.55 (m, 1H), 7.49–7.45 (m, 2 H), 7.39–7.32 (m, 3 H), 7.23–7.14 (m, 2 H), 7.03–7.02 (m, 1H), 5.24 (s, 1 H), 4.75–4.74 (m, 1 H) , 4.03–4.01 (m, 1 H), 3.91–3.89 (m, 1 H), 3.21–3.19 (m, 1 H), 2.94–2.82 ppm (m, 3 H).

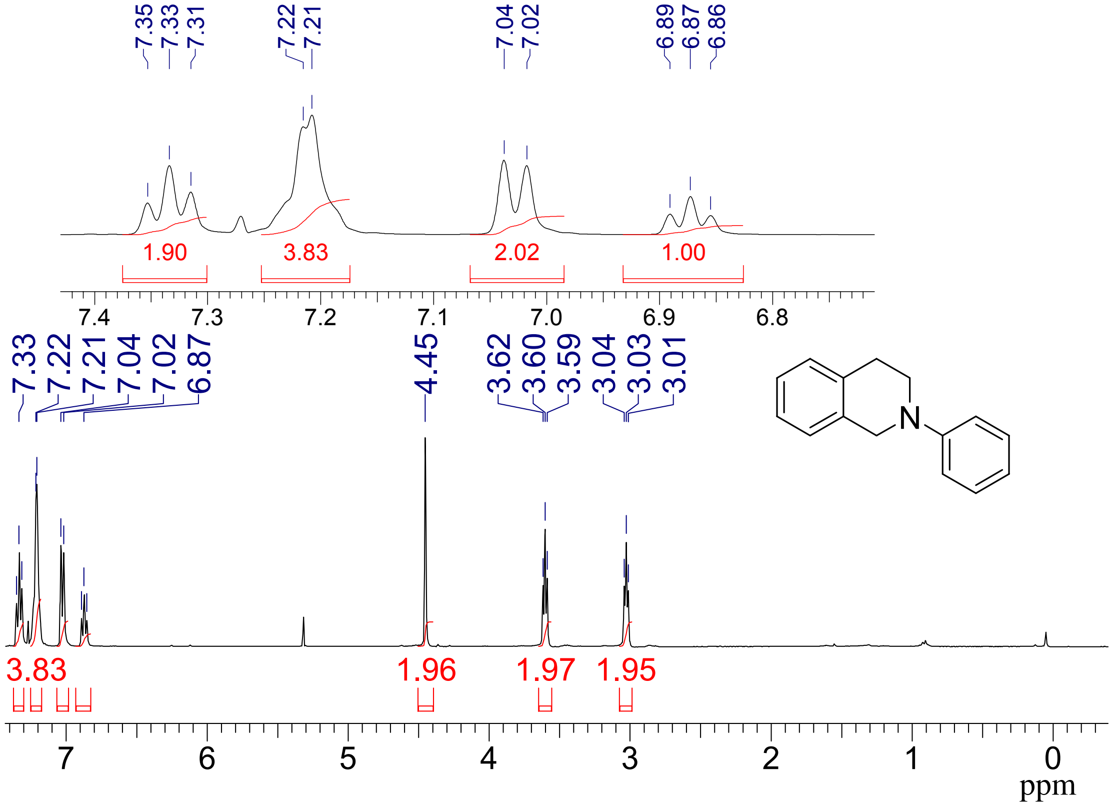

Figure S1. ^{1}H NMR of **1a** (400 MHz, $CDCl_3$).

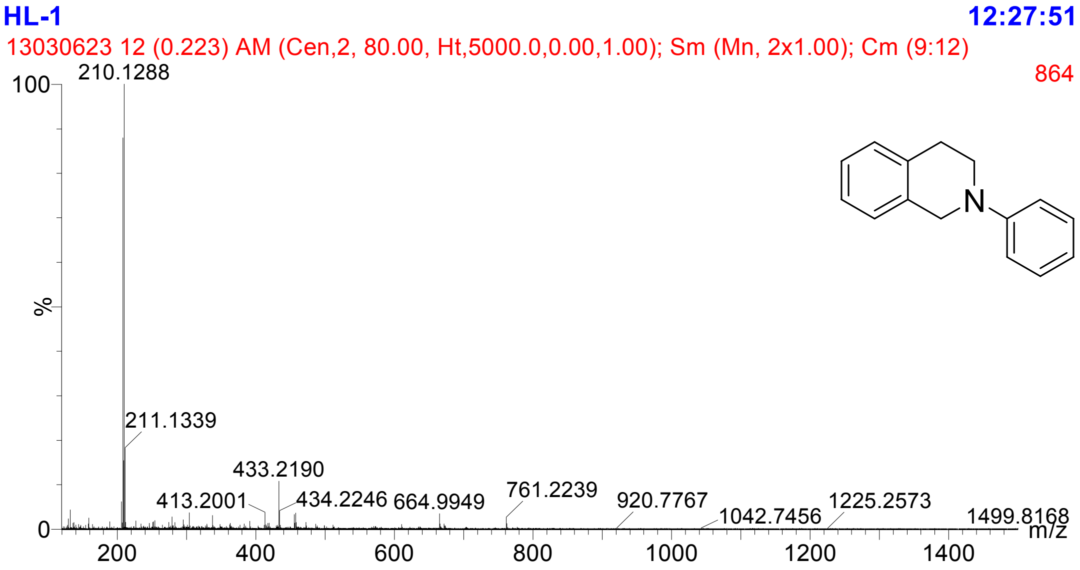

Figure S2. TOF HRMS ESI$^+$ of **1a**.

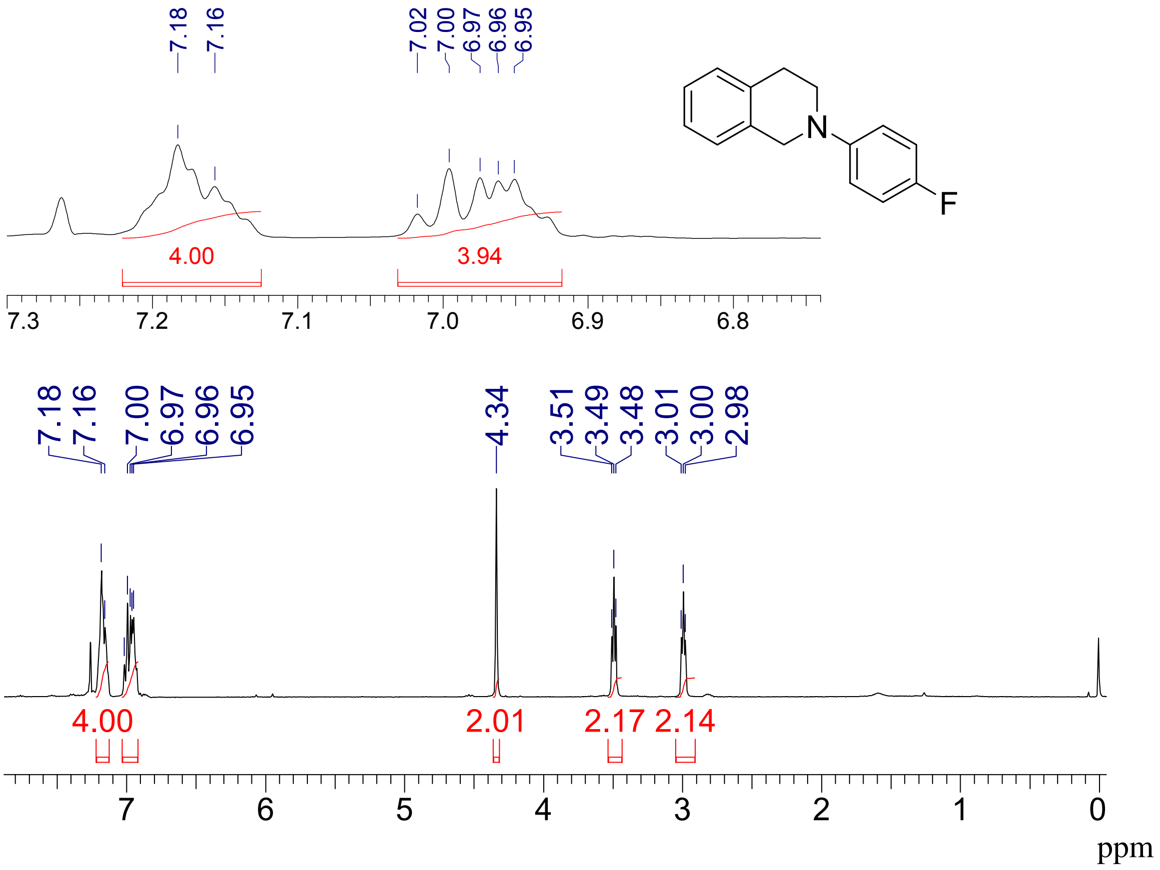

Figure S3. ^{1}H NMR of **1b** (400 MHz, $CDCl_3$).

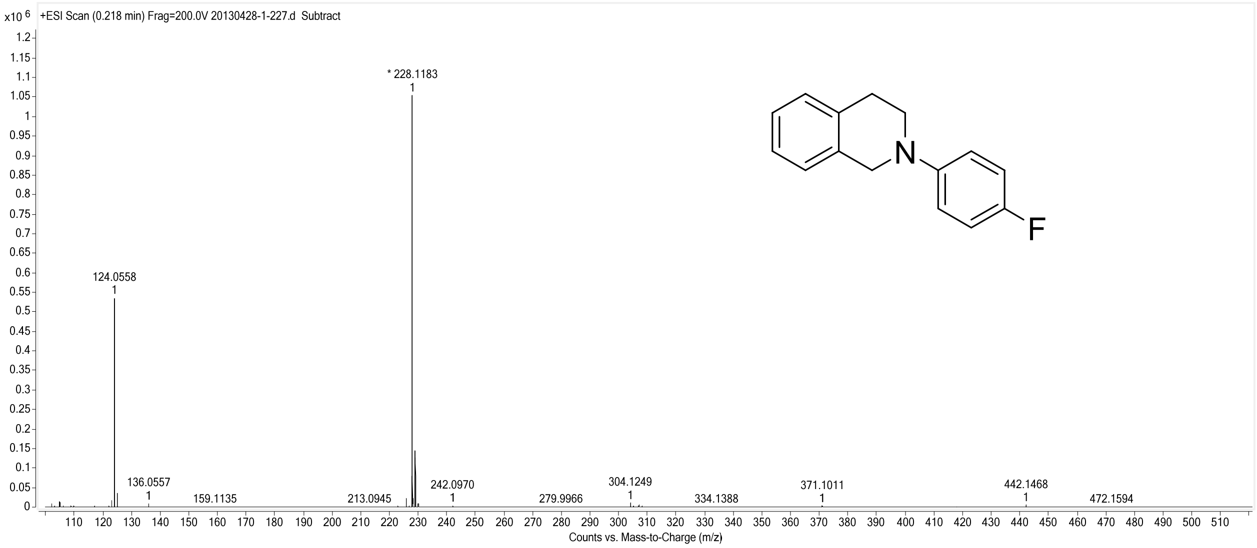

Figure S4. TOF HRMS ESI$^+$ of **1b**.

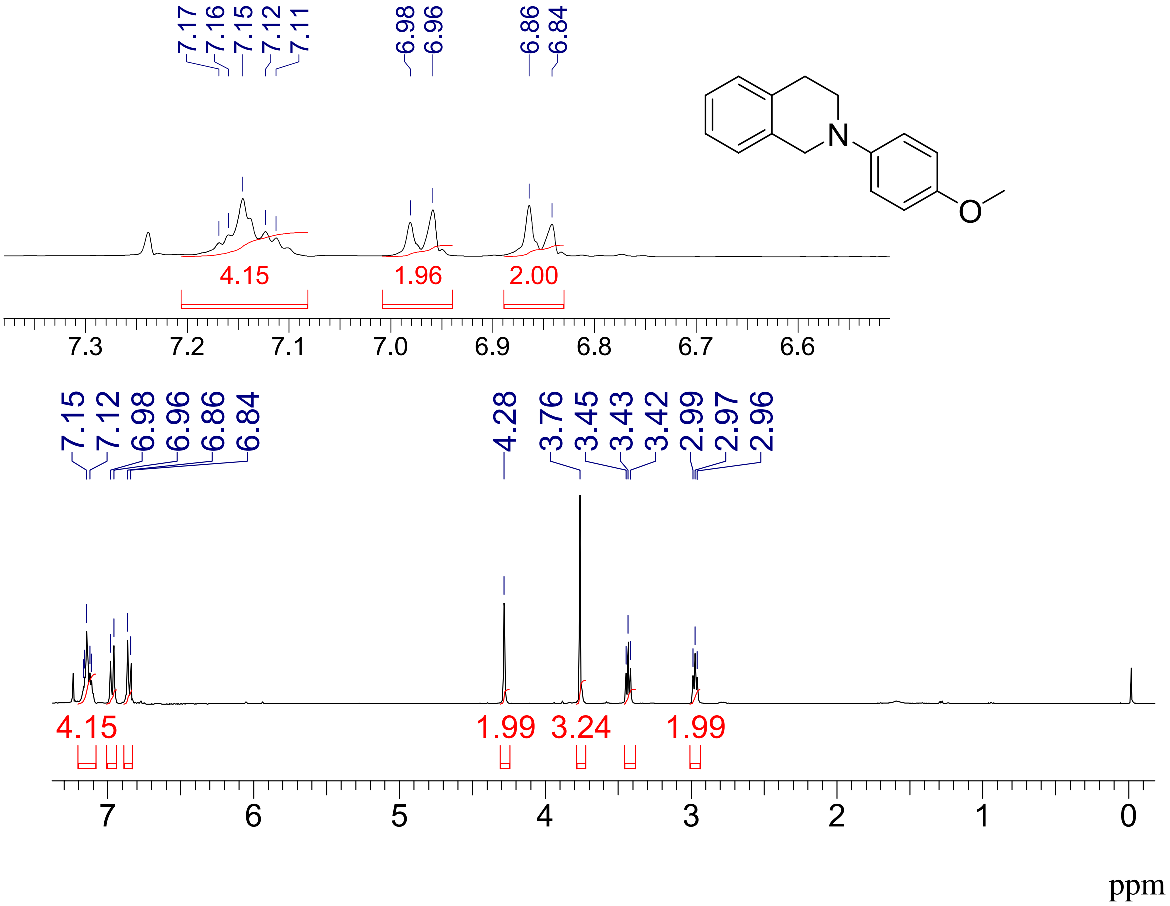

Figure S5. ^{1}H NMR of **1c** (400 MHz, $CDCl_3$).

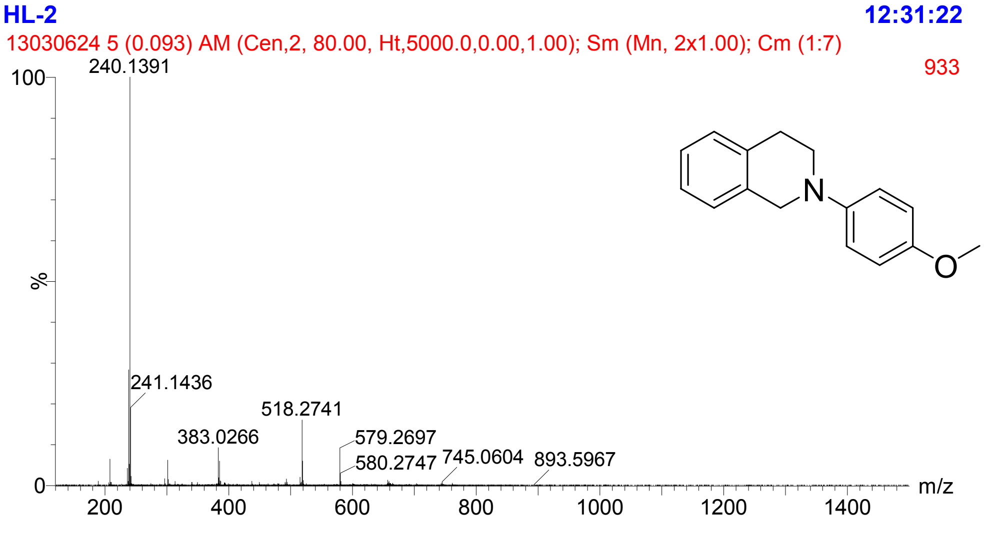

Figure S6. TOF HRMS ESI$^+$ of **1c**.

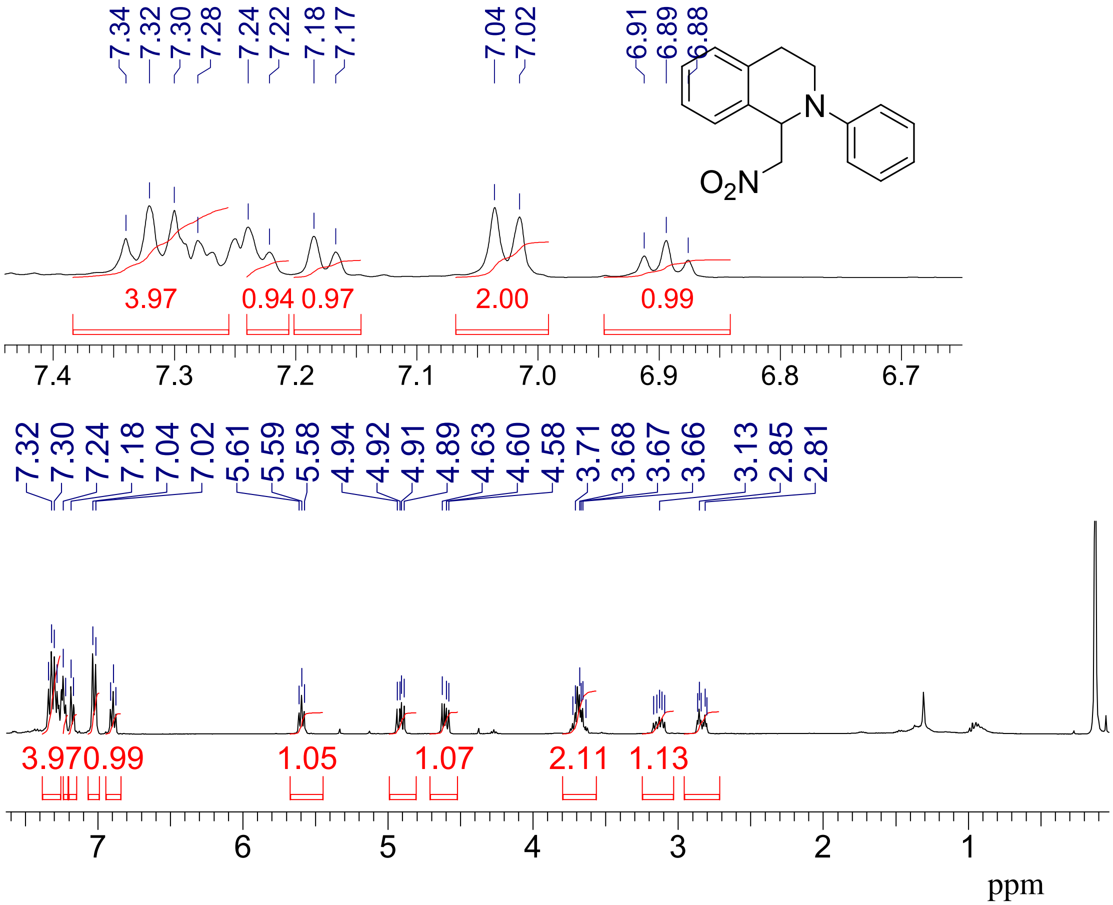

Figure S7. ^{1}H NMR of **2ad** (400 MHz, CDCl$_3$).

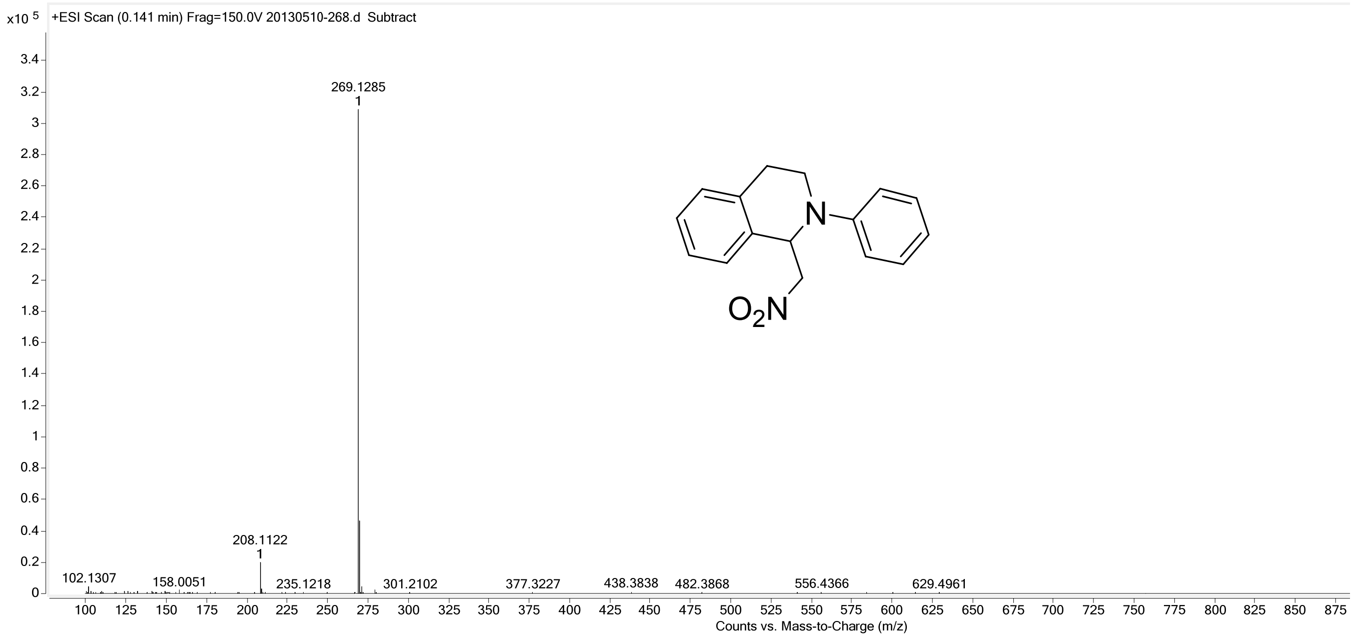

Figure S8. TOF HRMS ESI$^+$ of **2ad**.

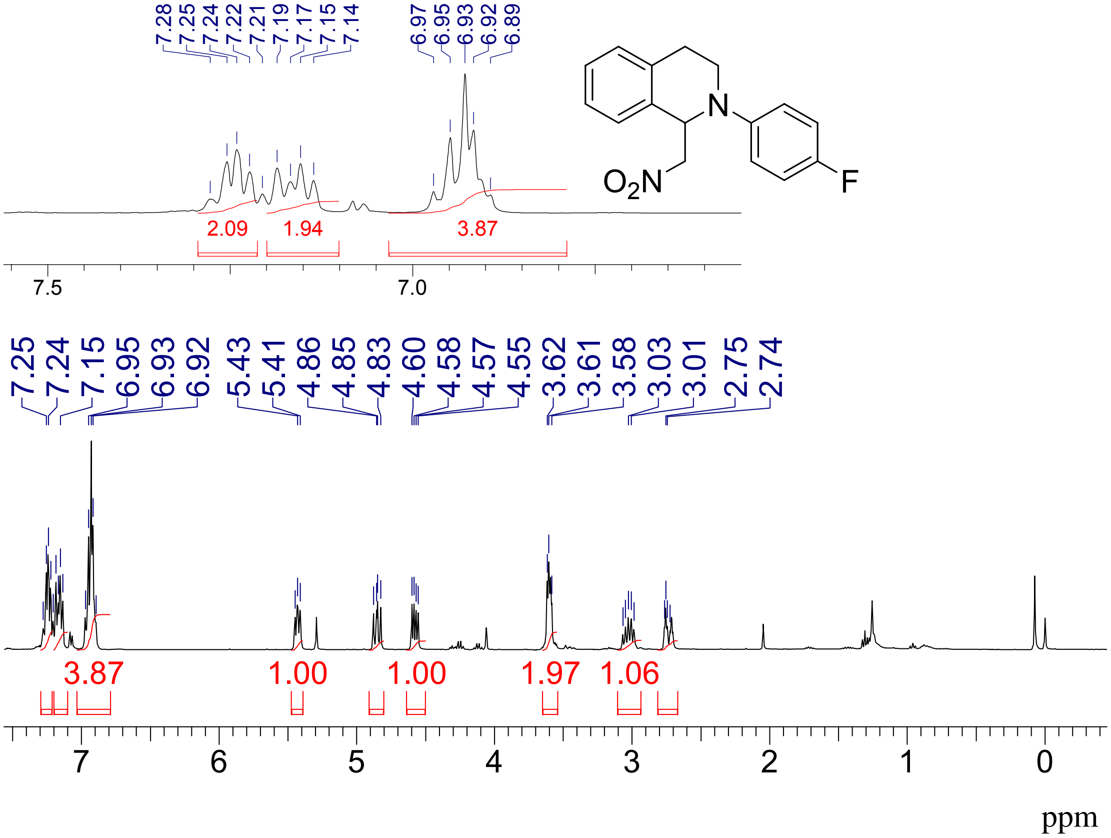

Figure S9. ^{1}H NMR of **2bd** (400 MHz, CDCl$_3$).

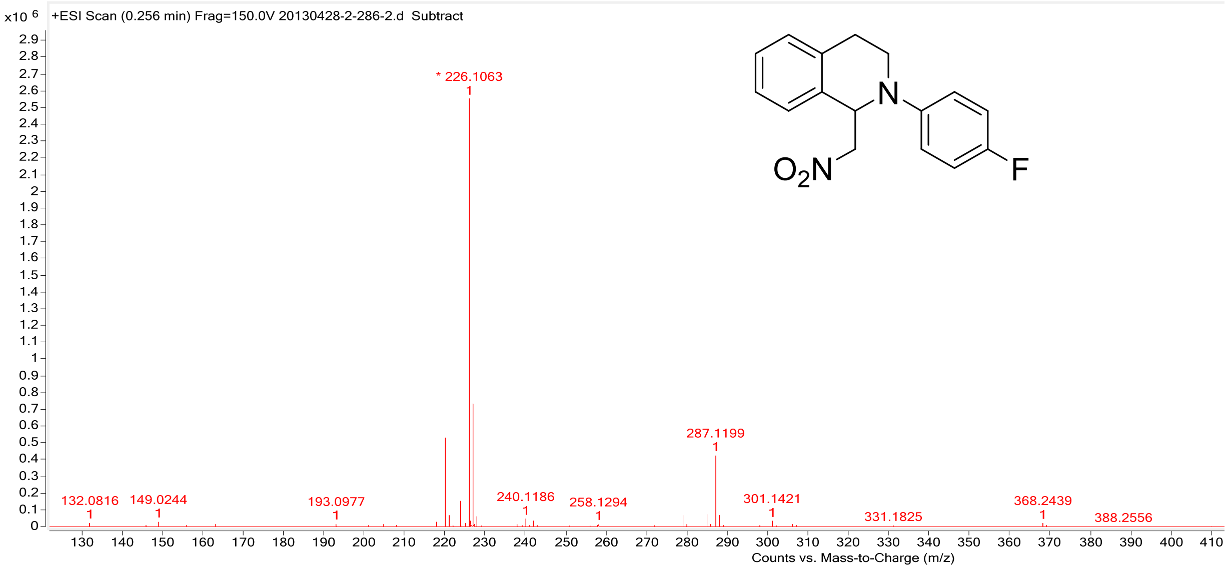

Figure S10. TOF HRMS ESI$^+$ of **2bd**.

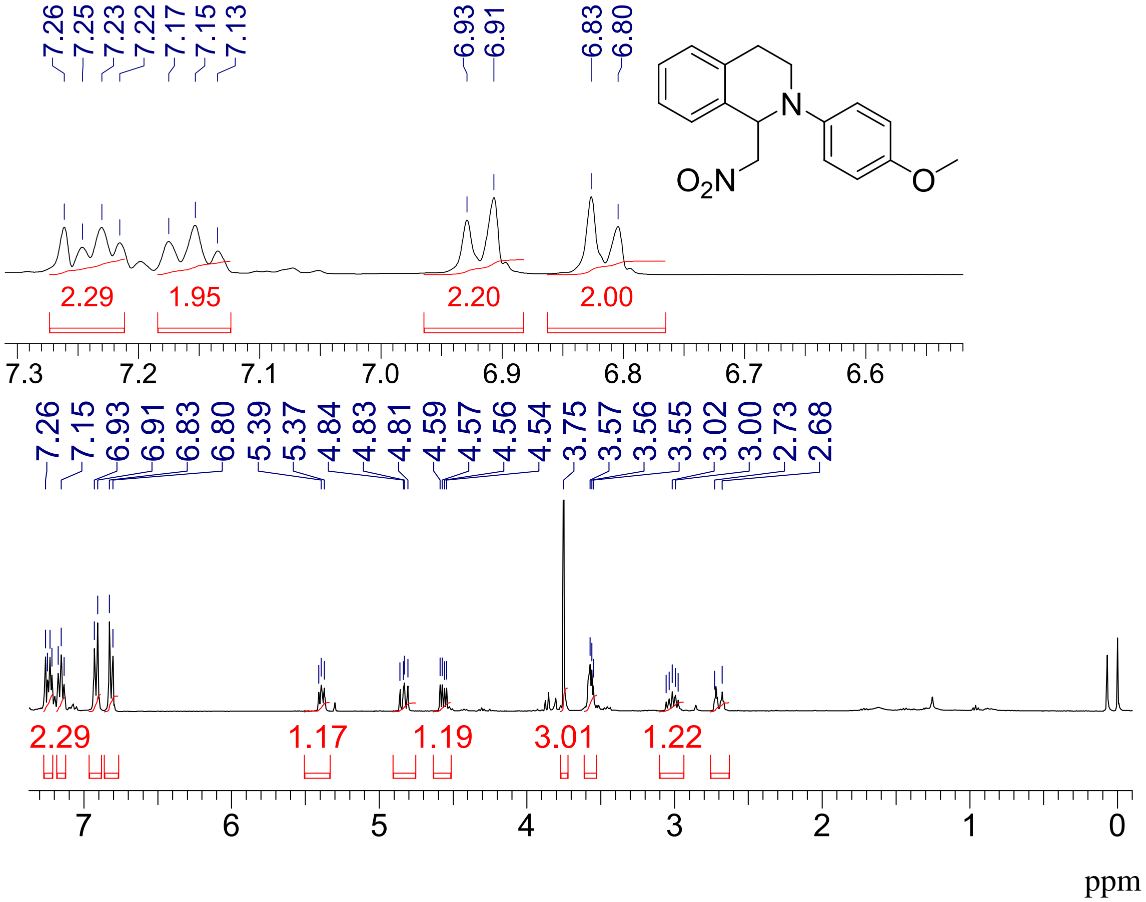

Figure S11. ^{1}H NMR of **2cd** (400 MHz, CDCl$_3$).

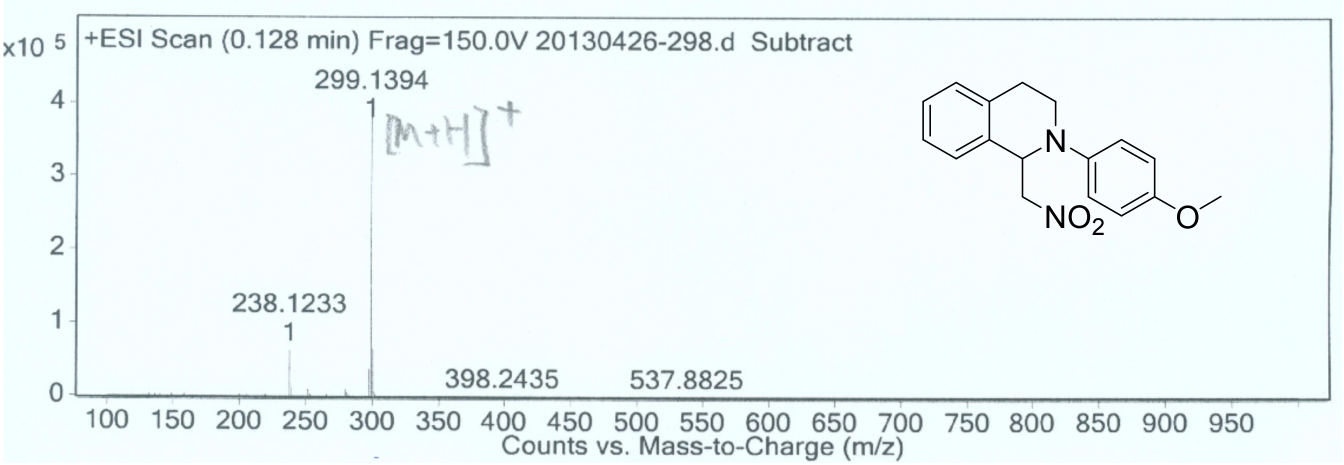

Figure S12. TOF HRMS ESI$^+$ of **2cd**.

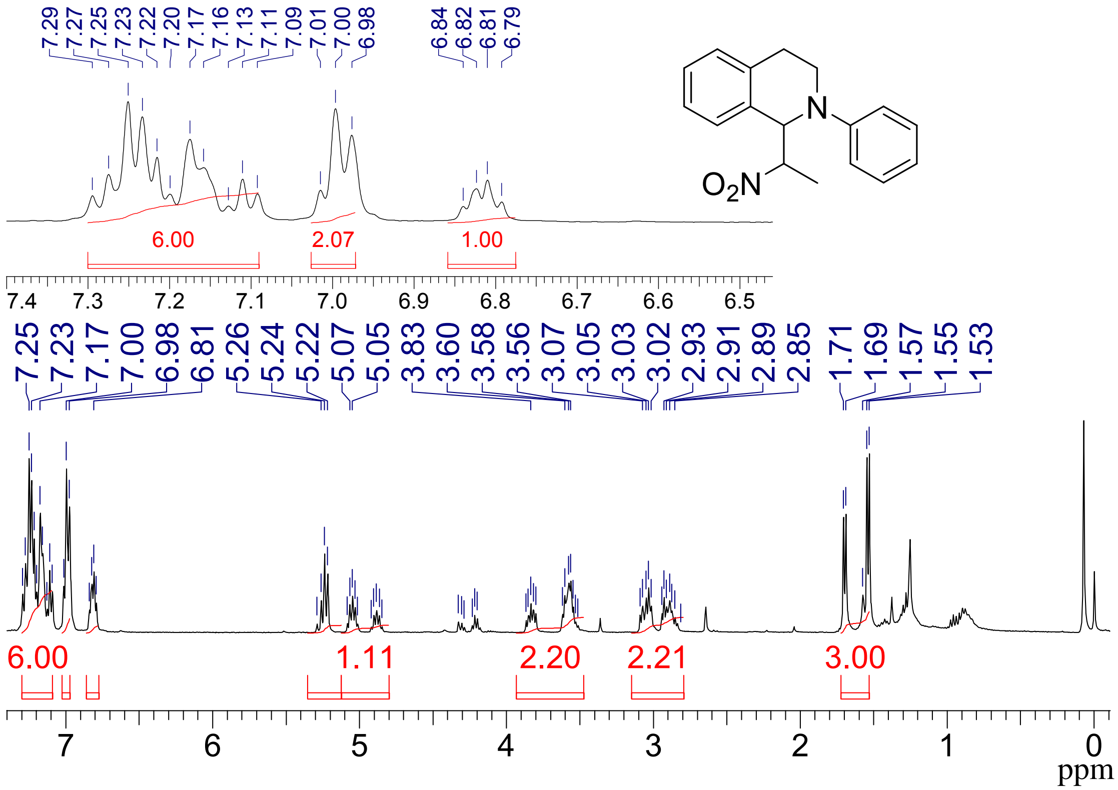

Figure S13. ^{1}H NMR of **2ae** (400 MHz, CDCl₃).

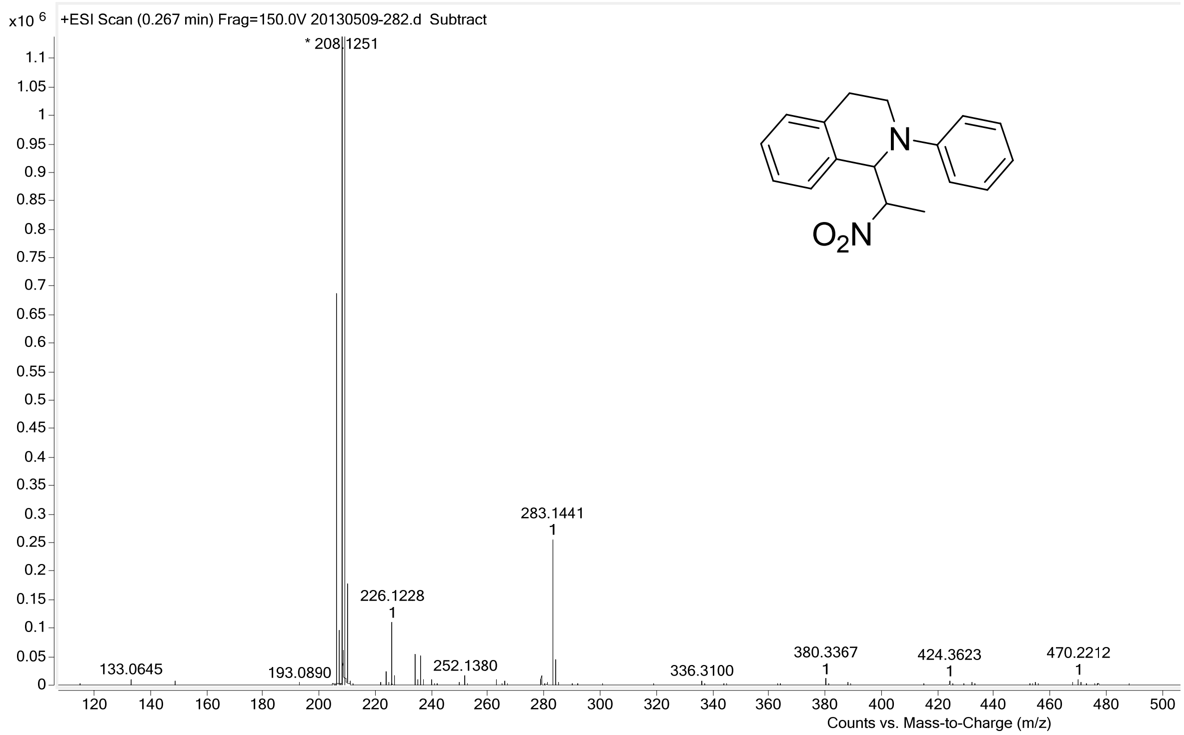

Figure S14. TOF HRMS ESI$^+$ **2ae.**

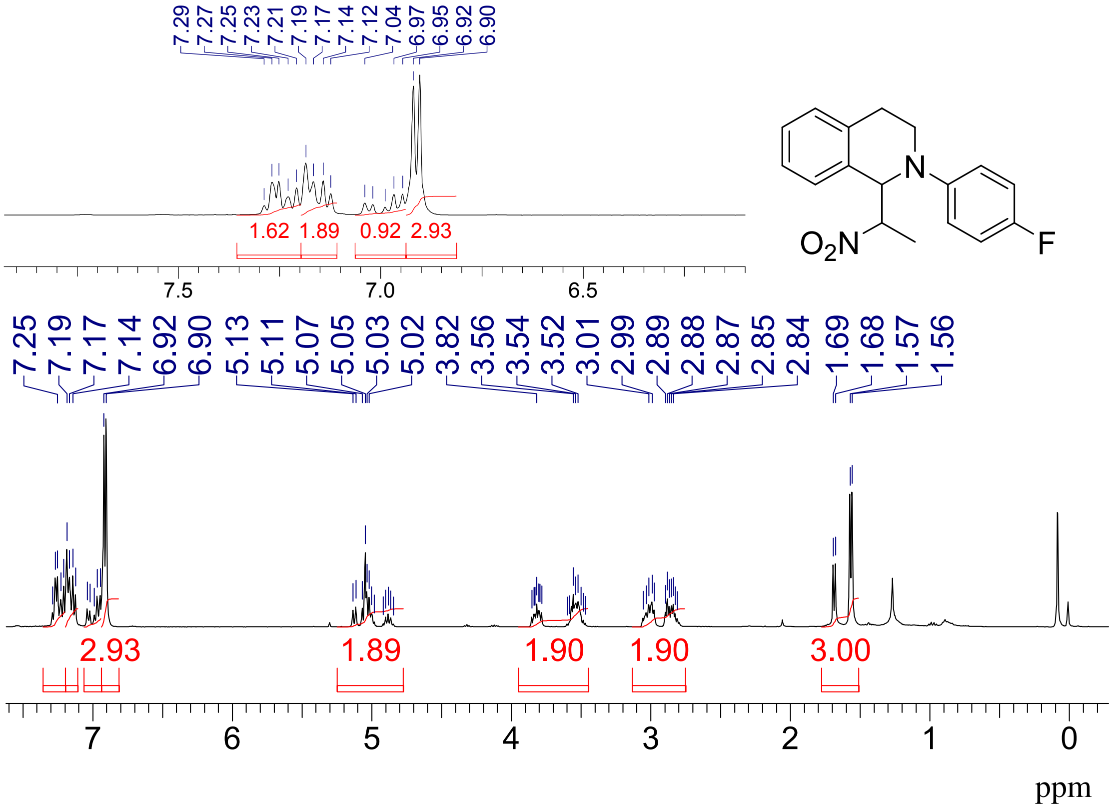

Figure S15. ^{1}H NMR of **2be** (400 MHz, $CDCl_3$).

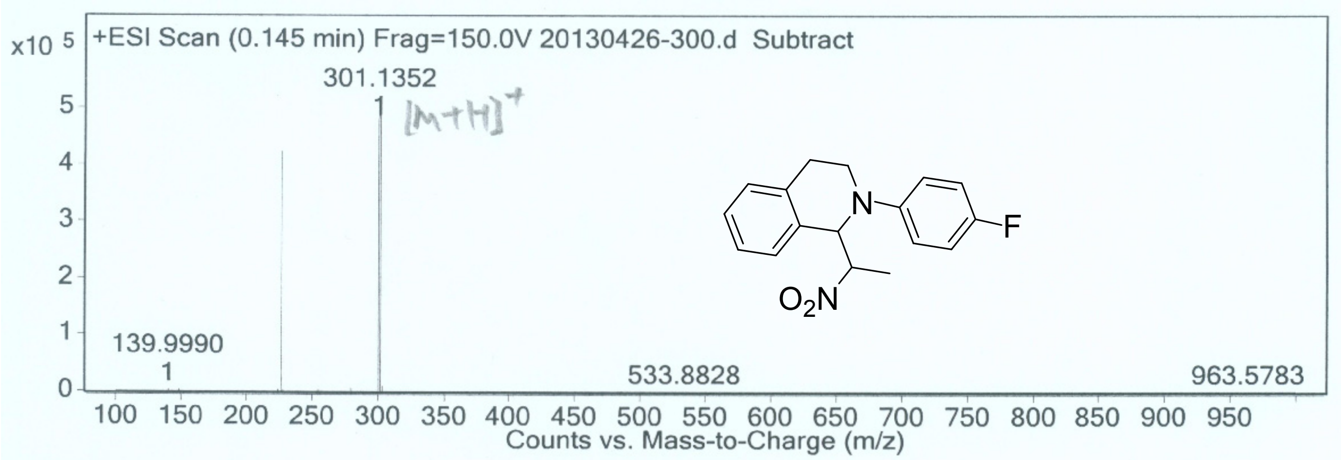

Figure S16. TOF HRMS ESI$^+$ **2be.**

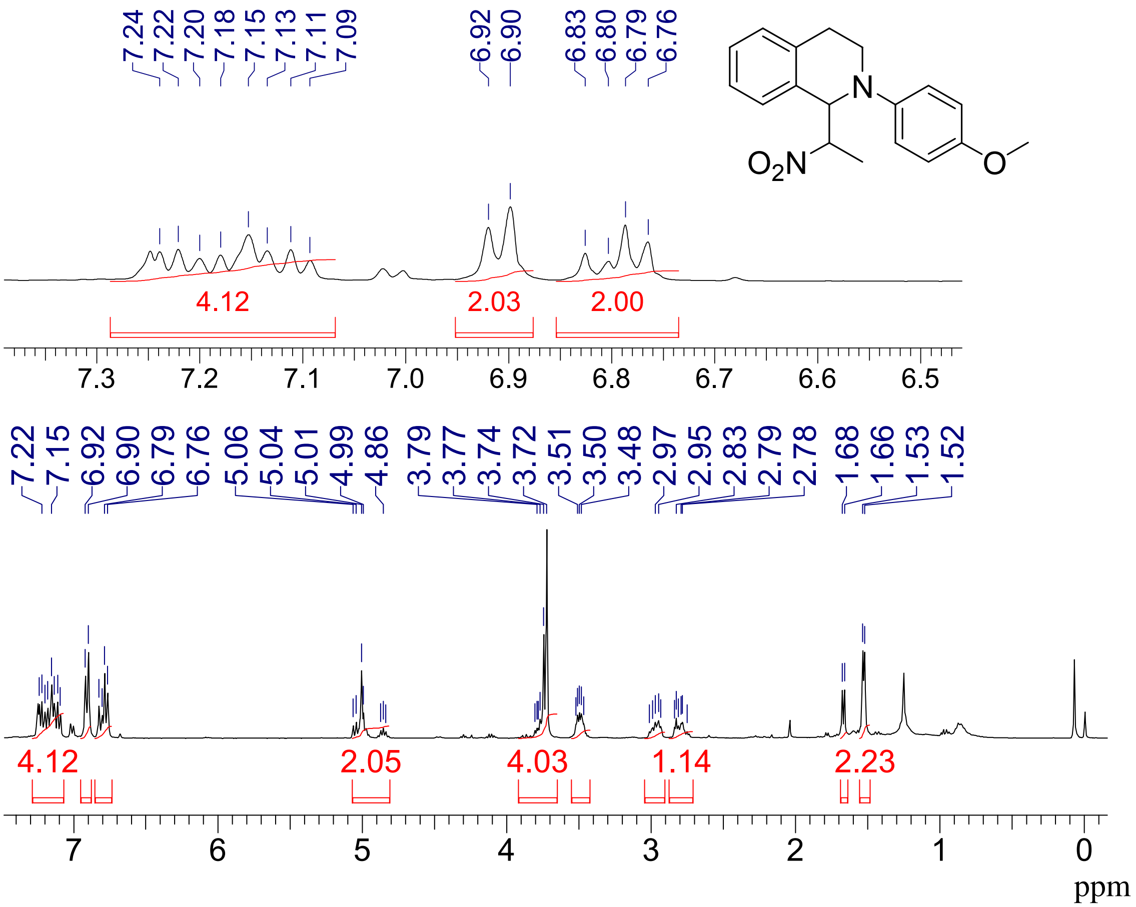

Figure S17. ^{1}H NMR of **2ce** (400 MHz, CDCl$_3$).

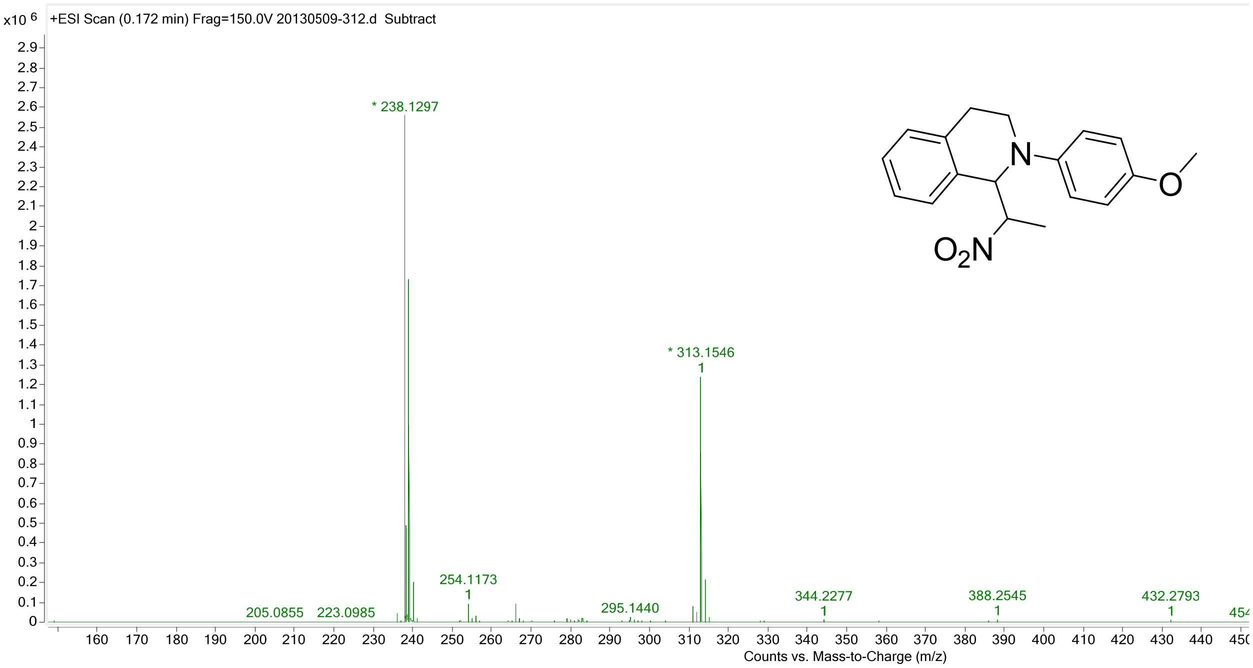

Figure S18. TOF HRMS ESI$^+$ **2ce**.

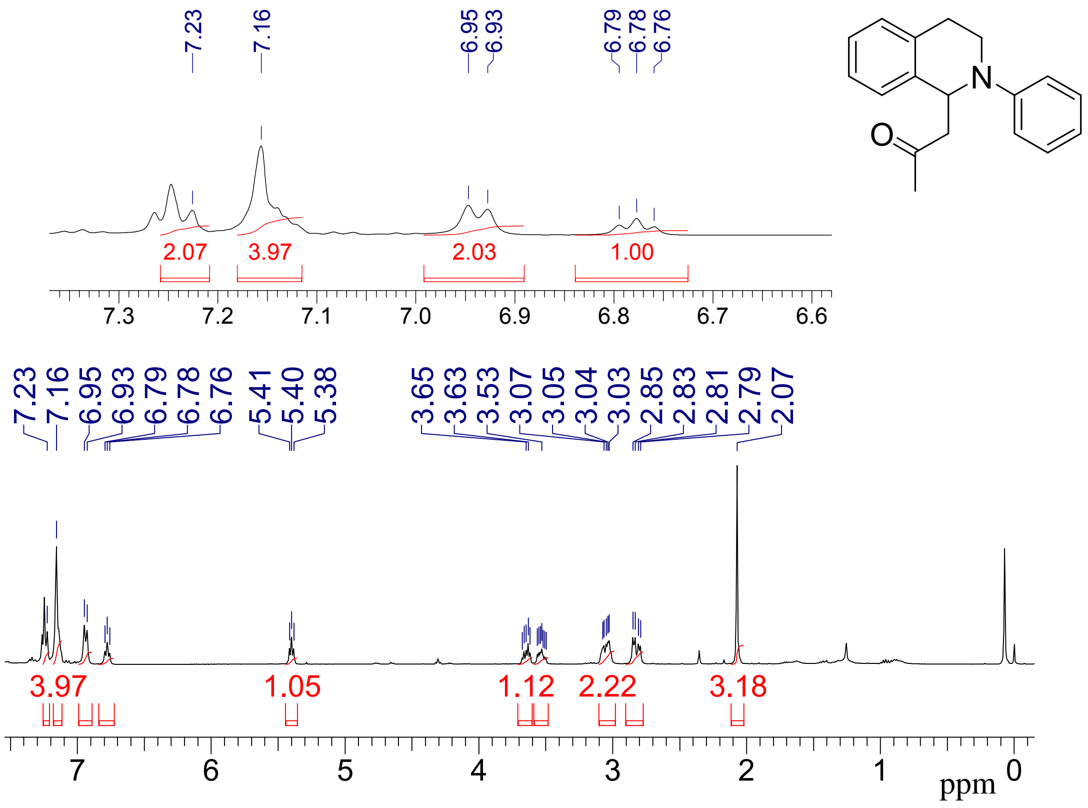

Figure S19. ^{1}H NMR of **2af** (400 MHz, $CDCl_3$).

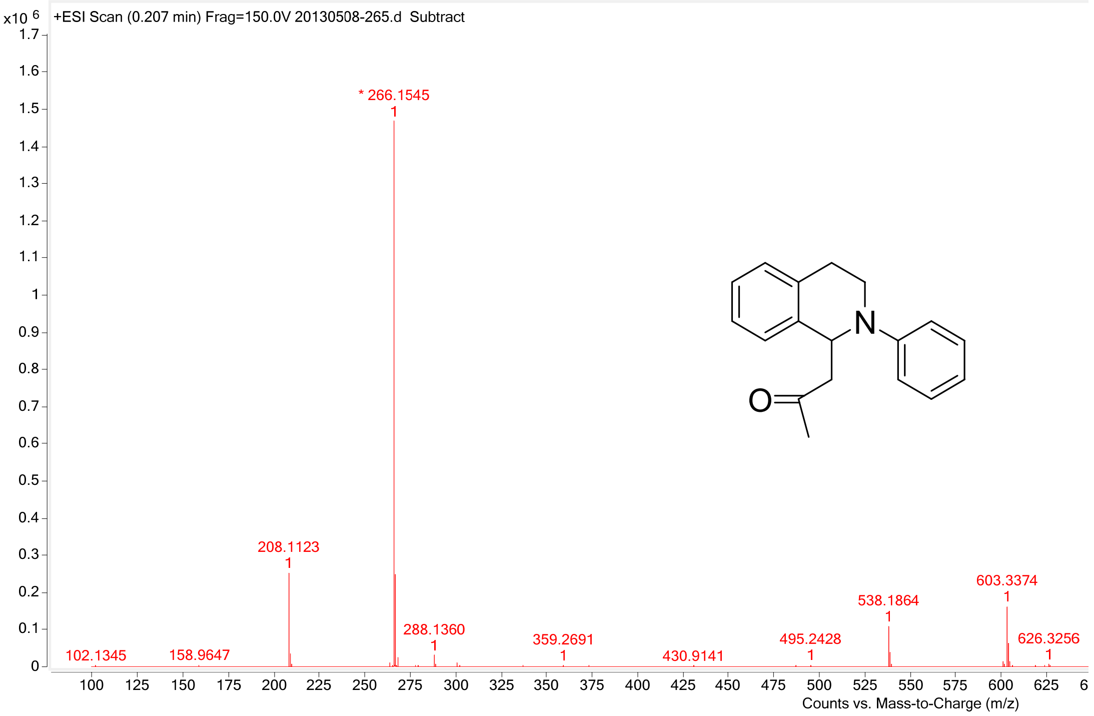

Figure S20. TOF HRMS ESI$^+$ **2af**.

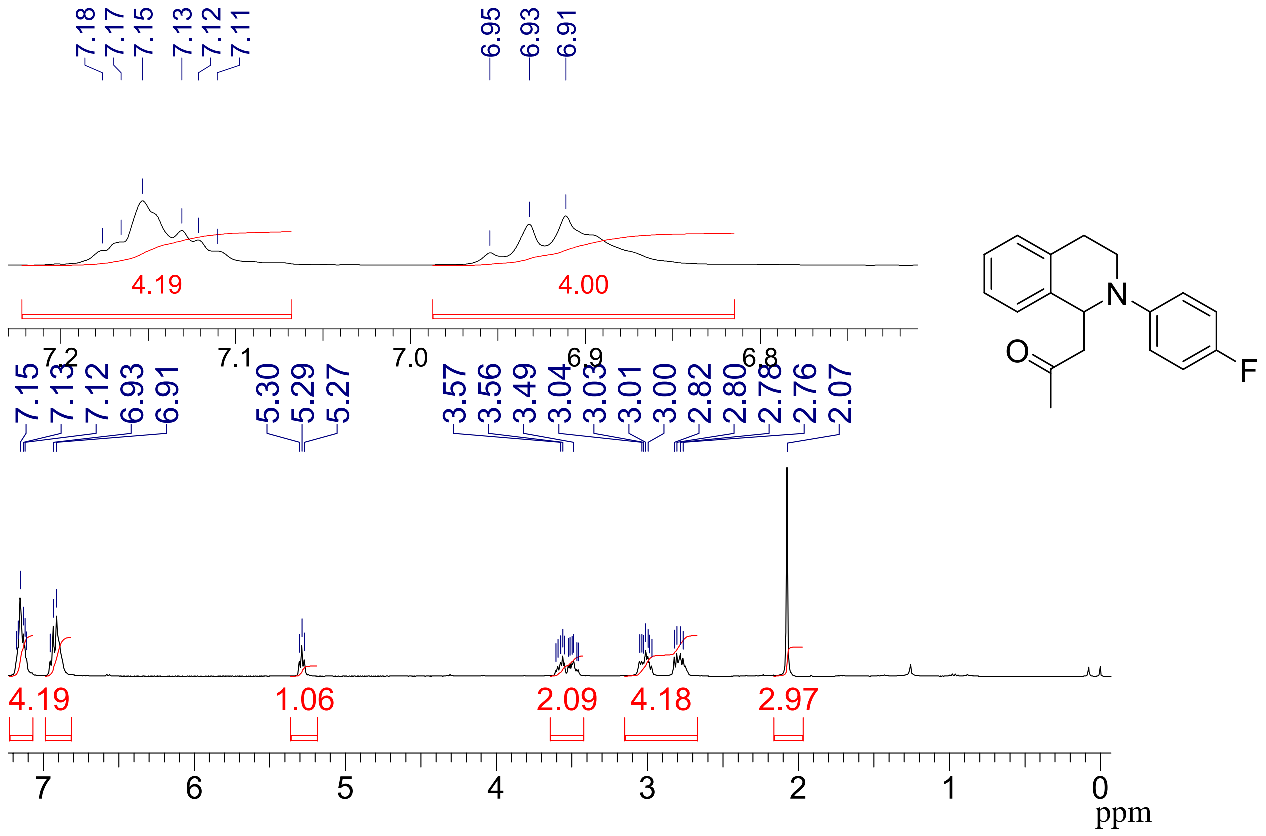

Figure S21. ^{1}H NMR of 2bf (400 MHz, CDCl$_3$).

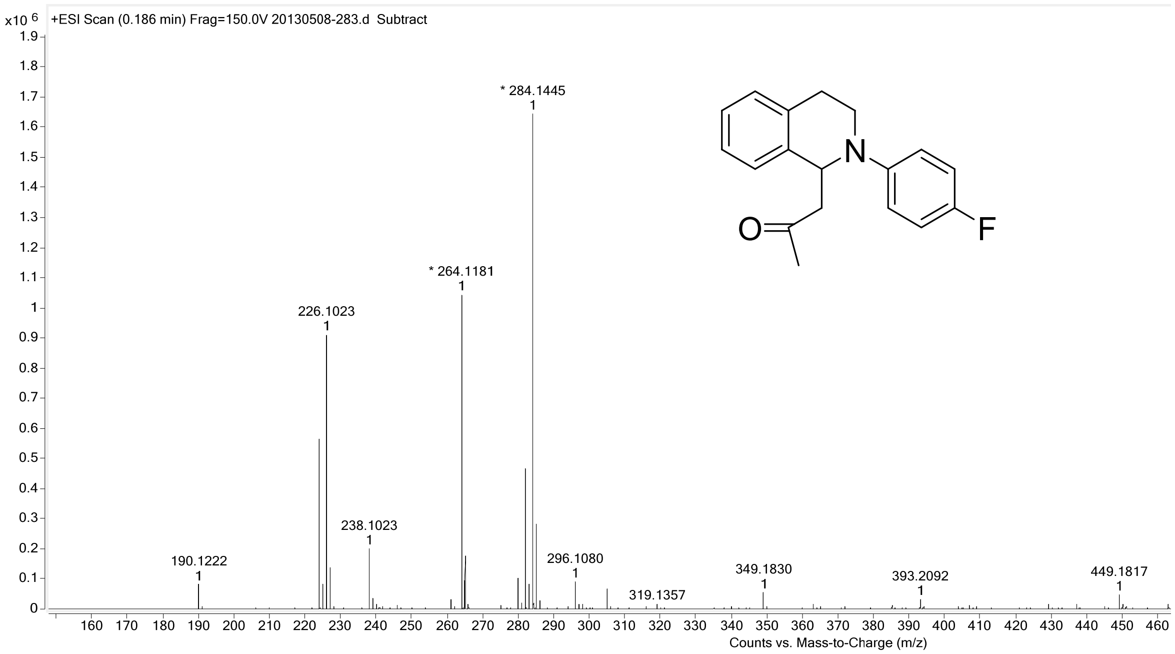

Figure S22. TOF HRMS ESI$^+$ **2bf**.

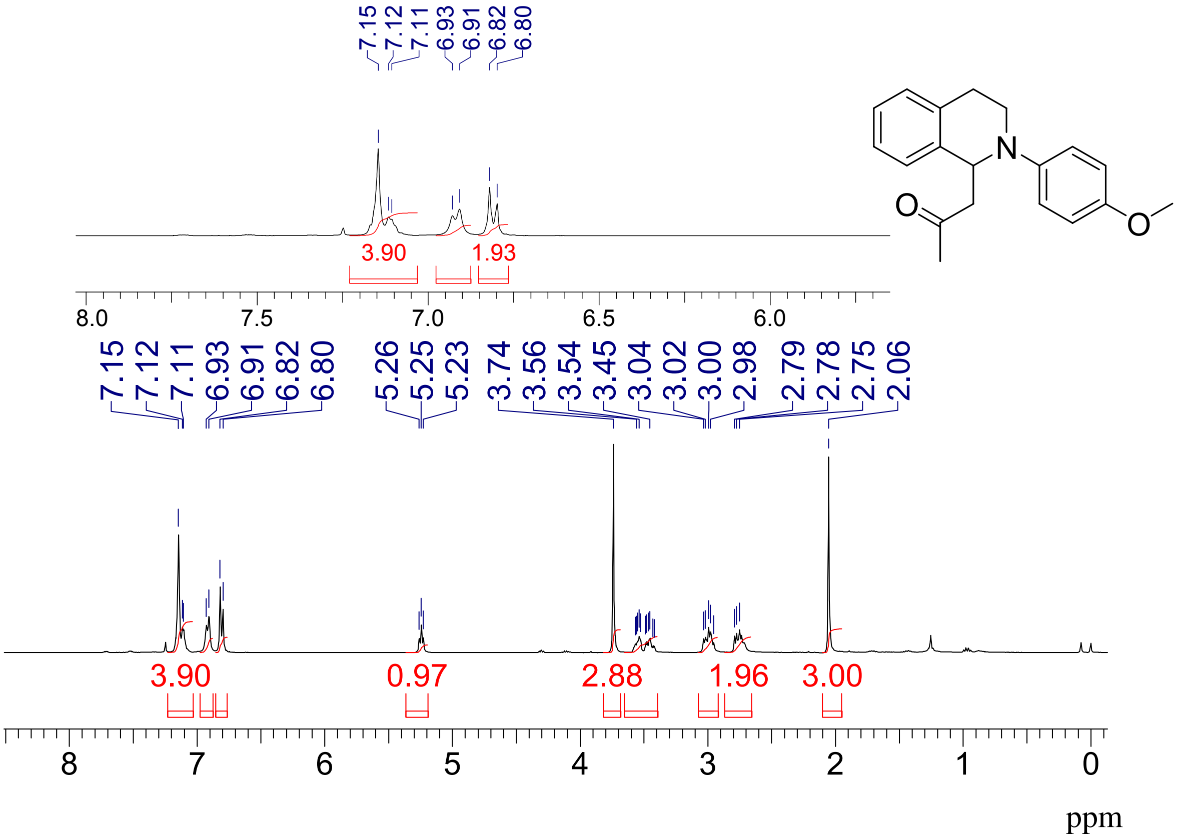

Figure S23. ^{1}H NMR of **2cf** (400 MHz, CDCl$_3$).

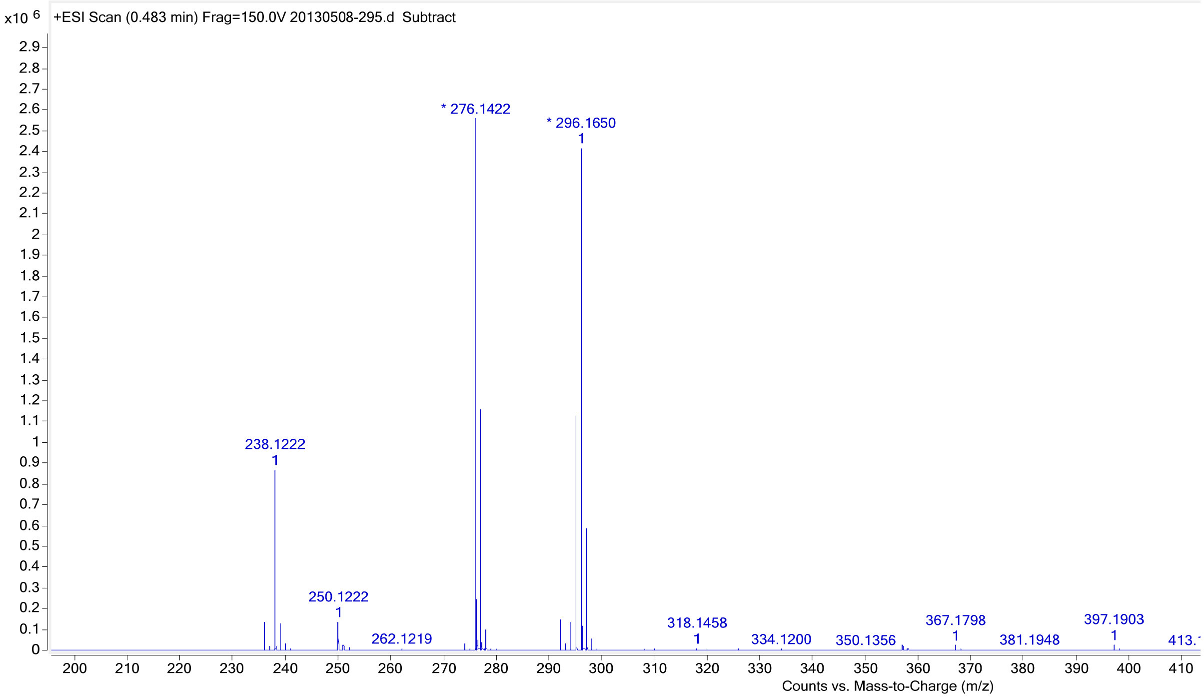

Figure S24. TOF HRMS ESI$^+$ **2cf**.

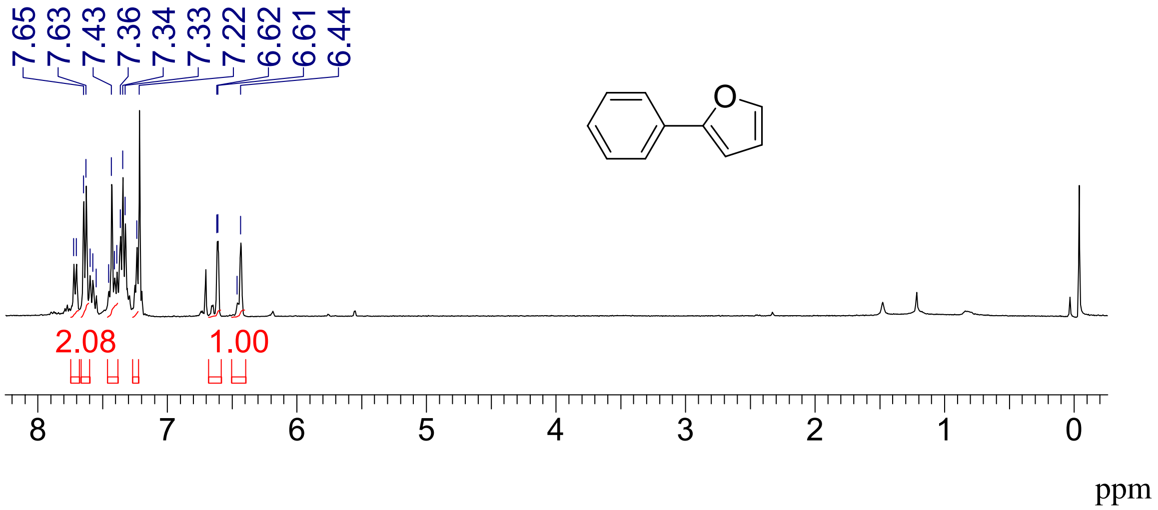

Figure S25. ^{1}H NMR of **2mr** (400 MHz, CDCl$_3$).

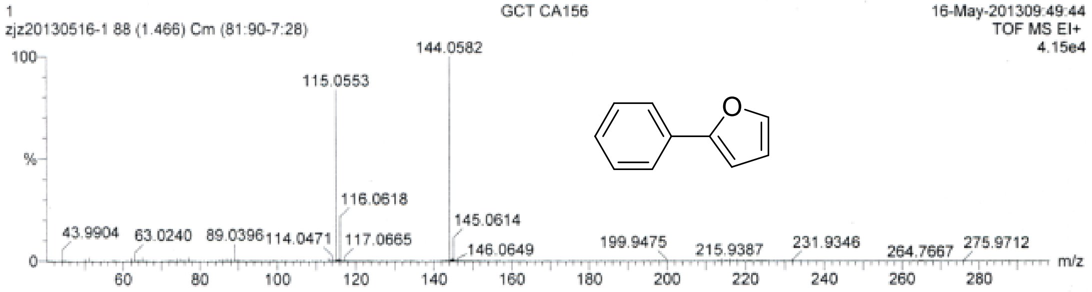

Figure S26. TOF HRMS EI$^+$ of **2mr.**

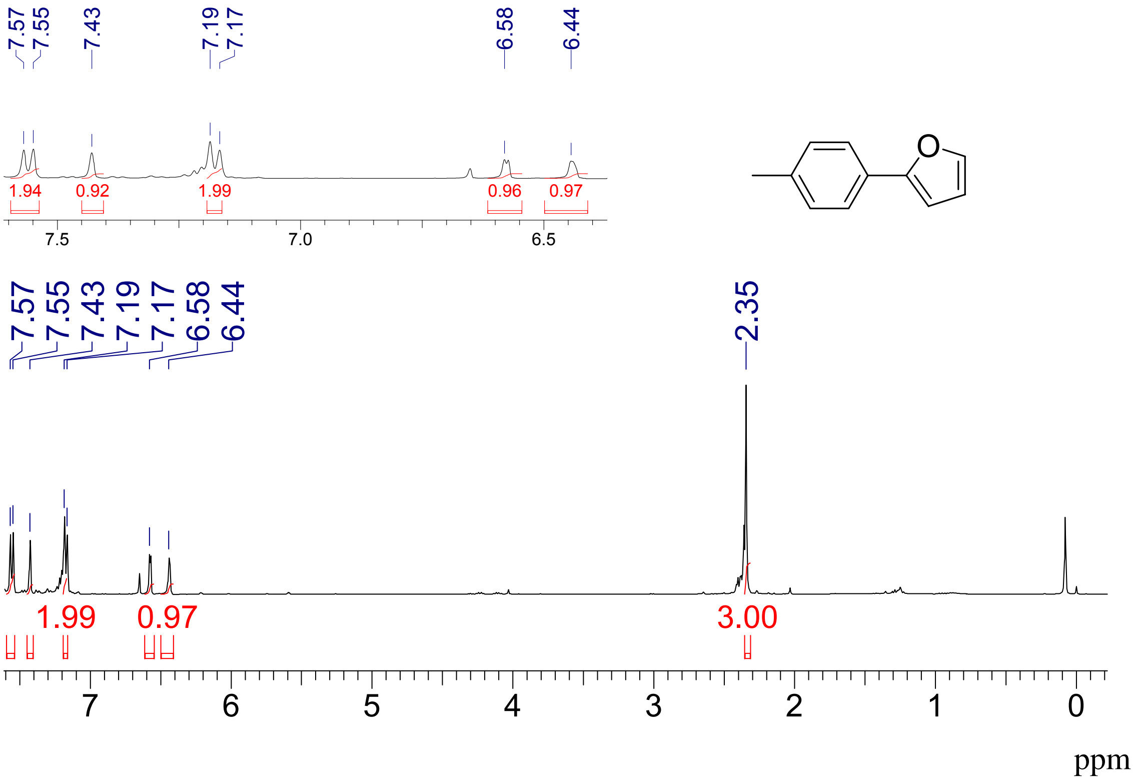

Figure S27. ^{1}H NMR of **2nr** (400 MHz, $CDCl_3$).

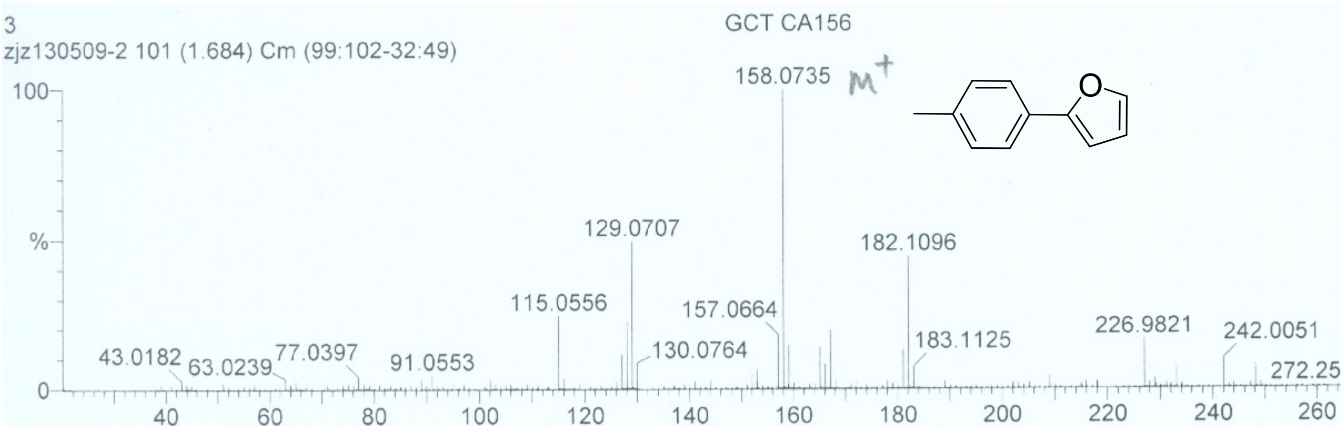

Figure S28. TOF HRMS EI^+ of **2nr.**

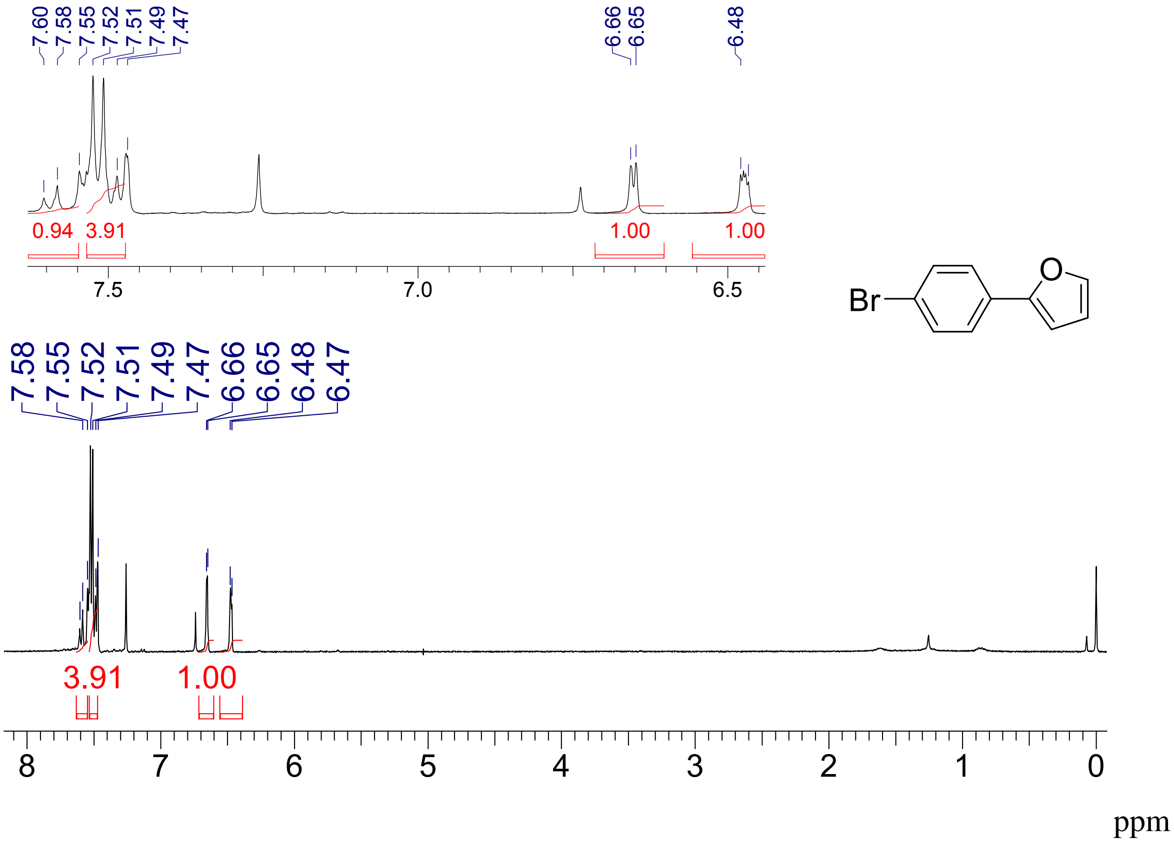

Figure S29. ^{1}H NMR of **2or** (400 MHz, CDCl$_3$).

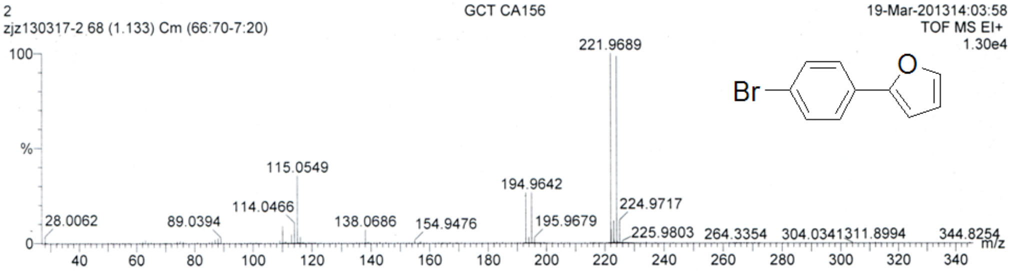

Figure S30. TOF HRMS EI$^+$ of **2or.**

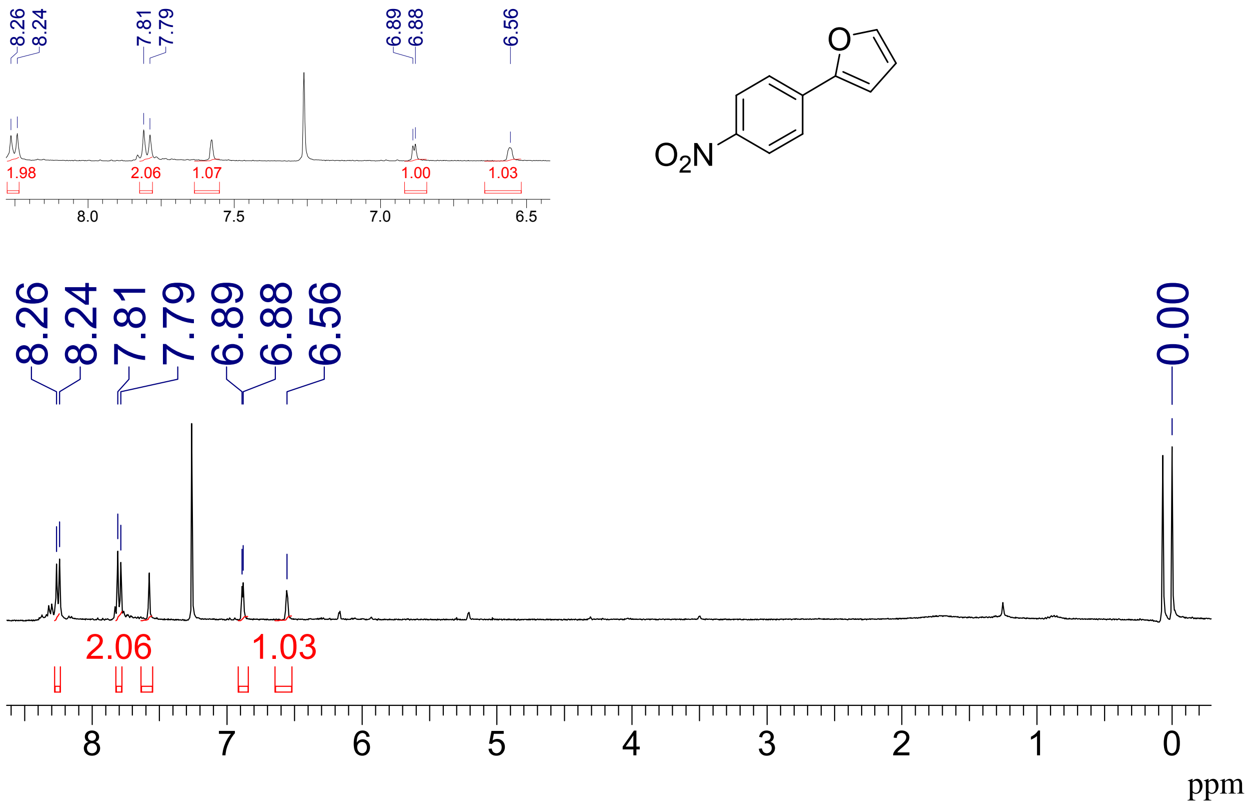

Figure S31. ^{1}H NMR of **2pr** (400 MHz, $CDCl_3$).

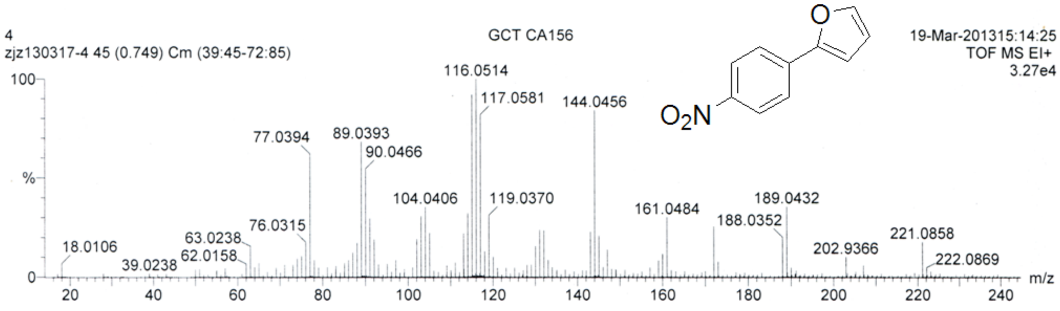

Figure S32. TOF HRMS EI$^+$ of **2pr.**

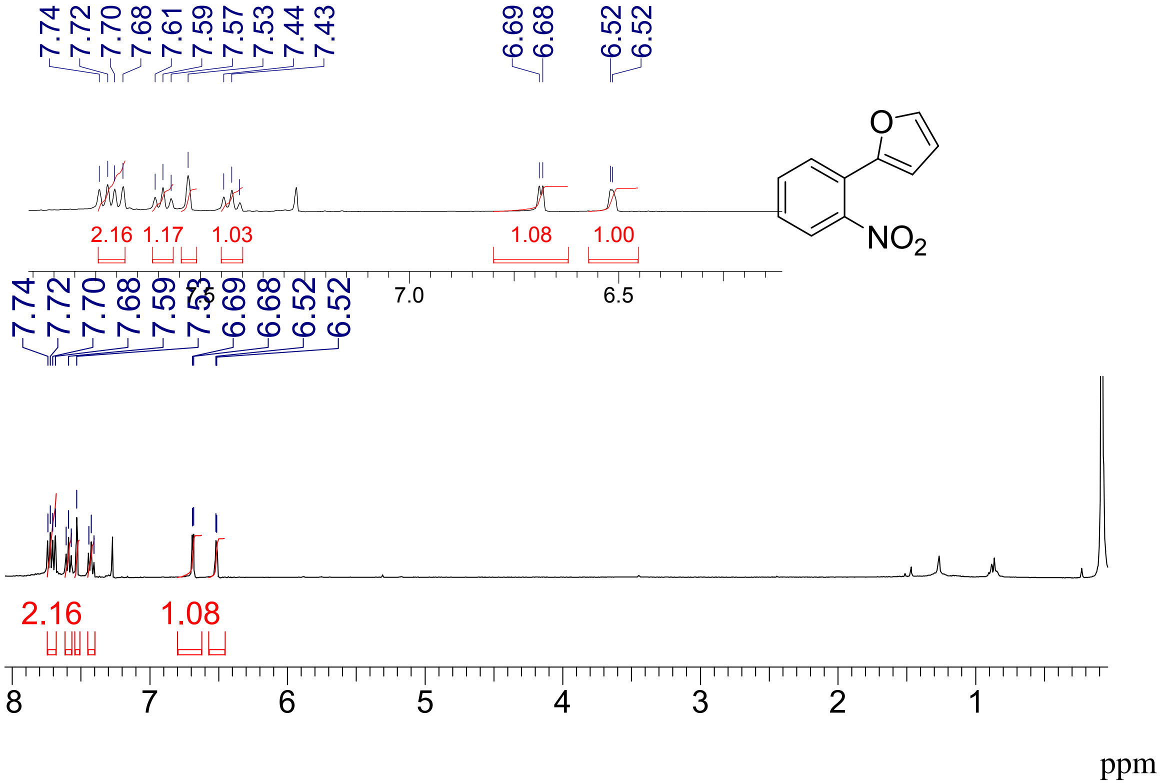

Figure S33. ^{1}H NMR of **2qr** (400 MHz, $CDCl_3$).

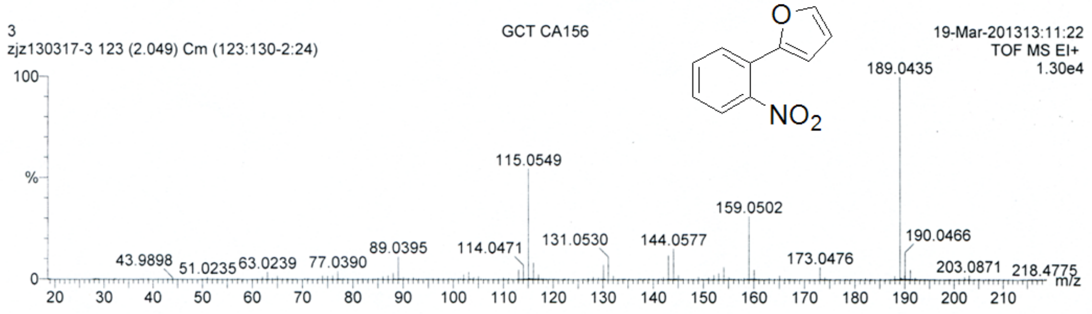

Figure S34. TOF HRMS EI$^+$ of **2qr.**

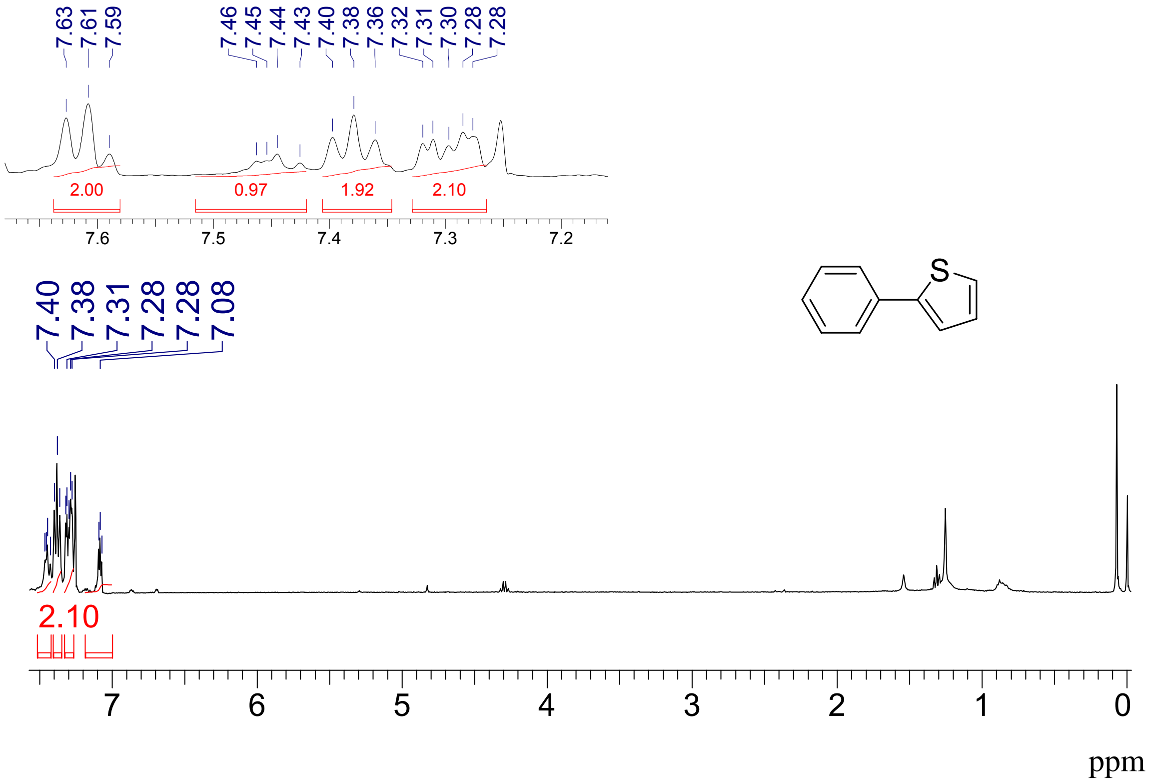

Figure S35. ^{1}H NMR of **2ms** (400 MHz, $CDCl_3$).

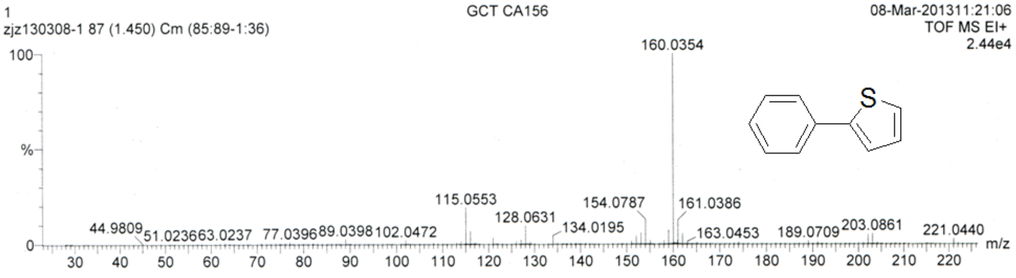

Figure S36. TOF HRMS EI$^+$ of **2ms.**

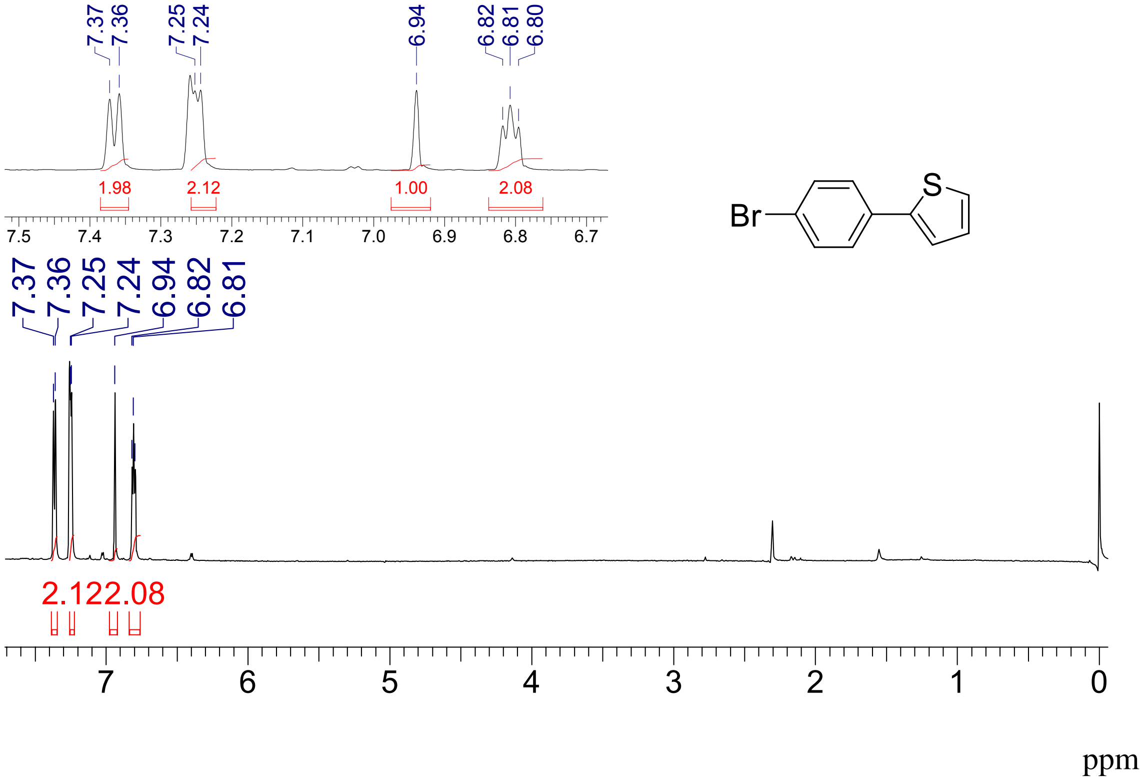

Figure S37. ^{1}H NMR of **2os** (400 MHz, $CDCl_3$).

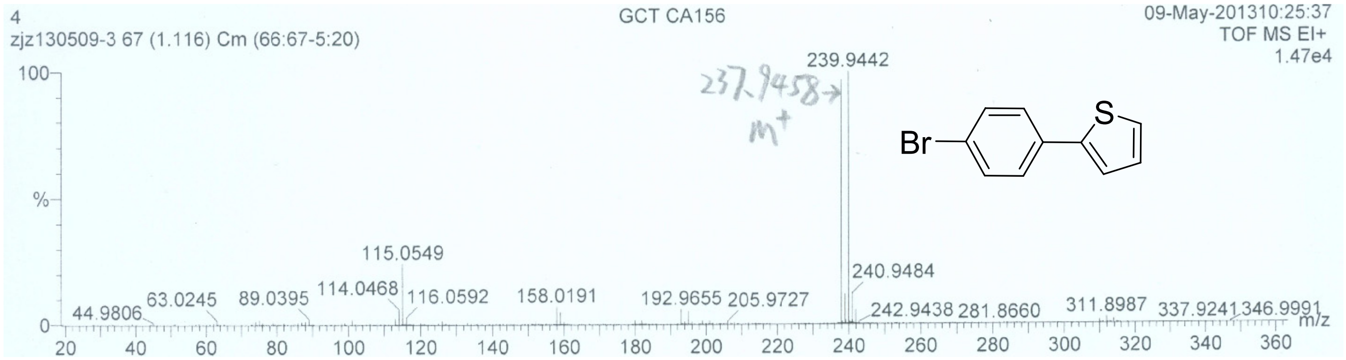

Figure S38. TOF HRMS EI$^+$ of **2os.**

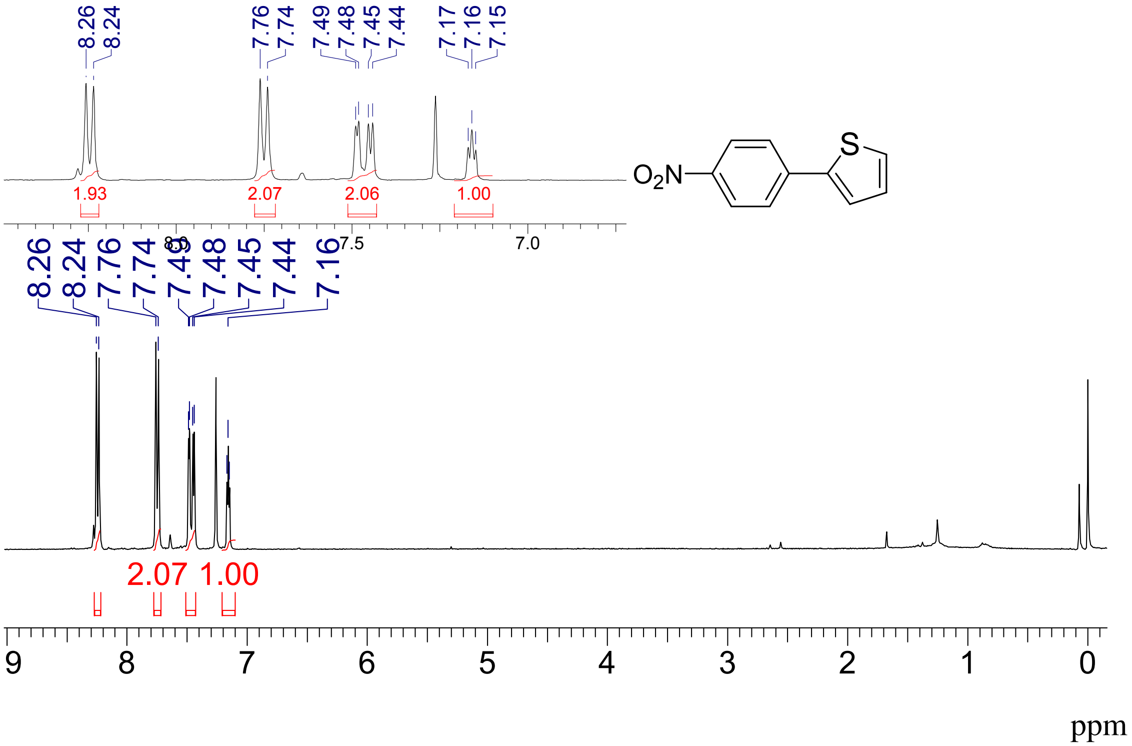

Figure S39. ^{1}H NMR of **2ps** (400 MHz, $CDCl_3$).

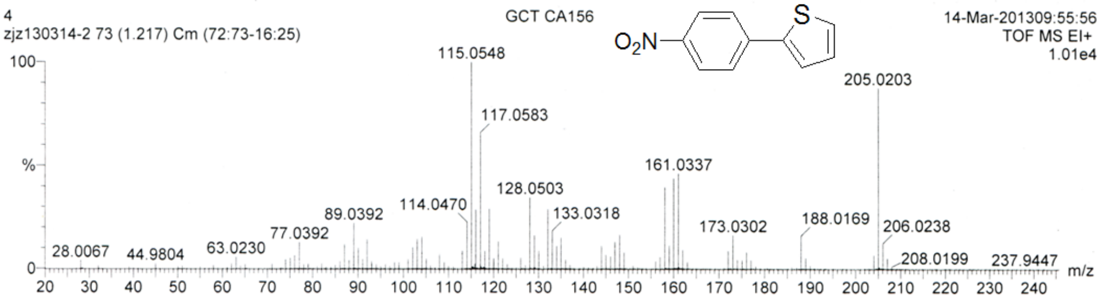

Figure S40. TOF HRMS EI$^+$ of **2ps** .

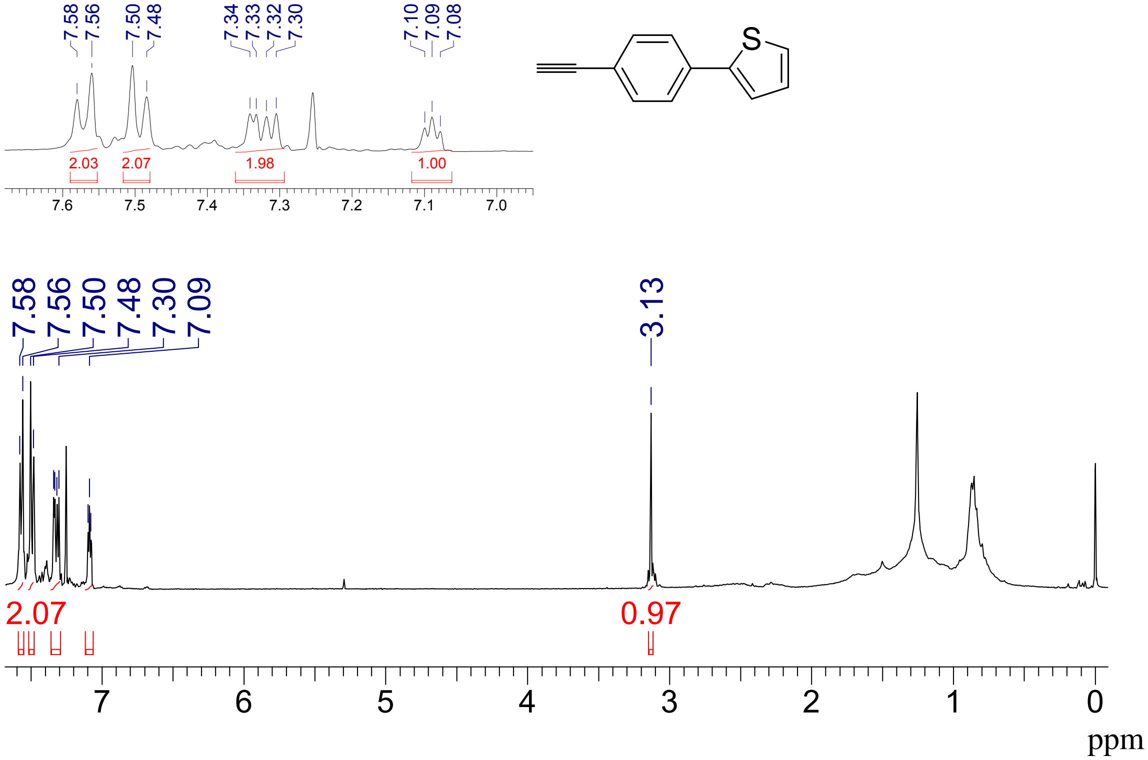

Figure S41. ^{1}H NMR of **1** (400 MHz, CDCl$_3$).

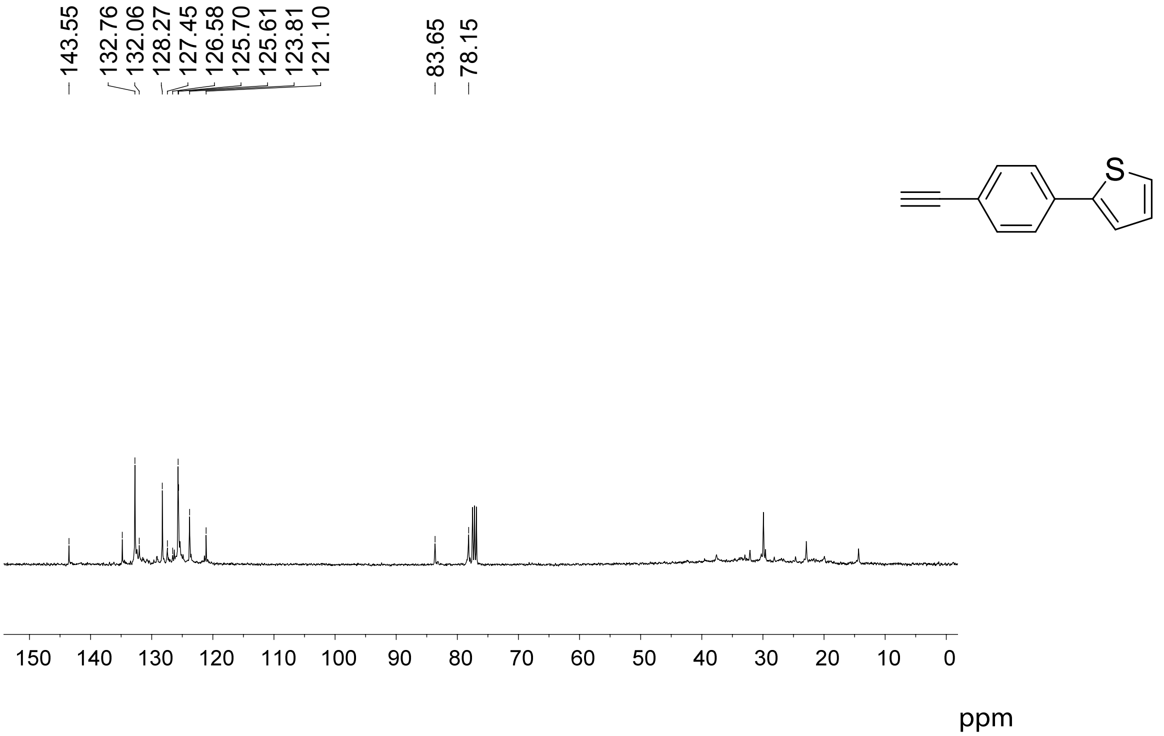

Figure S42. ^{13}C NMR of **1** (100 MHz, CDCl$_3$).

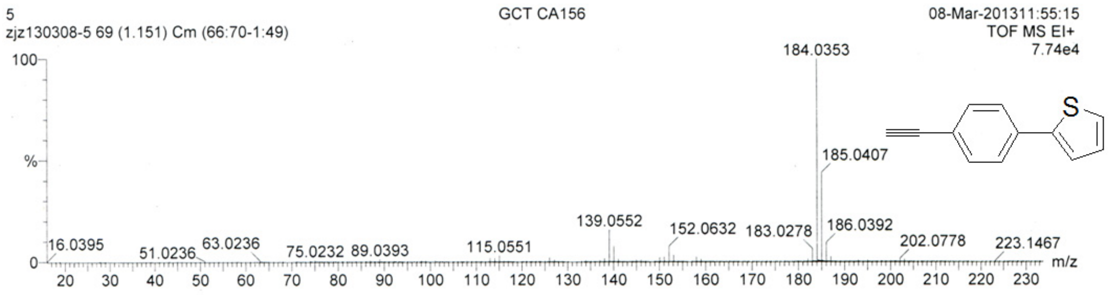

Figure S43. TOF HRMS EI$^+$ of **1** .

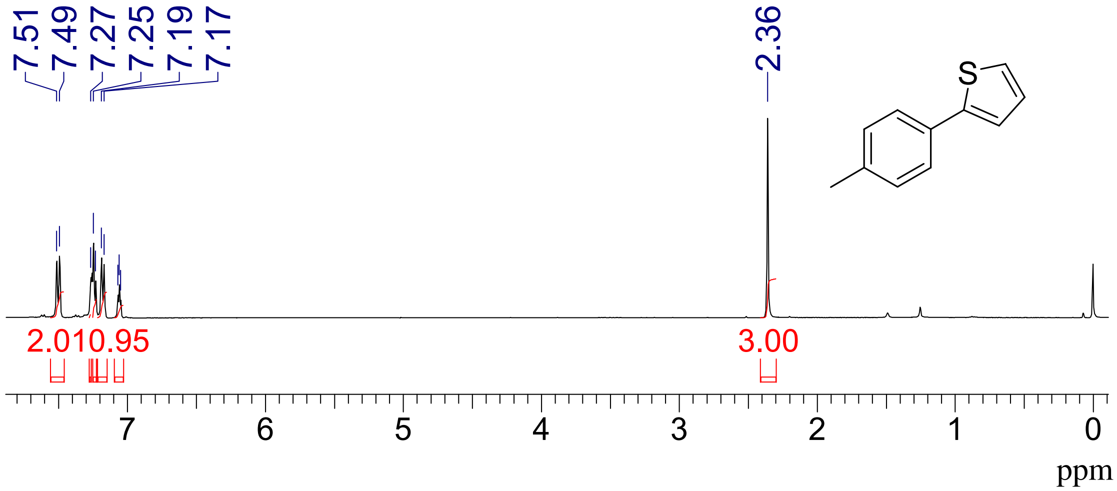

Figure S44. ^{1}H NMR of **2ns** (400 MHz, CDCl$_3$).

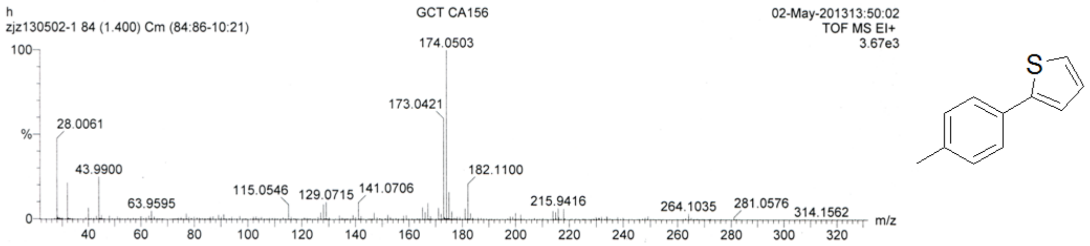

Figure S45. TOF HRMS EI⁺ of **2ns**.

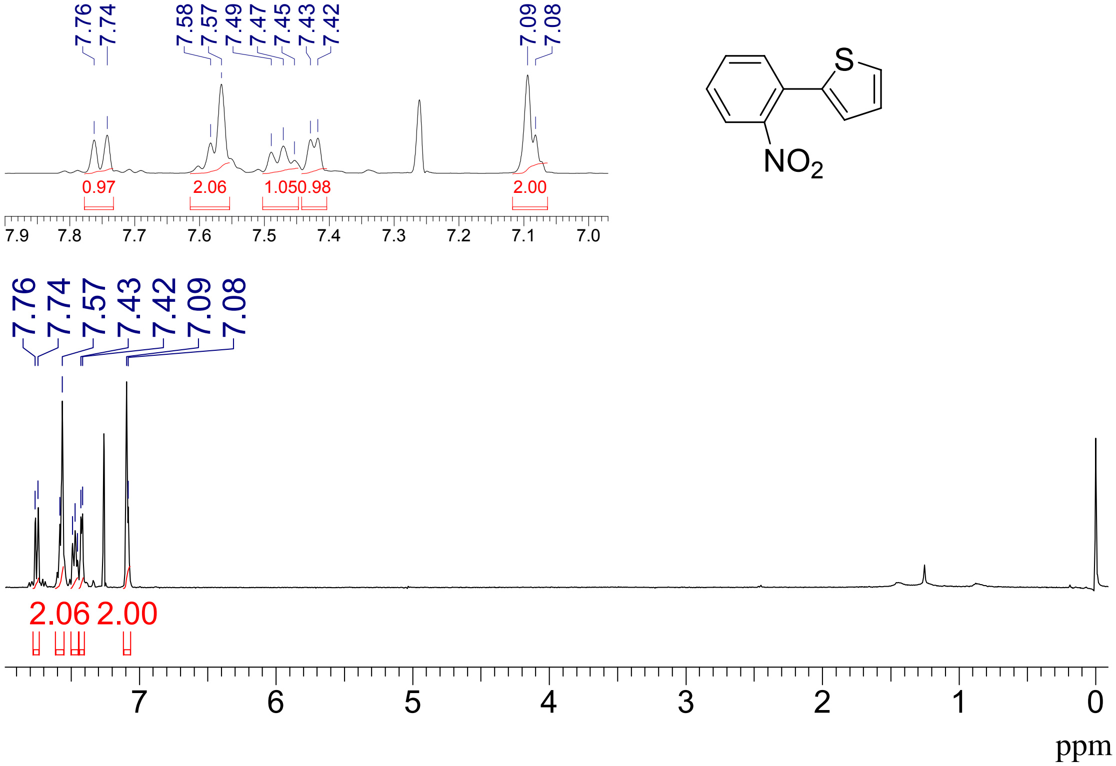

Figure S46. ^{1}H NMR of **2qs** (400 MHz, CDCl$_3$).

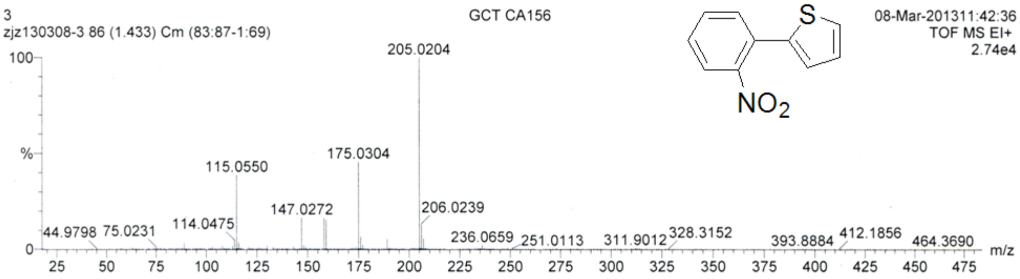

Figure S47. TOF HRMS EI$^+$ of **2qs**.

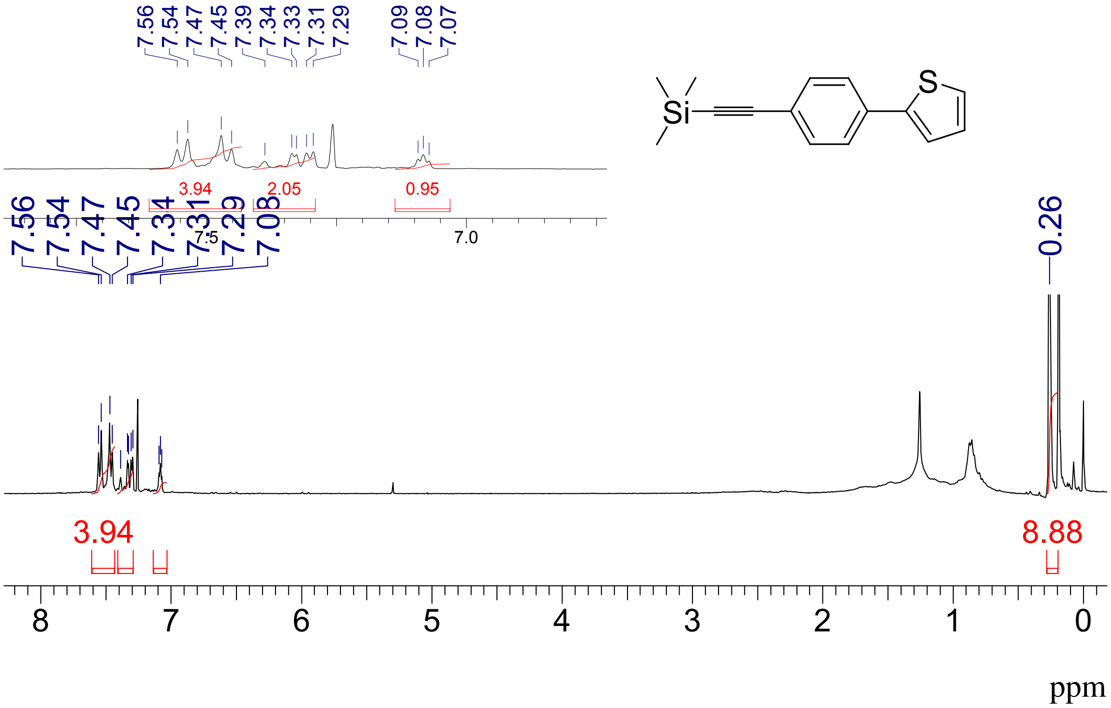

Figure S48. ^{1}H NMR of **2x** (400 MHz, $CDCl_3$).

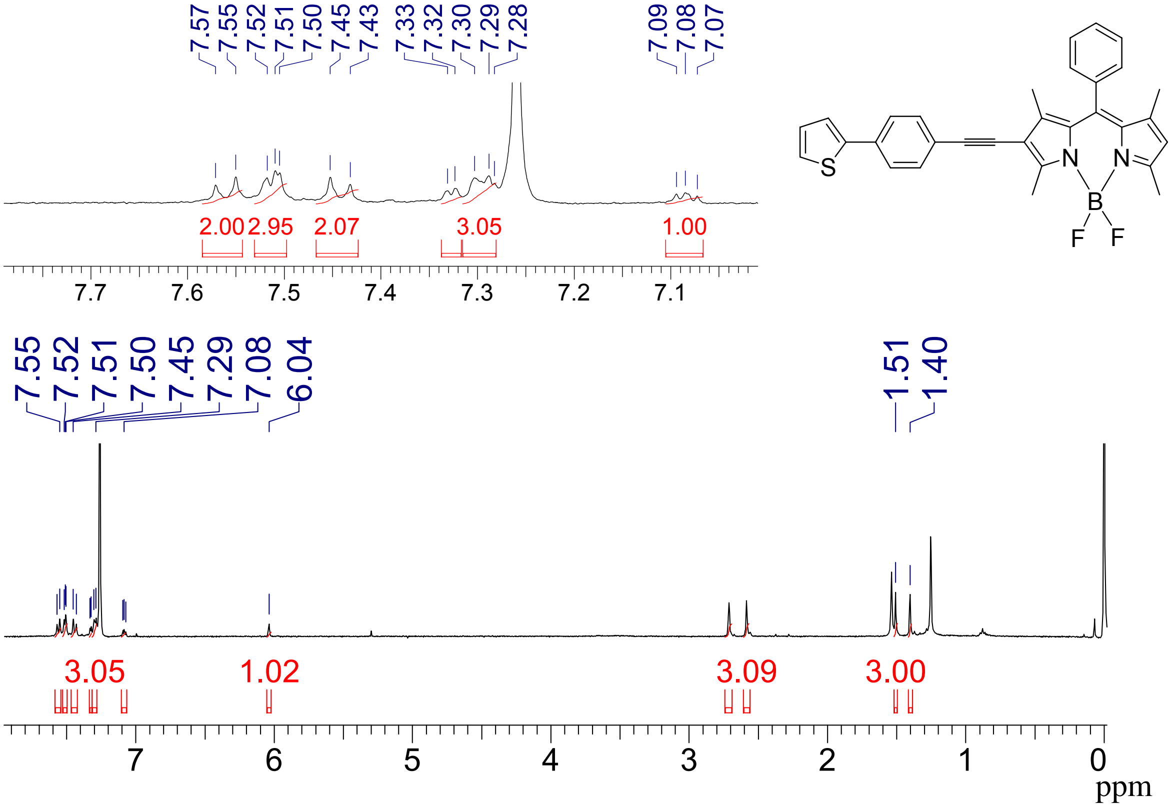

Figure S49. ^{1}H NMR of **T-1** (400 MHz, CDCl$_3$).

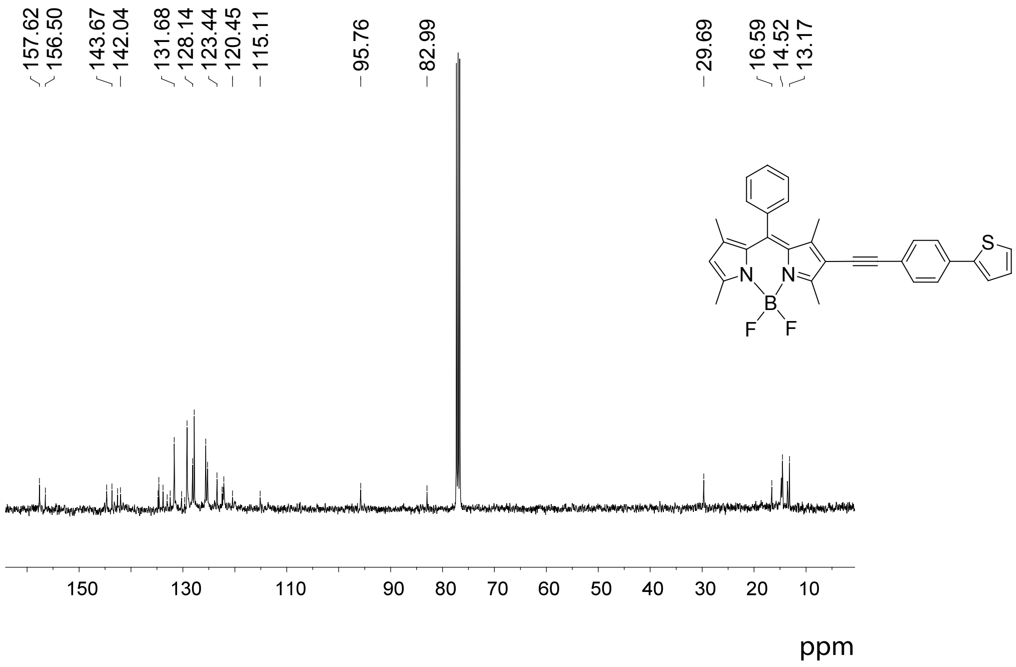

Figure S50. ^{13}C NMR of **T-1** (100 MHz, CDCl$_3$).

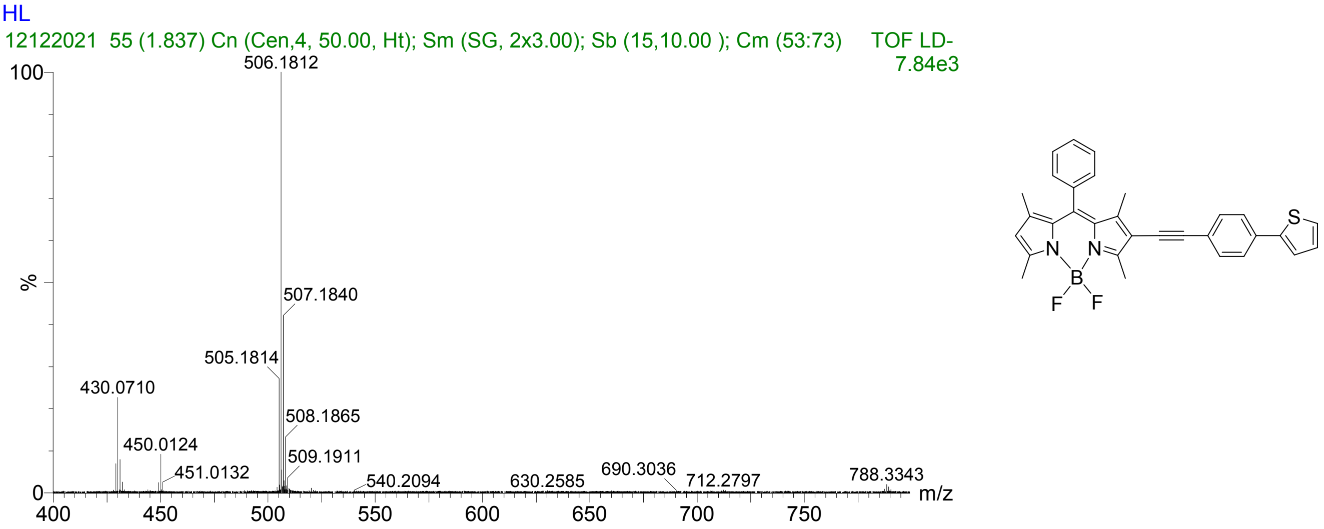

Figure S51. TOF HRMS MALDI of **T-1**.

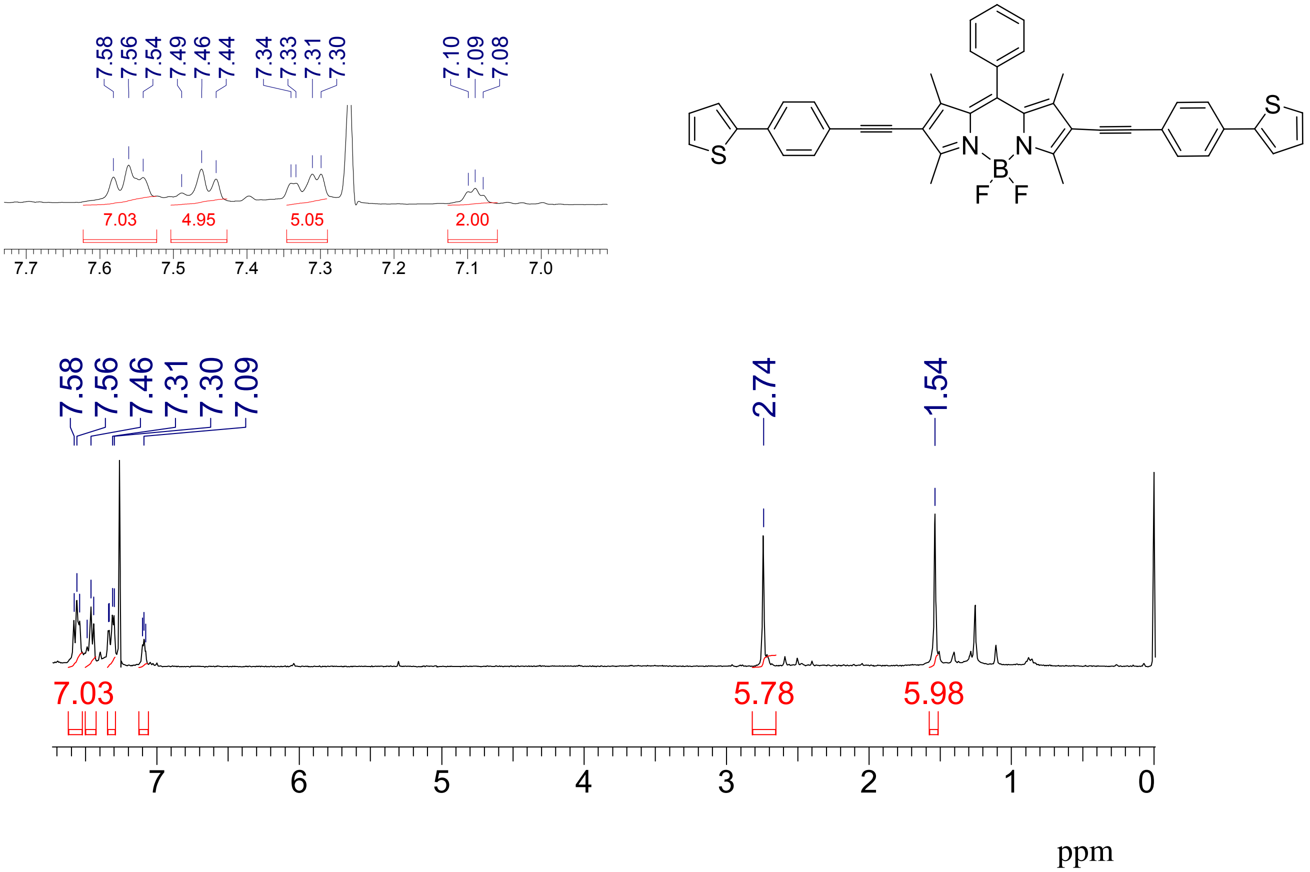

Figure S52. ^{1}H NMR of **T-2** (400 MHz, CDCl$_3$).

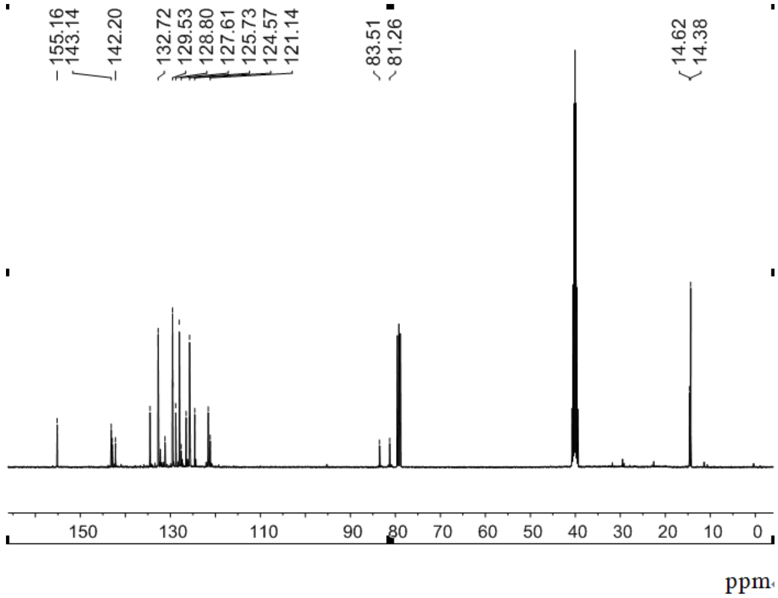

Figure S53. ^{13}C NMR of **T-2** (100 MHz, CDCl$_3$).

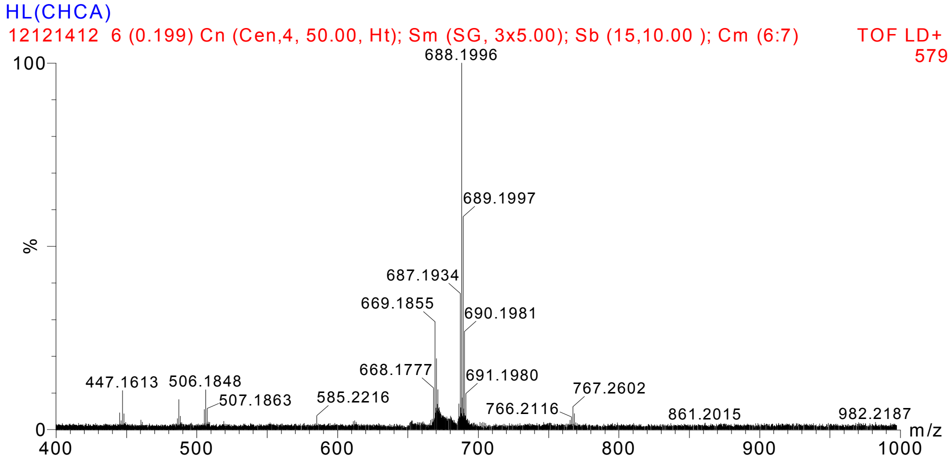

Figure S54. TOF HRMS MALDI of **T-2**.

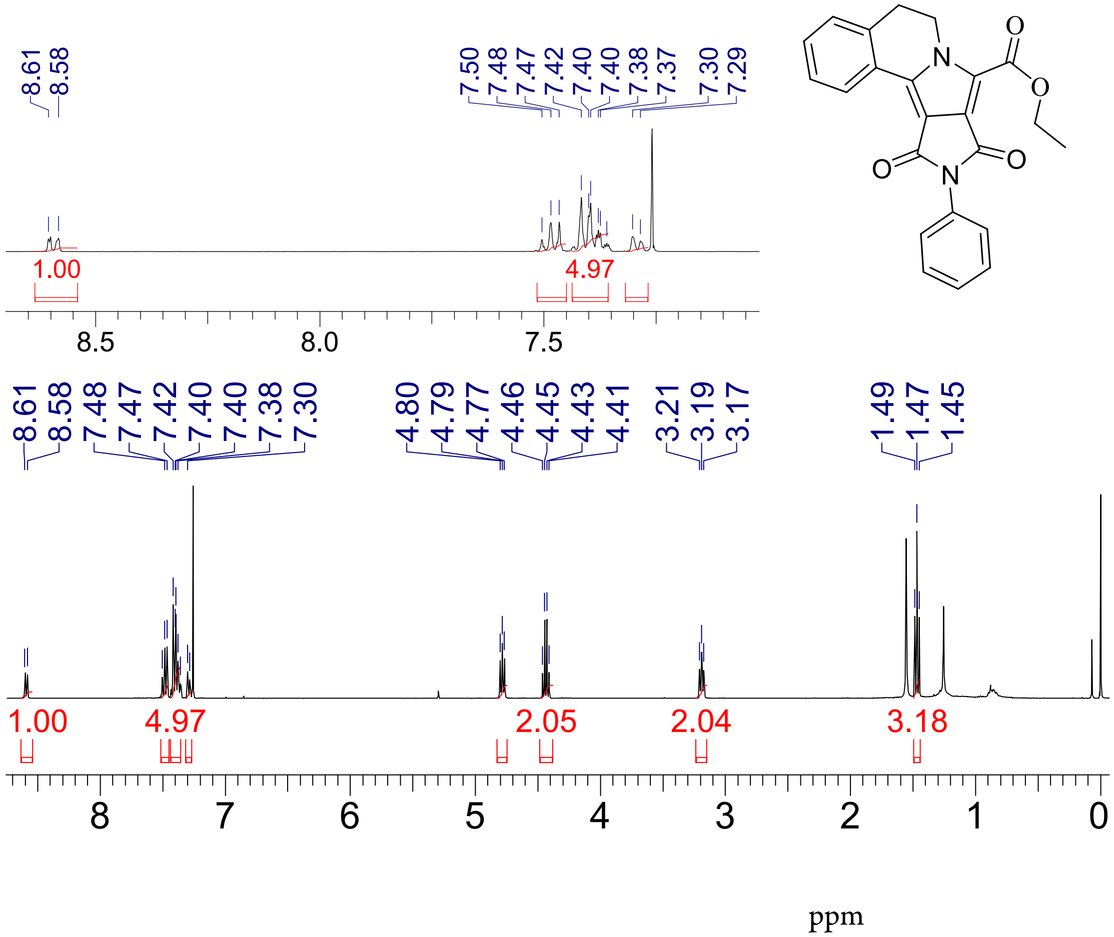

Figure S55. ^{1}H NMR of **2gh** (100 MHz, CDCl$_3$).

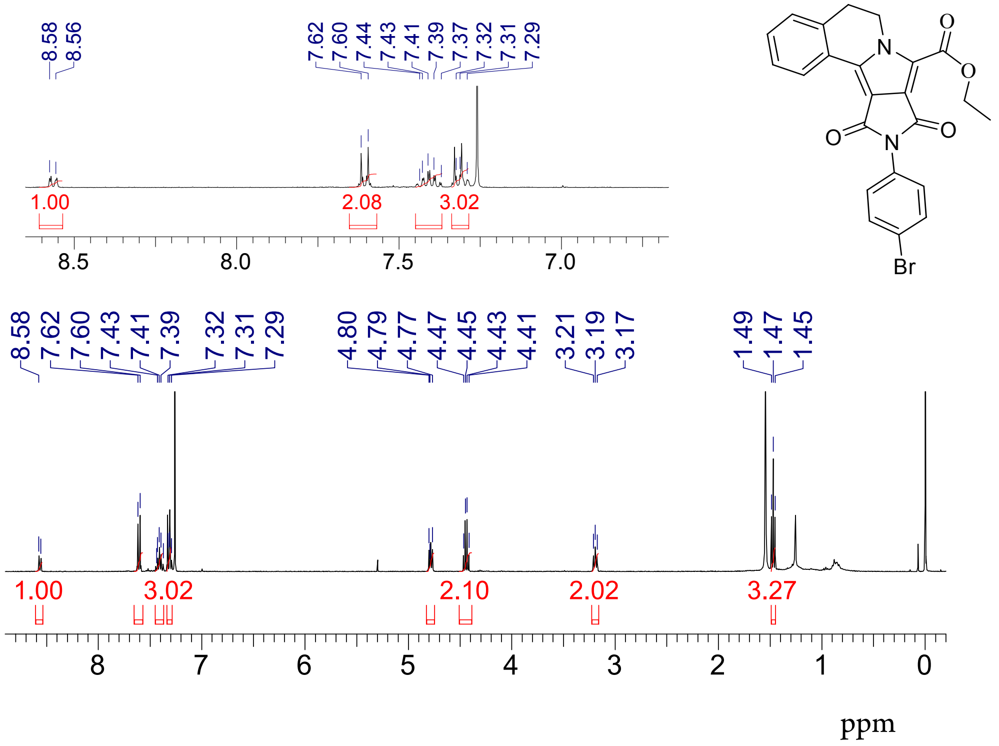

Figure S56. ^{1}H NMR of **2gi** (100 MHz, CDCl$_3$).

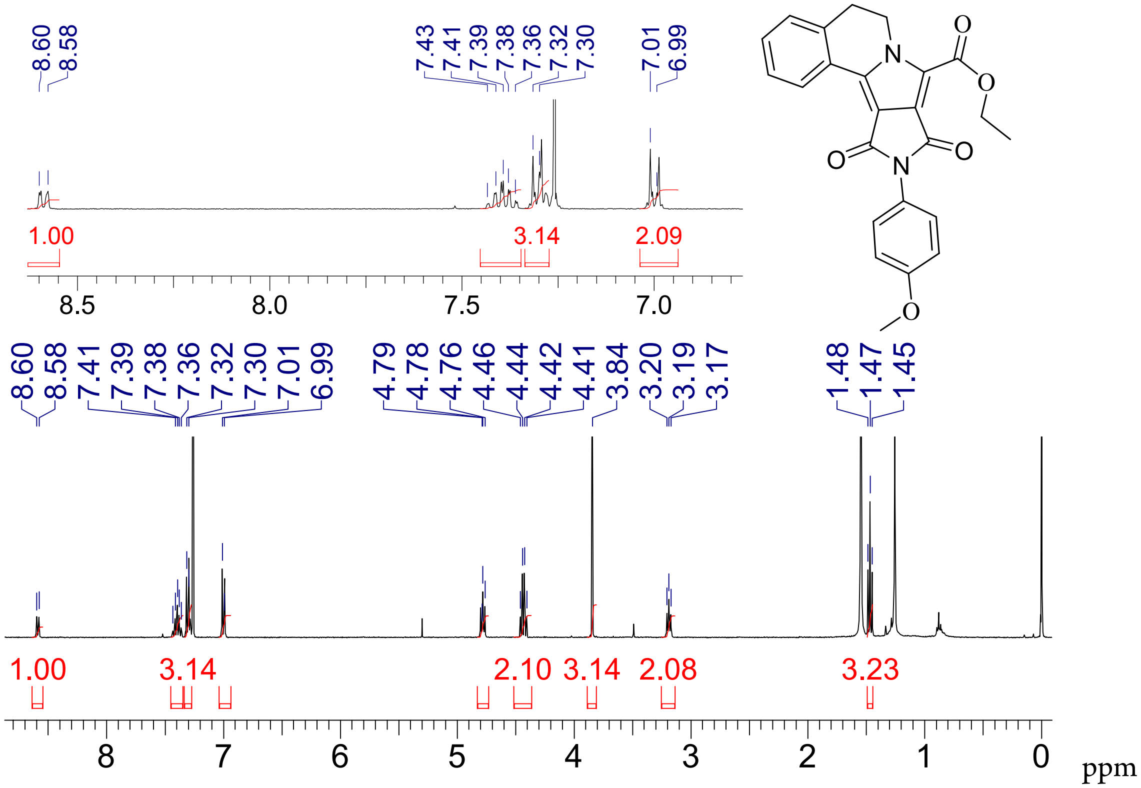

Figure S57. ^{1}H NMR of **2gj** (100 MHz, CDCl$_3$).

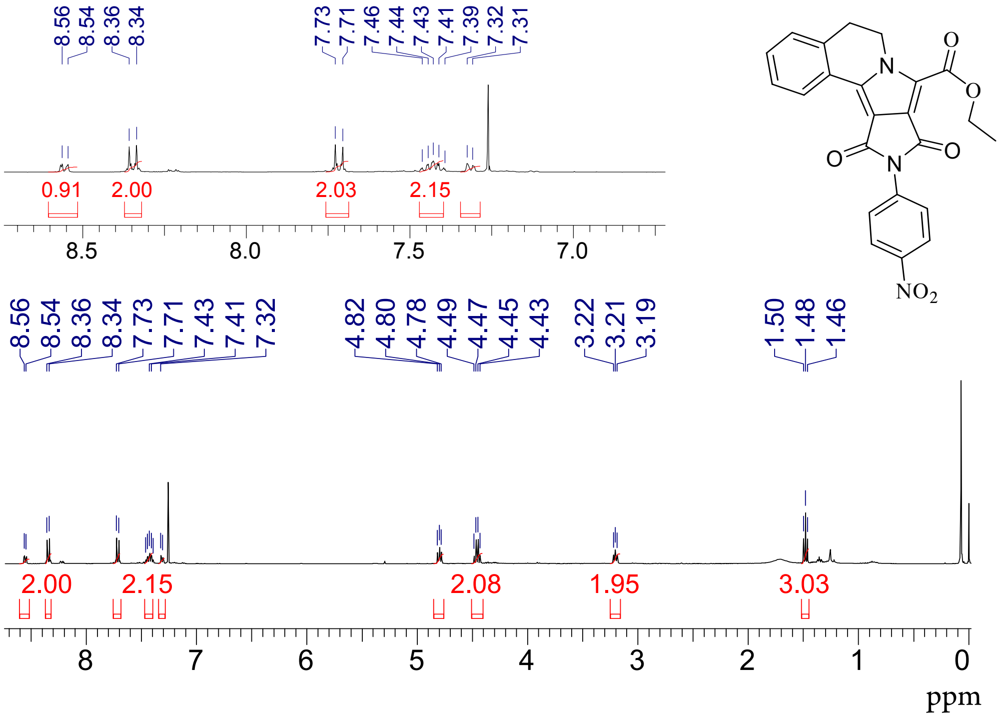

Figure S58. ^{1}H NMR of **2gk** (100 MHz, CDCl$_3$).

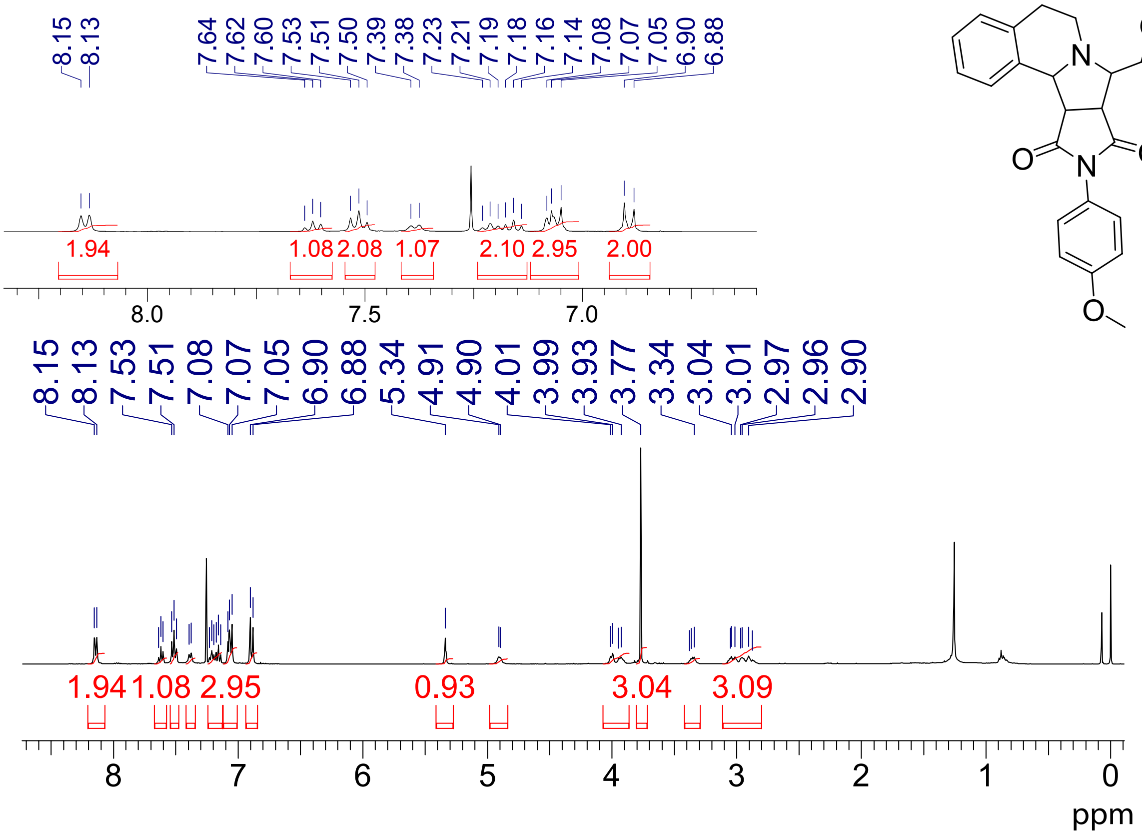

Figure S59. ^{1}H NMR of **2lh** (100 MHz, CDCl$_3$).

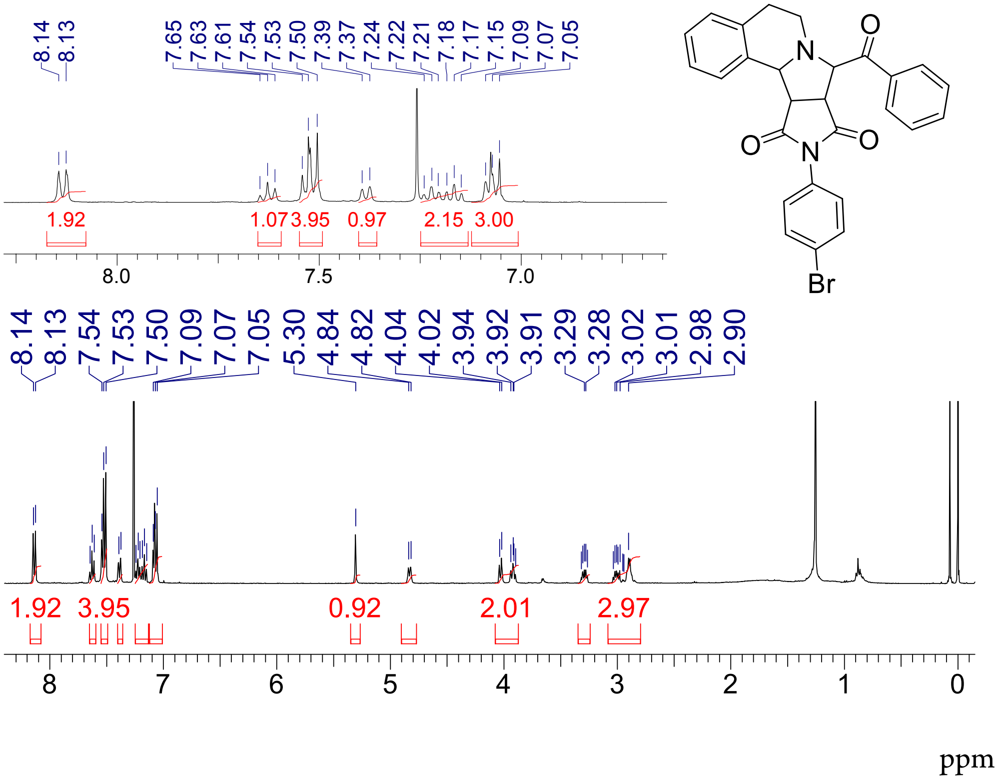

Figure S60. ^{1}H NMR of **2li** (100 MHz, CDCl$_3$).

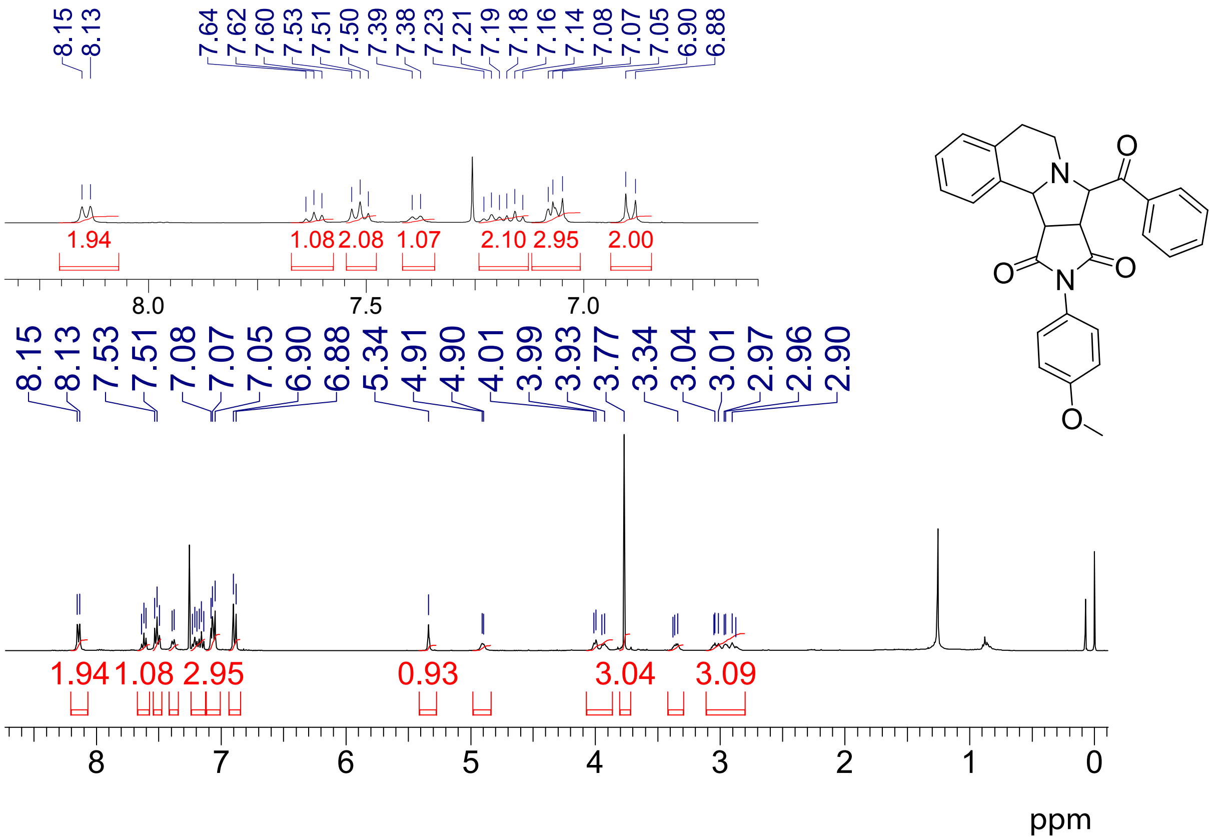

Figure S61. ^{1}H NMR of **2lj** (100 MHz, CDCl$_3$).

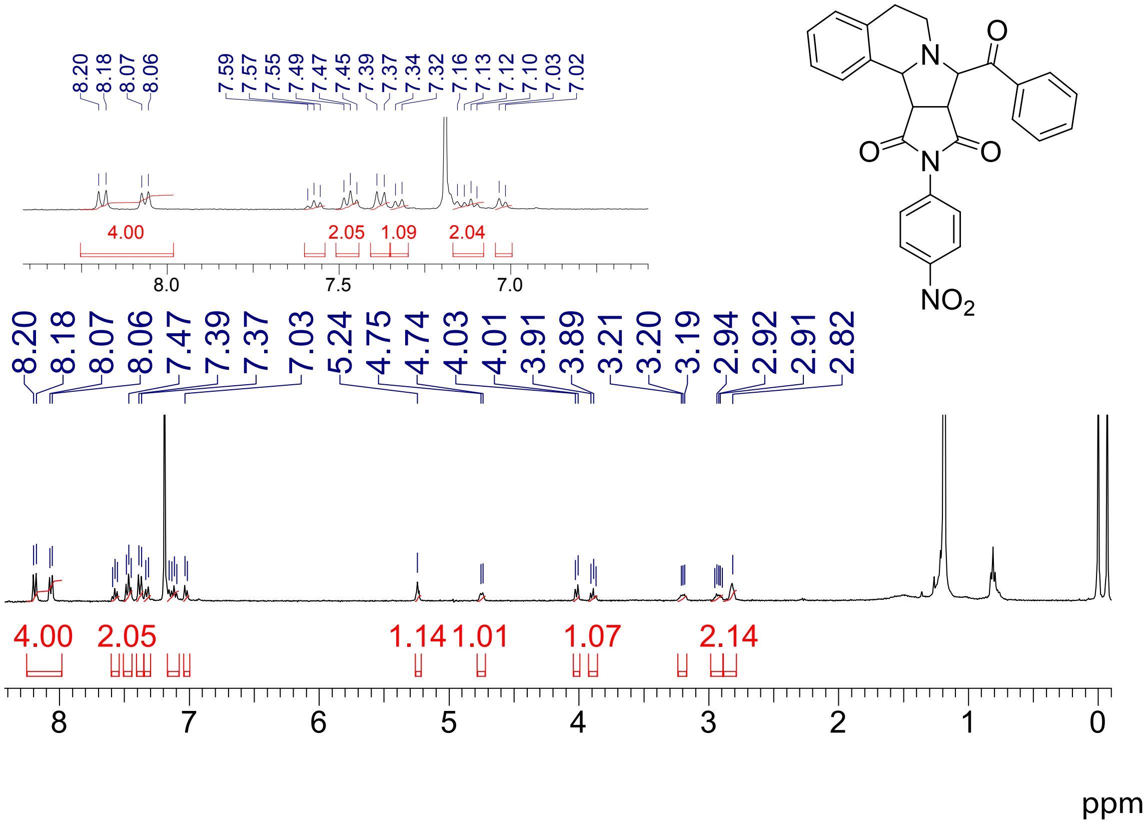

Figure S62. ^{1}H NMR of **2lk** (100 MHz, CDCl$_3$).

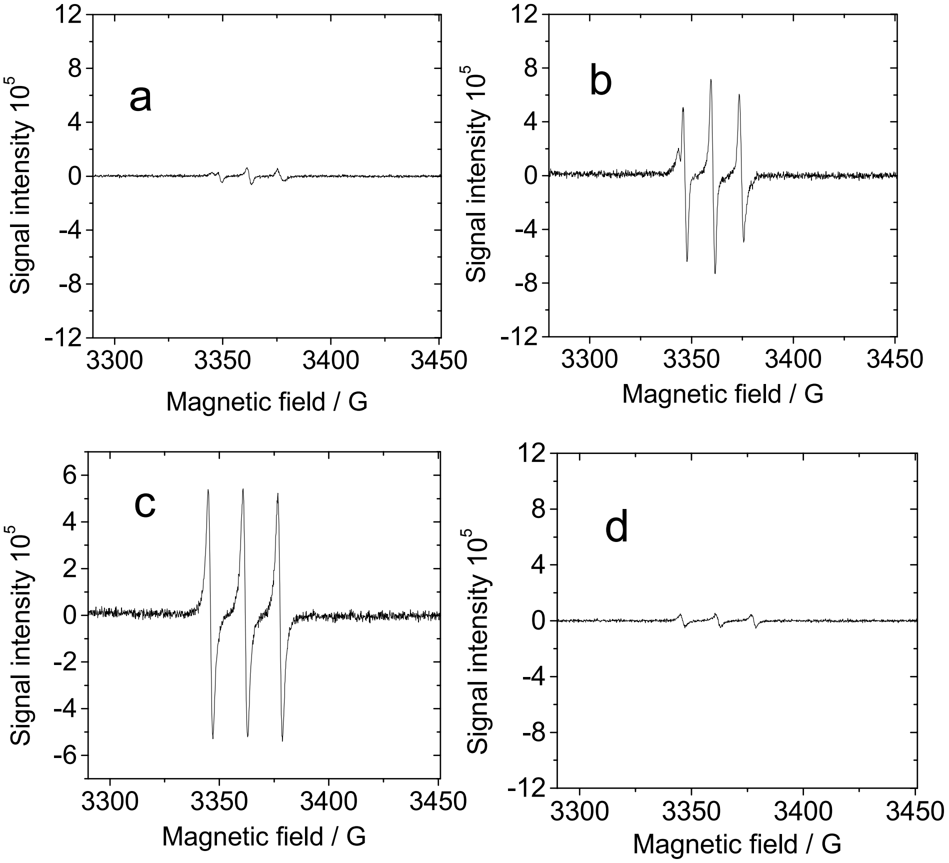

Figure S63. (a) ESR spectra of the mixture **B-1** (1.0×10^{-5} M) and DMPO (1.0×10^{-2} M) in air-saturated CH_2Cl_2 upon irradiation; (b) ESR spectrum of the mixture **B-1** (1.0×10^{-5} M), **1a** (3.0×10^{-3} M) and DMPO (1.0×10^{-2}M) in air-saturated CH_2Cl_2 upon irradiation; (c) ESR spectrum of a solution of **B-1** (1.0×10^{-4} M), TEMP (0.10 M), in air-saturated CH_2Cl_2 (d) ESR spectrum of **B-1** (1.0×10^{-5} M), TEMP (0.10 M), 1a (3.0×10^{-3} M) in air-saturated CH_2Cl_2 upon irradiation. All the irradiations were performed with 532 nm continuous laser and the duration is 300 s (141 mW/cm^2). 22 °C.

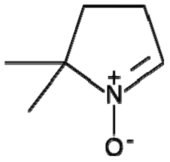

5,5-dimethyl-1-pyrroline-Noxide (DMPO)

For detection of $O_2^{\bullet-}$

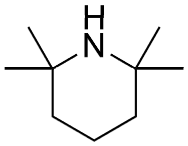

2,2,6,6-tetramethylpiperidine (TEMP)

For detection of $^1O_2$

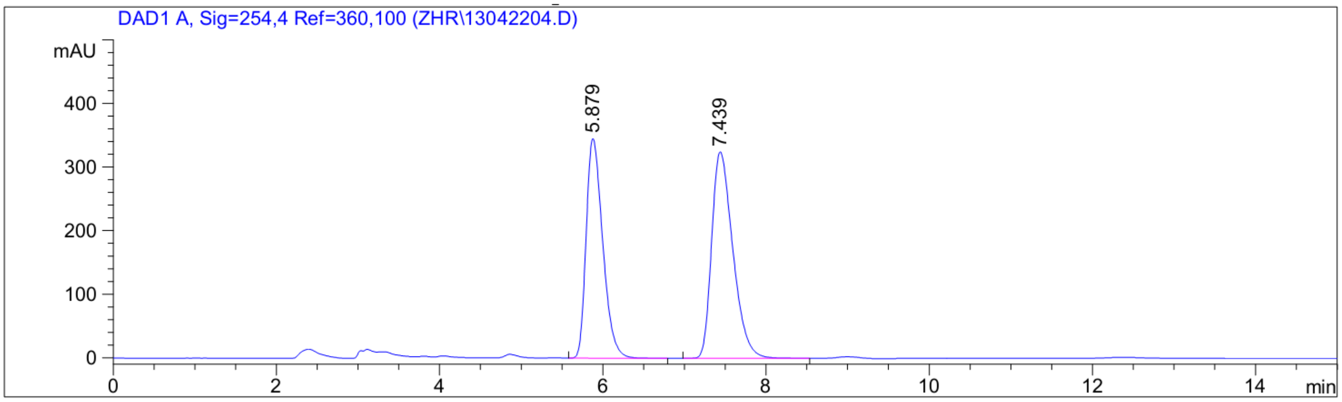

```
Peak RetTime  Type   Width      Area       Area
  #   [min]          [min]    [mAU*s]        %
----|-------|------|-------|----------|--------
   1   5.879 VB      0.2183 4861.79932  45.3664
   2   7.439 BB      0.2765 5854.95264  54.6336
```

Figure S64. Determination of the *e.e*% of **2af**, the mobile phase is isopropanol/ n-hexane = 95/5 (v/v), AD-H column.

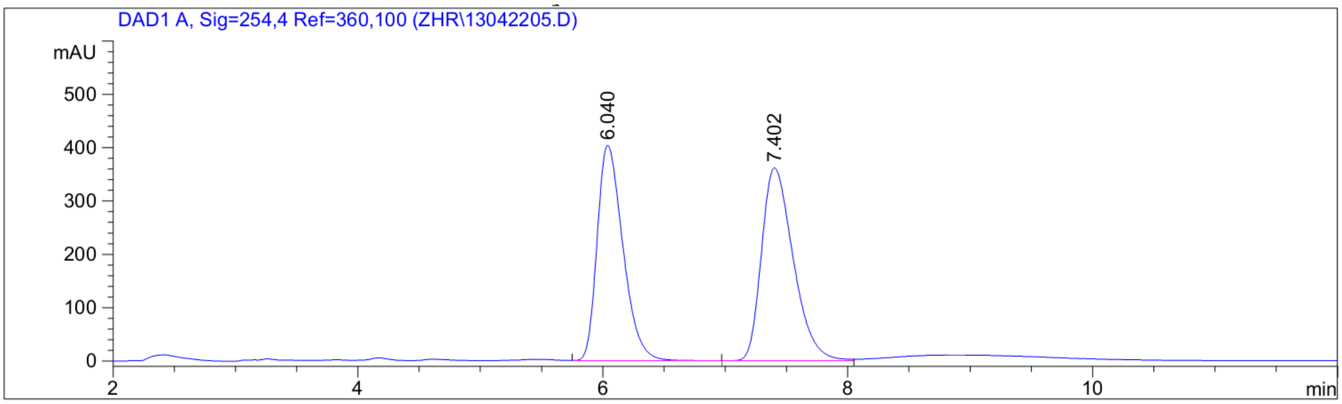

```
Peak RetTime  Type   Width      Area       Area
  #   [min]          [min]    [mAU*s]        %
----|-------|------|-------|----------|--------|
   1   6.040 VV      0.2269 5908.99512  47.5649
   2   7.402 VV      0.2792 6514.02002  52.4351
```

Figure S65. Determination of the *e.e.* % of **2bf**, the mobile phase is isopropanol/ n-hexane = 95/5 (v/v), AD-H column.

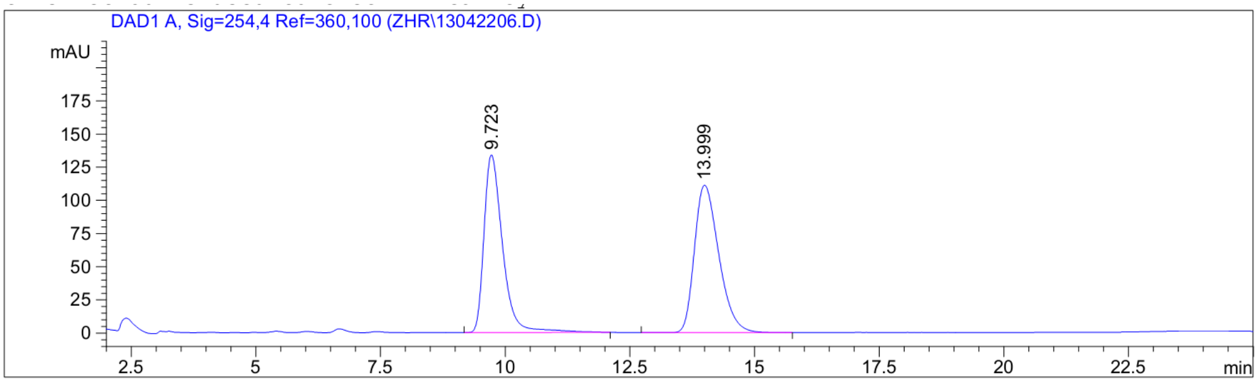

```
Peak RetTime  Type   Width     Area
  #   [min]          [min]   [mAU*s]
----|-------|------|-------|----------|
  1    9.723 BB     0.3957 3478.52563
  2   13.999 BB     0.5257 3780.00293
```

Figure S66. Determination of the *e.e.* % of **2cf**, the mobile phase is isopropanol/ *n*-hexane = 95/5 (v/v), AD-H column.

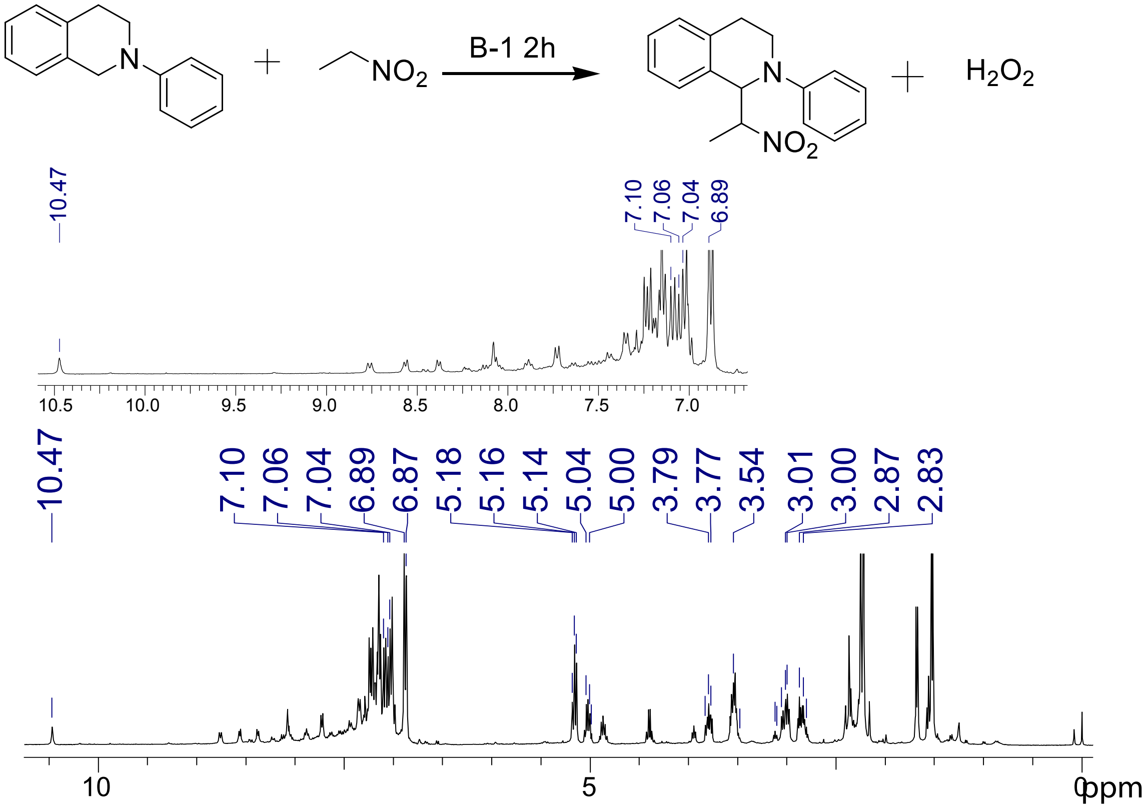

Figure S67. ^{1}H NMR determination of the H_2O_2 generated in the photocatalytic reactions. The peak at 10.47 ppm is due to H_2O_2 ($CDCl_3$, 400 MHz).

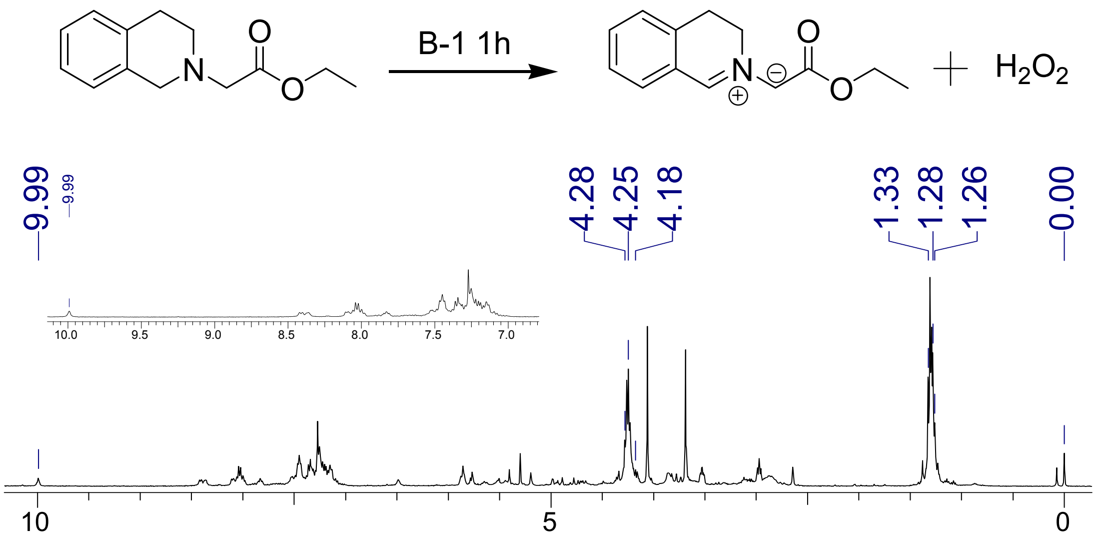

Figure S68. ^{1}H NMR determination of the H_2O_2 generated in the photocatalytic reactions, 9.99 ppm peak is H_2O_2 (in $CDCl_3$,400 MHz).

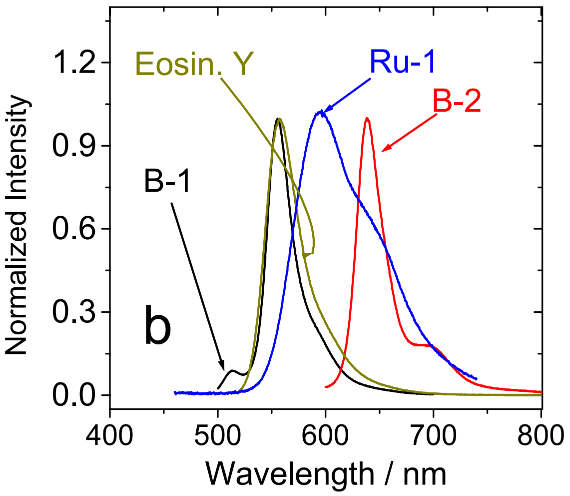

Figure S69. Normalized emission spectra of **B-1**– **B-2**， **Eosin. Y** and **Ru-1** Excited at 505 nm, 590 nm, 510 nm, 462 nm. in CH_2Cl_2 (1.0×10^{-5} M; 25 °C).

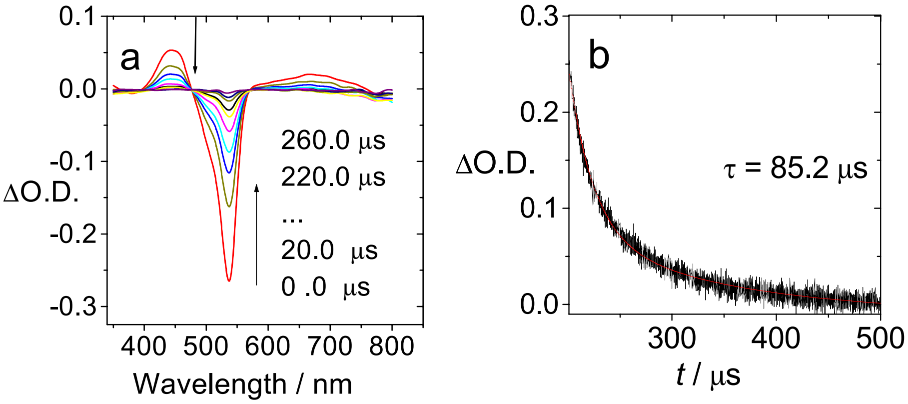

Figure S70. Nanosecond time-resolved transient difference absorption of **B-1**. (a) transient absorption difference spectra and (b) decay trace at 520 nm. In deaerated CH_2Cl_2. λ_{ex} = 532 nm, 20 °C.

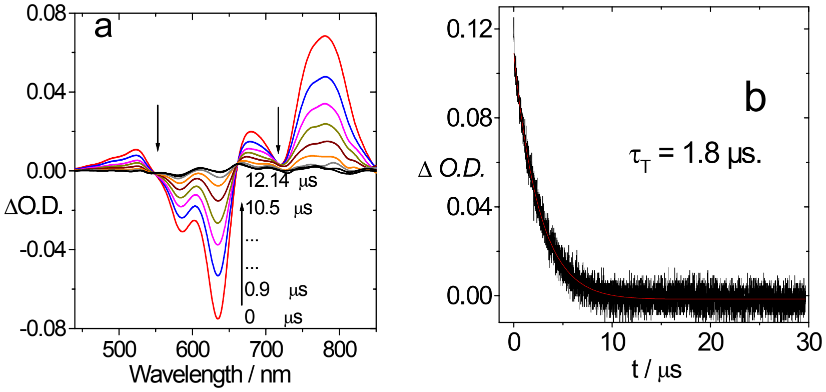

Figure S71. Nanosecond time-resolved transient difference absorption of **B-2**. (a) transient absorption difference spectra and (b) decay trace at 630 nm. In deaerated CH_2Cl_2 . λ_{ex} = 532 nm, 20 °C.

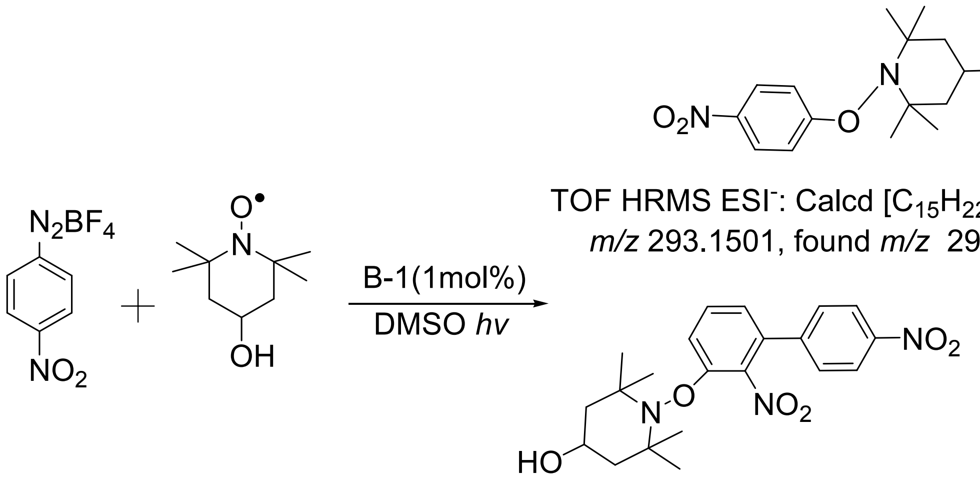

TOF HRMS ESI$^-$: Calcd $[C_{15}H_{22}N_2O_4\text{-}H]^-$ *m/z* 293.1501, found *m/z* 293.1511

TOF HRMS ESI$^-$: Calcd $[C_{21}H_{25}N_3O_6\text{-}H]^-$ m/z 414.1665, found m/z 414.1680

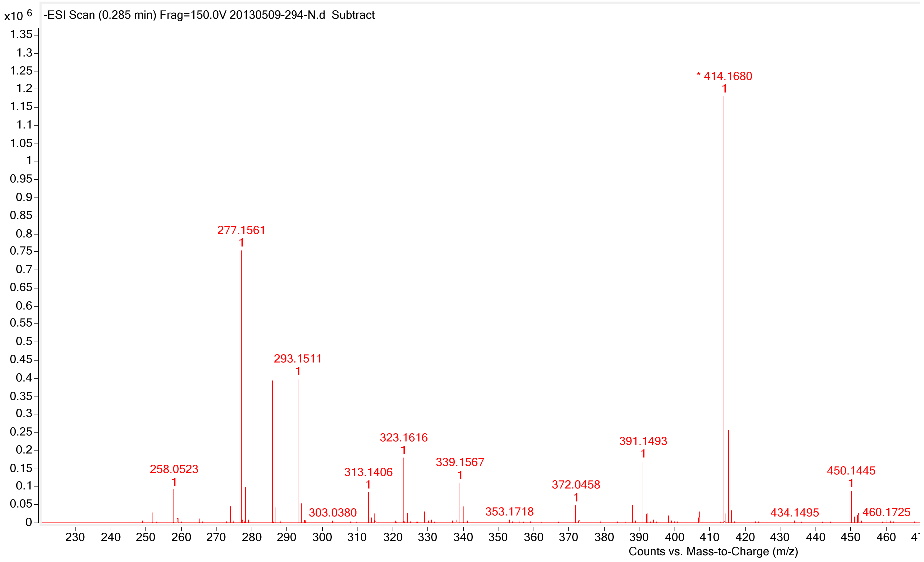

Figure S72. HRMS-ESI$^-$ evidence for 4–Hydroxy TEMPO trapped free radicals.

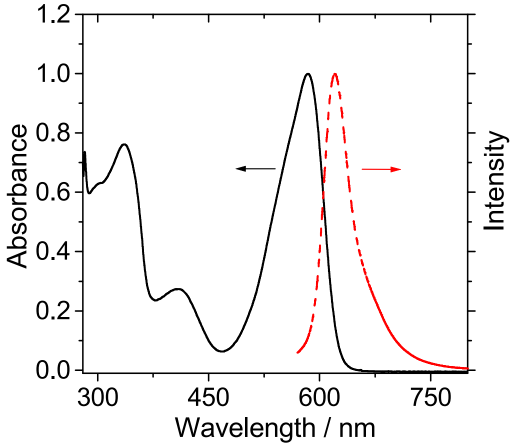

Figure S73. Normalized UV–vis absorption spectra and emission spectra of **T-2** (in toluene, 1.0 × 10^{-5} M, 20 °C).

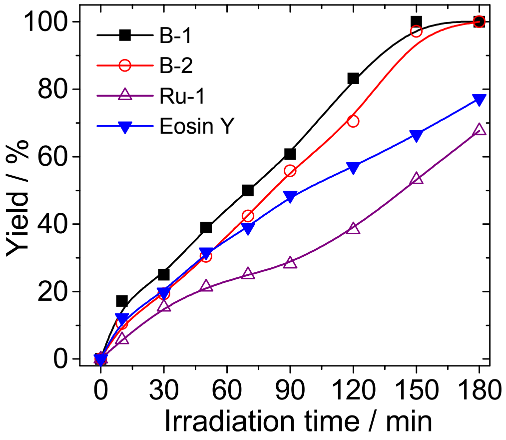

Figure S74. Plot of the photocatalysis yields vs. photoirradiation time with different photocatalysts.

Typical procedures: to a flask were added photocatalysts (1 mol%), tetrahydroisoquinoline derivatives (0.4 mmol), nitromethane (6 mL). The reaction mixture was stirred at rt under air. The solution was then irradiated using a 35 W xenon lamp through a cut off filter (0.72 M $NaNO_2$ aqueous solution, transparent for light > 385 nm). Aliquot of 0.3 mL of the solution was taken, the solvent was removed under reduced pressure. Proton nuclear magnetic resonance (^1H NMR) in $CDCl_3$ was carried out to determine the reaction yield. Peaks at 4.42 ppm are the substrate characteristic peak, the peak at 5.53 ppm is the characteristic peak of the product.

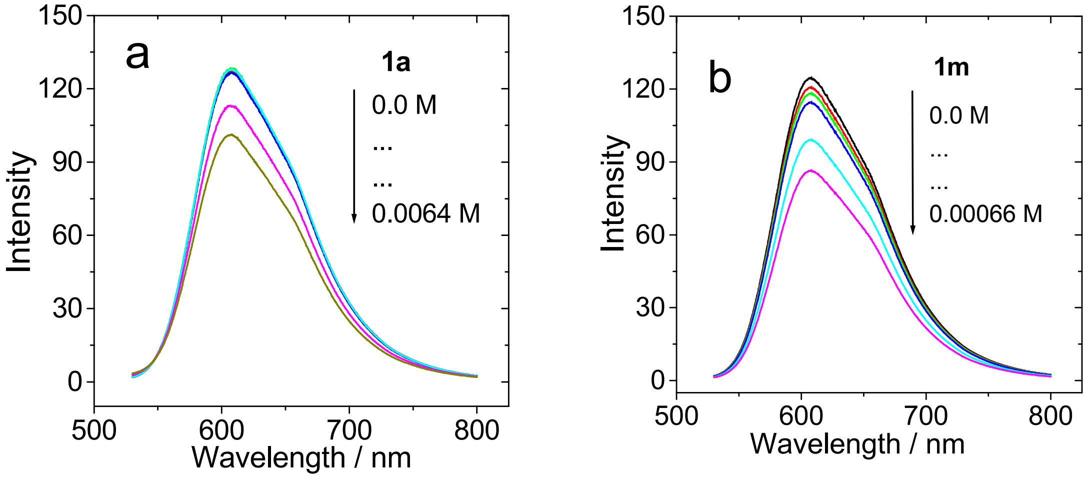

Figure S75. Quenching of the triplet excited state of Ru-1 by the substrate of the photocatalytic reactions. (a) quenching of the Ru(bpy)$_3^{2+}$ phosphorescence by **1a** (*N*-phenyl-1,2,3,4-tetrahydroisoquinoline), (b) quenching of the Ru(bpy)$_3^{2+}$ phosphorescence by **1m** (phenyl diazonium salts), λ_{ex} = 452 nm. In deaerated CH$_3$CN. 20 °C.

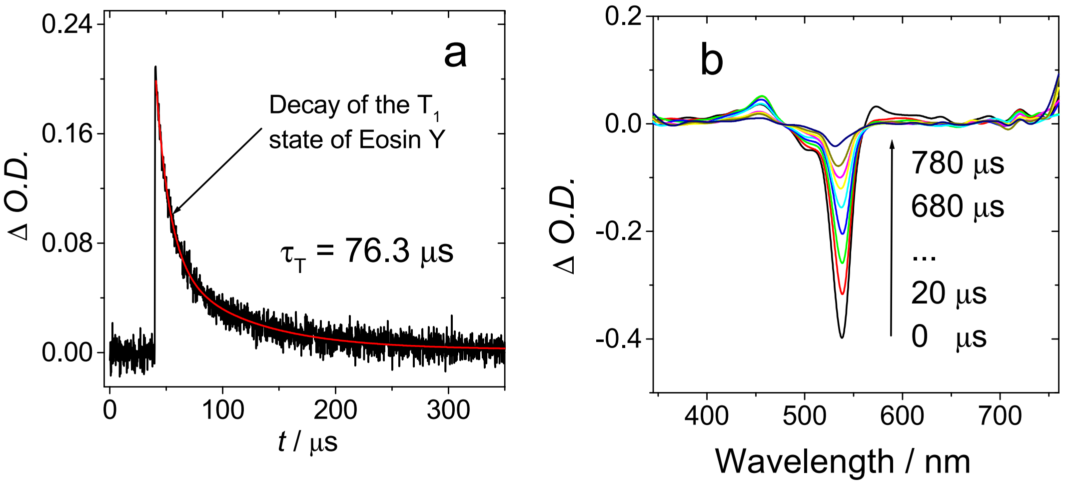

Figure S76. Nanosecond time-resolved transient difference absorption spectra of **Eosin Y**. (a) Decay trace of **Eosin Y** at 520 nm, (b) Transient difference absorption spectra of **Eosin Y**. Excited with pulsed laser (λ_{ex} = 532 nm). In deaerated CH$_3$CN. 1.0 × 10^{-5} M, 20 °C.

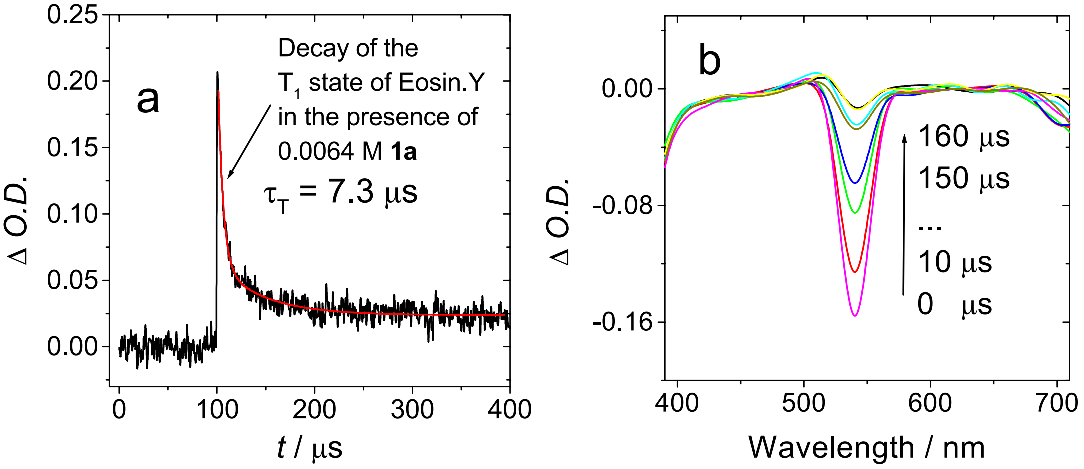

Figure S77. Nanosecond time-resolved transient difference absorption spectra of Eosin Y in the presence of 64 mM **1a**. (a) Decay trace of Eosin Y at 520 nm, (b) Transient difference absorption spectra of Eosin Y in the presence of 64 mM **1a**. Excited with nanosecond pulsed laser (λ_{ex} = 532 nm). In deaerated CH_3CN. 1.0×10^{-5} M, 20 °C.

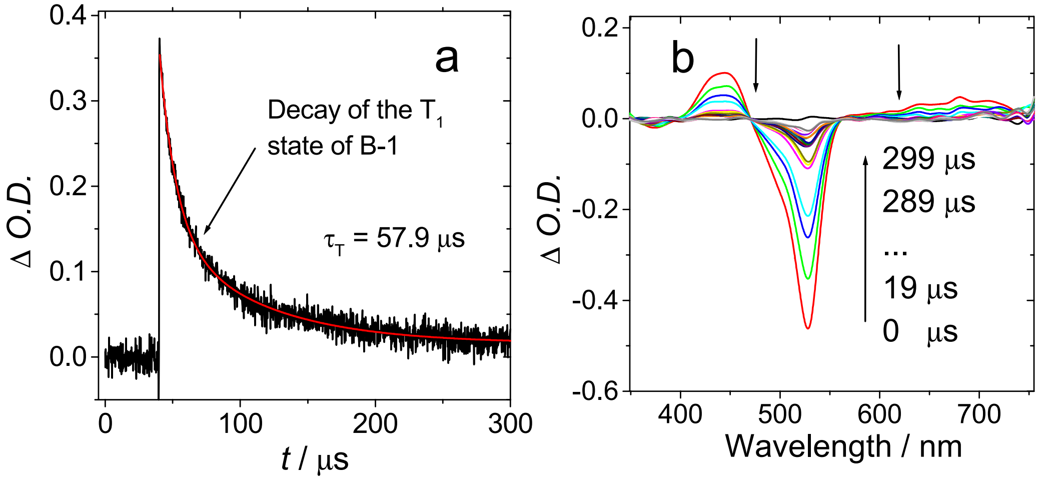

Figure S78. Nanosecond time-resolved transient difference absorption spectra of **B-1**. (a) Decay trace of **B-1** at 540 nm, (b) Transient difference absorption spectra of **B-1**. Excited with nanosecond pulsed laser (λ_{ex} = 532 nm). In deaerated CH_3CN. 1.0×10^{-5} M, 20 °C.

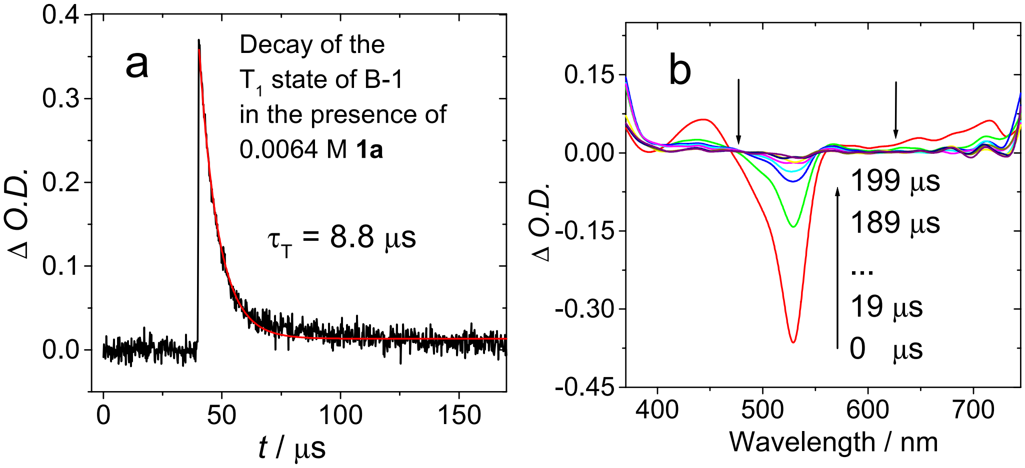

Figure S79. Nanosecond time-resolved transient difference absorption spectra of **B-1** added 6.4 mM **1a** (a) Decay trace of **B-1** at 540 nm, (b) Transient difference absorption spectra of **B-1** added 0.0064 M^{-1} **1a**. Excited with nanosecond pulsed laser (λ_{ex} = 532 nm). In deaerated CH_3CN. 1.0 × 10^{-5} M, 20 °C.

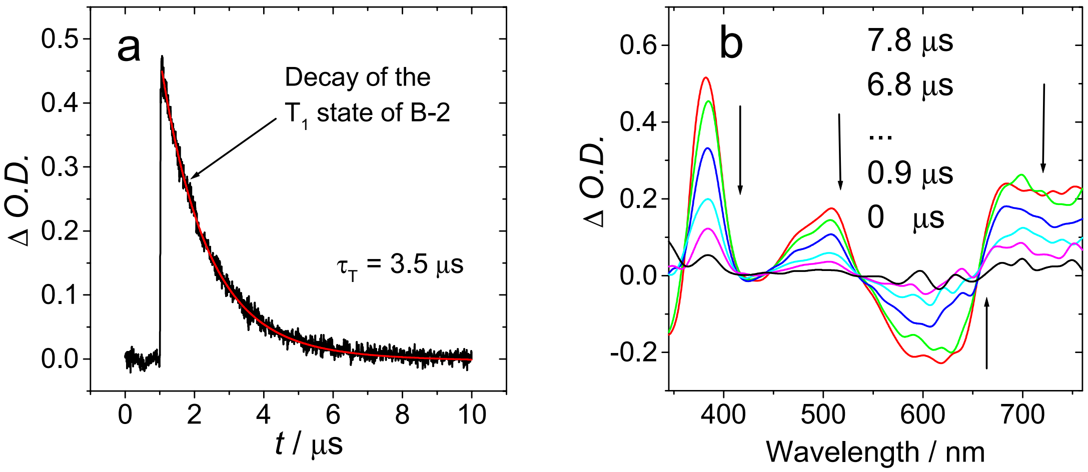

Figure S80. Nanosecond time-resolved transient difference absorption spectra of **B-2**. (a) Decay trace of **B-2** at 380 nm, (b) Transient difference absorption spectra of **B-2**. Excited with nanosecond pulsed laser (λ_{ex} = 532 nm). In deaerated CH_3CN. 1.0 × 10^{-5} M, 20 °C.

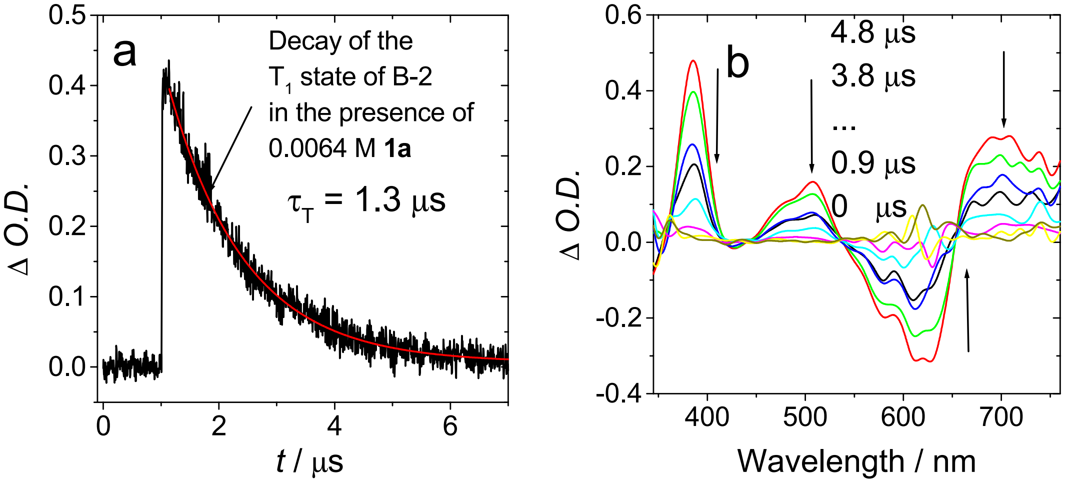

Figure S81. Nanosecond time-resolved transient difference absorption spectra of **B-2** in the presence of 6.4 mM **1a.** (a) Decay trace of **B-2** at 540 nm, (b) Transient difference absorption spectra of **B-2** in the presence of 6.4 mM **1a**. Excited with nanosecond pulsed laser (λ_{ex} = 532 nm). In deaerated CH_3CN. 1.0×10^{-5} M, 20 °C.

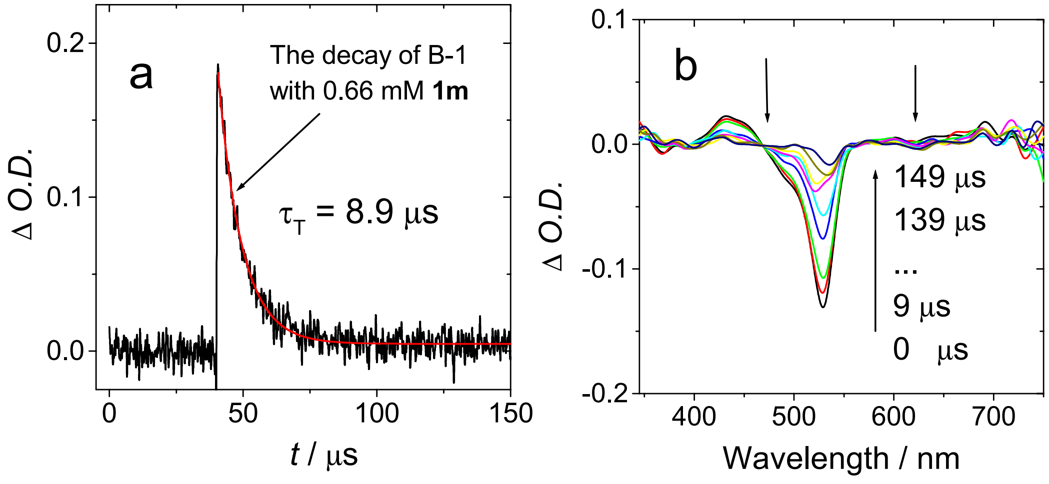

Figure S82. Nanosecond time-resolved transient difference absorption spectra of **B-1** in the presence of 6.4 mM **1m.** (a) Decay trace of **B-1** at 540 nm, (b) Transient difference absorption spectra of **B-1** added 6.4 mM **1m**. Excited with nanosecond pulsed laser (λ_{ex} = 532 nm). In deaerated CH_3CN. 1.0×10^{-5} M, 20 °C.

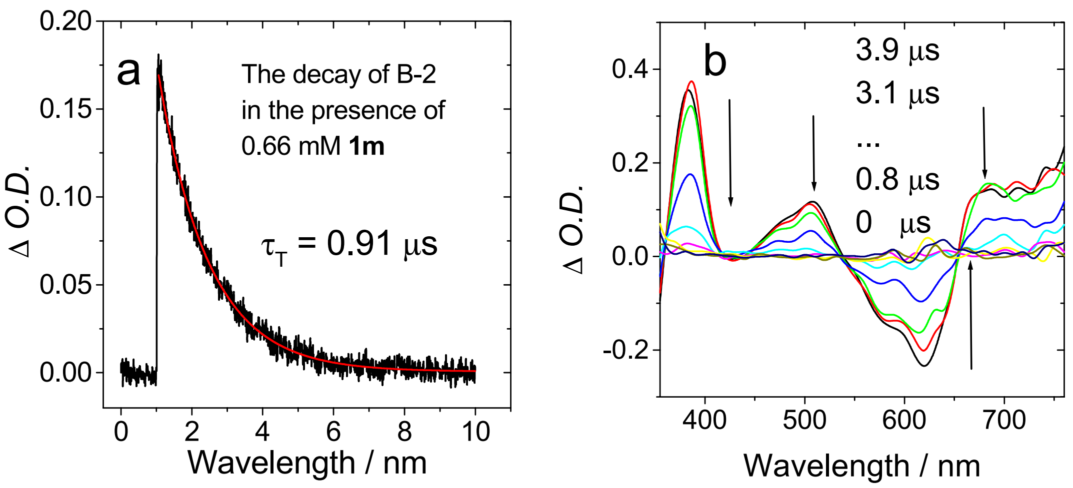

Figure S83. Nanosecond time-resolved transient difference absorption spectra of **B-2** in the presence of 0.66 mM **1m**. (a) Decay trace of **B-2** at 380 nm, (b) Transient difference absorption spectra of **B-2** in the presence of 0.66 mM **1m**. Excited with nanosecond pulsed laser (λ_{ex} = 532 nm). λ_{ex} = 532 nm (in deaerated CH_3CN. 1.0 × 10^{-5} M, 20 °C).

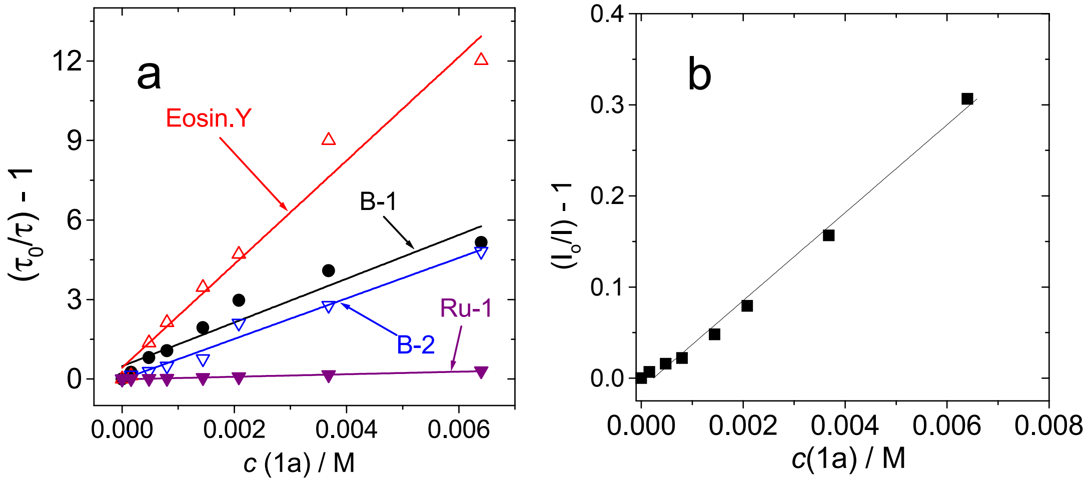

Figure S84. (a) The Stern–Volmer quenching of the triplet state lifetimes of the different triplet photosensitizers **B-1**, **B-2** and Eosin Y in the presence of **1a** (*N*-phenyltetrahydroisoquinione). *c* [photocatalysts] = 1.0 × 10^{-5} M, λ_{ex} = 532 nm. (b) The Stern–Volmer quenching of the phosphorescence of **Ru-1** in the presence of **1a** (*N*-phenyltetrahydroisoquinione). *c* [**Ru-1**] = 1.0 × 10^{-5} M. In CH_3CN, λ_{ex} = 452 nm, 20 °C.

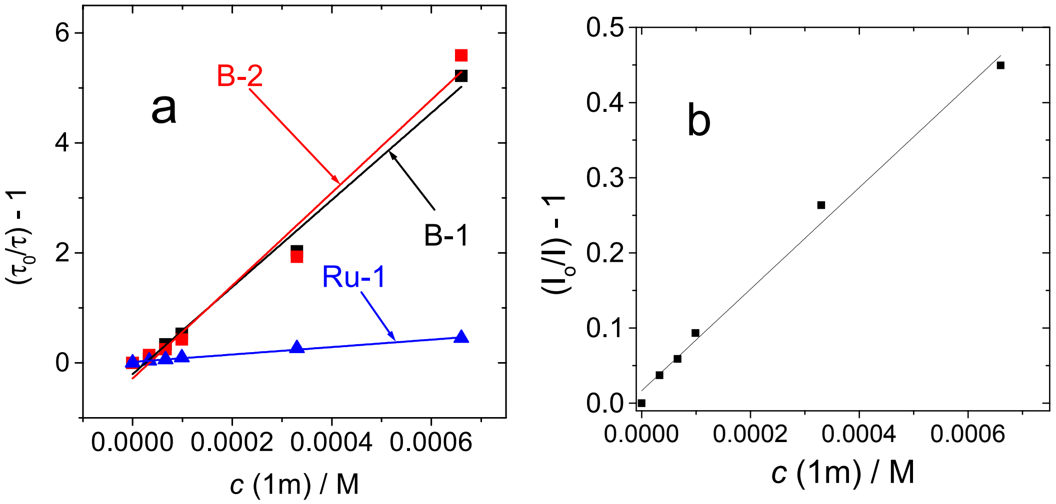

Figure S85. (a) The Stern–Volmer quenching of the triplet state lifetimes of the photocatalysts **B-1** and **B-2** in the presence of **1m** (Aryl diazonium salts). *c* [photocatalysts] = 1.0 × 10^{-5} M, λ_{ex} = 532 nm. (b) The Stern–Volmer quenching of the phosphorescence in the presence of **1m** (phenyl diazonium salts). *c* [**Ru-1**] = 1.0 × 10^{-5} M. In CH_3CN, λ_{ex} = 452 nm, 20 °C.

Table S1. Triplet Excited-State Lifetimes (τ_T), Stern–Volme Quenching Constant (K_{sv}), and Bimolecular Quenching Constants (k_q) of photocatalysts with *N*-phenyl-1,2,3,4-tetrahydroisoquinoline as quencher [a]

	τ_T / μs	K_{sv} / 10^2 M^{-1}	K_q / 10^7 $M^{-1}s^{-1}$
B-1	56.9	8.25	1.45
B-2	3.6	7.65	36.4
Eosin Y	76.3	19.5	2.56
$Ru(bpy)_3^{2+}$	0.9	0.49 [b]	5.47 [b]

[a] The data were obtained with photocatalysts concentration at 1.0 × 10^{-5} M in deaerated CH_3CN solution, excited with pulsed 532 nm laser, 20 °C. [b] The data were obtained by measurement of the quenching of the phosphorescence of $Ru(bpy)_3^{2+}$ excited with 452 nm, 20 °C.

Table S2. Triplet Excited State Lifetimes (τ_T), Stern–Volme Quenching Constant (K_{sv}), and Bimolecular Quenching Constants (k_q) of photocatalysts with phenyl diazonium salt as quencher. [a]

	τ_T / μs	K_{sv} / 10^3 M^{-1}	K_q / 10^8 M^{-1} s^{-1}
B-1	56.9	7.91	1.39
B-2	2.1	8.44	40.2
Eosin Y	76.3	—	—
$Ru(bpy)_3^{2+}$	0.9	0.68 [b]	7.51 [b]

[a] The data were obtained with photocatalysts concentration at 1.0×10^{-5} M in deaerated CH_3CN solution, excited with 532 nm laser, 20 °C. [b] The data were obtained quenching of the phosphorescence excited with 452 nm, 20 °C.